Advanced Numerical Methods

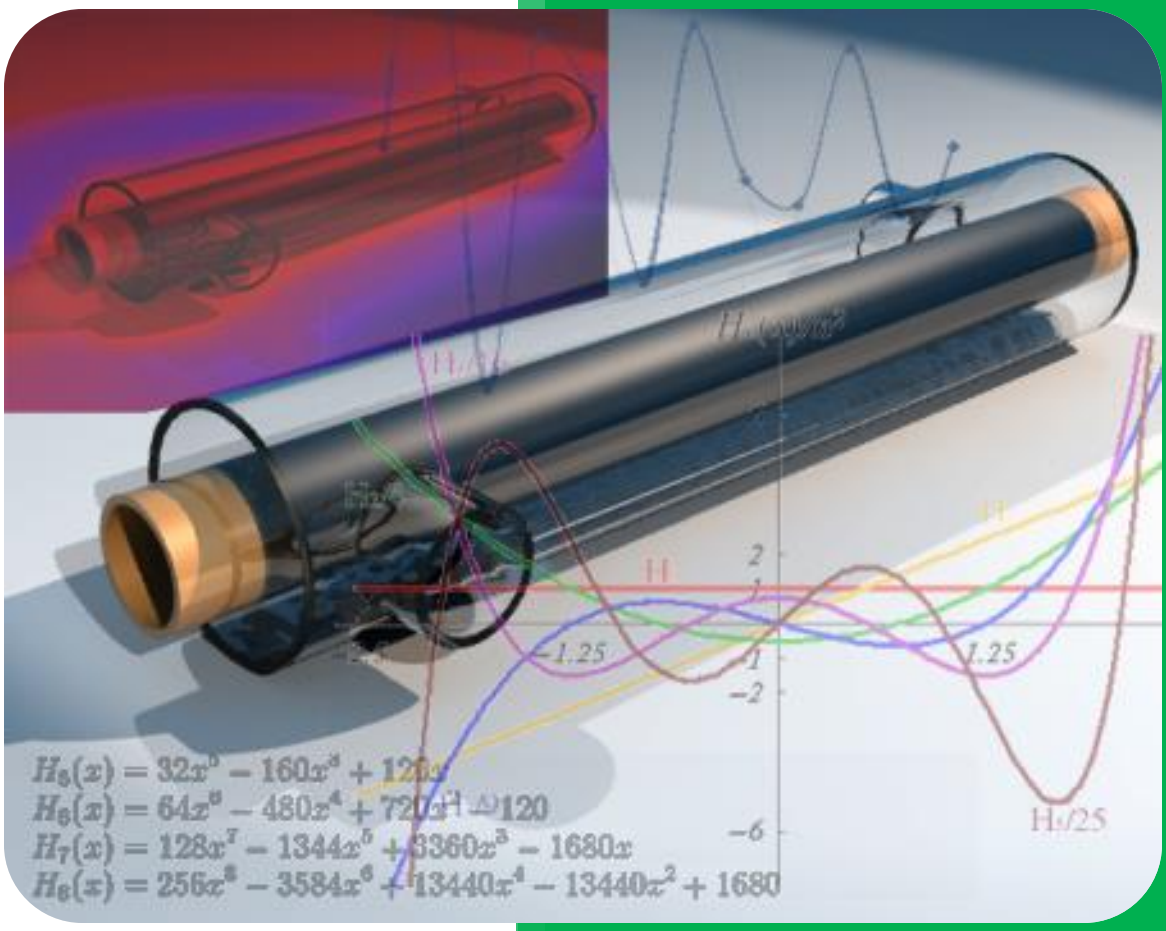

Esmail Ansari 88200782
Ahmad Siahati 88200425
Supervised By: Dr. Bozorgmehri
Term Project
Chemical and Petroleum department
Sharif University of Technology

march.2010

Contents

Abstract-preface **1**

Acknowledgement **2**

Table of figures **3**

Table of tables **5**

Table of flowcharts **5**

Nomenclature **6**

1-1 Outlines **8**

1-2 Objective **9**

1-3 Literature Review **9**

1-3-1 Governing Equations **9**

1-3-1-1 Two-phase flow inside ducts **10**

1-3-1-2 Heat conduction in the internal tube wall **12**

1-3-1-3 Evaluation of empirical coefficients **12**

1-3-1-4 Single-phase **13**

1-3-1-5 Annulus **13**

1-3-1-6 Condensing flow **13**

1-3-2 Numerical resolution **14**

1-3-2-1 Spatial and temporal discretization **14**

1-3-2-2 Two-phase flow inside ducts **14**

1-3-2-3 Discretization equations **14**

1-3-2-4 Boundary conditions **16**

1-3-2-5 Heat conduction in the internal tube wall **17**

1-3-2-6 Heat conduction in the external tube and insulation **17**

1-3-2-7 Numerical algorithm **18**

1-4 Used correlations **19**

1-5 Assumptions **21**

1-6 Explicit methods **23**
1-6-1 Explicit codes flowchart **23**
1-6-2 Explicit codes structure **29**
1-7 Implicit methods **30**
1-7-1 Unsteady implicit flowcharts **30**
1-7-2 Implicit codes structure **34**
1-8 Results **35**
1-8-1 steady state study of heat exchanger: **35**
1-8-2 Study the effect of various parameters on steady state results: **42**
1-8-3 Study of unsteady state behavior of Co-current flows: **55**
1-8-3-1 case study **56**
1-8-3-2 comparison **61**
1-8-4 Simulating Counter-Current flows: **62**
1-8-5 Study of Super-heat entrance: **69**
1-8-5-1 without conduction **69**
1-8-5-2 with conduction **71**
1-8-5-3 General form of inlet superheat vapor **73**
1-8-6 Study of two dimensional wall and heat transfer with environment: **79**
1-9 Challenges and rewards **84**

Chapter 2 - Hermite polynomials **85**
2-1 Outlines **87**
2-2 Objective **87**
2-3 Introduction **87**
2-4 Assumptions **87**
2-5 Program Flowchart **87**
2-6 Program Results **89**
2-7 Challenges **91**
2-8 Program GUI **93**

Chapter 3- Spline Interpolation **93**
3-1 Outlines **94**
3-2 Objective **94**
3-3 Introduction **94**
3-4 Assumptions **95**
3-5 Program results **97**
Suggestions **98**
Appendix A-Program Profile **99**
Appendix B- Fluent work failure **107**
References **108**

Abstract

The heat exchanger simulation of both co-current and counter-current flows will be carried out. All implicit, explicit and semi-implicit methods will be implemented. House-holder-Broyden method will be incorporated into Newton method. Superheated steam will be investigated. The effect of various parameters, such as angle, on the results will be explained. Heat transfer with environment will be analyzed. Hermite polynomials will be studied. Spline interpolation will be looked into. Attained results will be compared, validated and discussed.

Preface

All parts of the project have been performed by written codes in MATLAB software. The provided codes can handle other conditions as well.

Figures

Fig1. Flow inside a control volume. 10
Fig2. Heat fluxes in a control volume of a solid. 12
Fig3. Node distribution along the double-pipe heat exchanger 13
Fig4 .Schematic illustration of steady state results in Matlab. 37
Fig5. Curves of convection heat transfer coefficient for inner and outer fluids. 38
Fig6. Water temperature and pressure profile in its steady state in steady state condition 39
Fig7. Steam temperature and pressure profile in its steady state condition. 40
Fig8. Temperature of pipe wall 41
Fig9. Comparing the time of convergence between different methods. 42
Fig10. Effect of Inner pipe diameter on the heat exchanger steady state condition 43
Fig11. Effect of Outer pipe diameter on heat exchanger steady state condition 44
Fig12. Effect of Inlet subcooled water temperature on heat exchanger steady state condition 45
Fig13. Effect of Inlet saturated steam temperature on the heat exchanger steady state condition 46
Fig14. Effect of heat exchanger's length on its steady state condition 47
Fig15. The impact of Inlet saturated steam flux on various data in steady state condition 48
Fig16. Effect of Inlet water flux on various data in steady state condition 49
Fig17. Effect of having one dimensional wall on steady state condition 50
Fig18. Effect of two dimensional walls on various results in steady state condition 51
Fig19. Effect of changing angle of heat exchanger on water temperature along the pipe 52
Fig20. Effect of changing angle of heat exchanger on various parameters in S.S condition 53
Fig21. Effect of changing angle of heat exchanger on various parameters in outlet section 54
Fig22. The moving effect of water temperature for uniform initial condition after 11.7 seconds. 57
Fig23. After some moments, the steady state is reached. The blinking line shows the steady state situation. 57
Fig24. Left to right. Moving front of steam mass flow after 1.8, 5.1 and 30 seconds. 58
Fig25. Liquid film after 2.1 and 23.1 seconds (steady state) for uniform initial condition. 58

Fig26. 2D and contour plots of steam velocity after 3.3 seconds (uniform initial condition). 59
Fig27. The reaction of water temperature towards its stable state after applying pulse. 59
Fig28. Profile of steam pressure after 3 seconds (left) and after steady state (right). 59
Fig29. Both plots shows steam temperature after 15 seconds (uniform initial condition). 60
Fig 30. Steady state results of the problem. 64
Fig31. These plots, both 2D and contour, represent the progress of liquid film. 64
Fig32. Pursuing the lines by zoom objects is required in order to estimate the exact steady state time. 65
Fig 33. Water temperature (lower) vs. steam temperature(upper) at 1.2 and 6.3 seconds. 65
Fig34. Water pressure (upper) vs. steam pressure (lower) at 9 seconds. 66
Fig35. Liquid film velocity (upper) vs. steam velocity (lower) at 3.3 seconds. 66
Fig 36. Steam mass flow (upper) vs. Steam velocity (lower). 67
Fig 37. Steam pressure vs. steam velocity at 21 seconds. 67
Fig38. Quality (lower) vs. condensate film (upper) at 8.1 sec. 67
Fig39.Plot of temperature of water for co-current and counter-current. 68
Fig40. The fantastic plot of liquid film for both co-current and counter-current. 69
Fig41. Changing temperature of steam where superheated vapor enters the heat exchanger. 75
Fig42. Condensate water 76
Fig 43. Changing temperature of steam for a long heat exchanger. 77
Fig 44. Liquid condensate for superheat entering. 78
Fig 45. Profile of temperature for two dimensional inner pipe wall (two mesh across the pipe). 82
Fig 46. Profile of temperature for two dimensional isolation and outer wall. 82
Fig 47. Finding Critical Radius 83
Fig48. Truncation of the numbers (round off errors) in Matlab. 91
Fig49. Hermite polynomials GUI 93
Fig 50. Spline GUI 97

Tables

Table 1. Results of various methods for steady state condition. 35
Table 2. Results of unsteady after 10.1 seconds for Uniform Initial Condition 60
Table 3. Results of unsteady after 10.1 seconds for pulsed Steady-State Initial Condition 61
Table 4. Comparison between co-current and counter-current flow. Note that the data of the problem are set as the default data. 67
Table 5. Results for inlet superheat vapor without conduction. No saturated steam will be produced in this length. 70
Table 6. Comparing the results with and without conduction assumption for various flux rates. 72
Table 7. Table of results for reformation of superheat to saturated vapor 73
Table 9- effect of isolation thickness on quality and insulation-air contact temperature. 80
Table 10- Results of Hermite polynomials 89

Flowcharts

Flowchart 1- The main part of unsteady state codes. 24
Flowchart 2- Simulating the inner pipe (subcooled water) by appending its equations. 25
Flowchart 3- Simulation of outer pipe (steam) 26
Flowchart 4- assembling the equations of inner pipe wall (one dimensional method) 27
Flowchart 5- superheat vapor changes the outer pipe simulation algorithm. Others parts remain the same. 28
Flowchart 6- Structure of main.m file in the implicit codes. 31
Flow chart 7- Newton function and its sub function jacobian which includes House Holder Broyden method. 32
Flow chart 8- Structure of important function “EquCalc”. 33
Flowchart 9- Bairstow algorithm 88
Flowchart 10– Spline 96

Latin letters

A	cross section area (m^2)
C_P	specific heat at constant pressure (J kg^{-1} K^{-1})
CV	control volume
D	diameter (m)
E	specific energy *(h* + $n^2/2$ + *gz* sin *0)* (J kg^{-1})
CV	control volume
F	friction factor
G	acceleration due to gravity (ms^{-2})
G	mass velocity (kg m^{-2} s^{-1})
L	length (m)
M	mass (kg)
M-dot	mass flux (kg s^{-1})
n	number of control volumes
p	*Pressure(pa)*
P	*PERIMETER(M)*
q	Heat flux per unit area(w/m2)
Nu	Nusselt number *(aD/l)*
Re	Reynolds number *(GD/J)*
T	time (s)
T	temperature (K)
V	velocity (ms^{-1})
X_g	vapour mass fraction
Z	axial coordinate

Greek letters

θ	angle (rad); see 1-1)
ρ	density (kg m^{-3})
Φ	two-phase frictional multiplier
α	heat transfer coefficient (W m^{-2} K^{-1})
δ	rate of convergence
ξ	absolute roughness (m)
τ	shear stress (Pa)
λ	thermal conductivity (W m^{-1} K^{-1})
μ	dynamic viscosity (Pa s)
ϵ_g	void fraction
Δt	temporal discretization step (s)
Δr	radial discretization step (m)
Δz	axial discretization step (m)

Subscript

A	Annulus
Amb	Ambient
Bc	begin condensation
E, e	East
Ec	end condensation
Exp	Experimental
g	gas or vapour
h	Hydraulic
l	Liquid
N, n	North
Num	Numerical
r	radial direction
Ref	Refrigerant
S, s	South
Tp	two-phase
W, w	West
z	axial direction

Superscripts

O	previous instant
*****	previous iteration

Chapter 1

Heat Exchanger Project

1-1 Outlines

1. Using fully explicit step by step method for every single grid, the properties of inner fluid (temperature and pressure), outer fluid (temperature, pressure and quality) and inner pipe wall (temperature) are simulated.
2. Considering the terms for time and using step by step fully explicit method for each grid, the unsteady state behavior of the problem is explored.
3. Using fully implicit method over the equations of all grids conjointly, the steady state equations are solved simultaneously and previous results are validated.
4. The unsteady state is simulated using fully implicit method over all grids equations collectively.
5. The effect of changing angle (between -90 to 90 degrees) is studied.
6. Crank-Nicholson method is adapted to the fully implicit codes.
7. The simulation is conducted premising both concurrent and countercurrent flows and the outcomes and differences are explained.
8. For reducing the time, the valuable methods of House-Holder and Broyden are implemented with the Newton method.
9. The entrance of Super heat vapor is taken into account and the results are investigated.
10. Finally, heat transfer with surrounding environment and marshal indexing of pipe are adapted to the codes.
11. Illustrated results are explained thoroughly using basic concepts.
12. Attempts have been made to provide easily legible and friendly codes.

1-2 Objective

The objective of this project is to simulate the behavior of double pipe heat exchangers by solving associated PDE's through finite difference approach.

1-3 Literature Review [1]

A detailed one-dimensional steady and transient numerical simulation of the thermal and fluid-dynamic behavior of double pipe heat exchangers has been carried out. The governing equations (continuity, momentum and energy) inside the internal tube and the annulus, together with the energy equation in the internal tube wall, external tube wall and insulation, are solved iteratively in both unified and segregated manner. The discretized governing equations in the zones with fluid flow are efficiently coupled. This formulation requires the use of empirical correlations for the evaluation of convective heat transfer, shear stress and void fraction. All the flow variables (enthalpies, temperatures, pressures, mass fractions, velocities, heat fluxes …) together with the thermophysical properties are evaluated at each point of the grid in which the domain is discretized. Different numerical aspects are presented in order to verify and validate the model.

1-3-1 Governing Equations

The numerical solution in the zones with fluid flow has been performed by discretization of the one-dimensional governing equations based on an efficiently coupled fully implicit and explicit method over control volumes (CVs). The energy equation is written in terms of the enthalpy to give generality and to allow a suitable treatment of mixtures. The different flow regimes produced in condensation phenomenon, have been taken into account. The refrigerants and water thermo physical properties are evaluated locally using Spline interpolation or related correlations. The solid elements are accurately solved considering multidimensional heat transfer effects.

1-3-1-1 Two-phase flow inside ducts

A characteristic CV is shown schematically in Fig. 1, where 'i' and 'i + 1' represent the inlet and outlet sections, respectively.

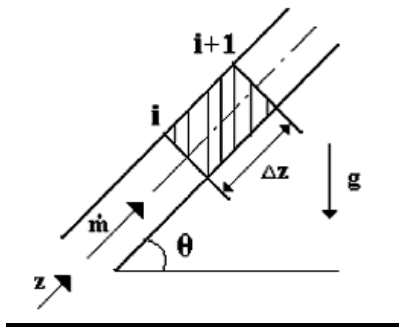

Fig1. Flow inside a control volume.

Taking into account the characteristic geometry of ducts (diameter, length, roughness, angle...), the governing equations have been integrated assuming the following assumptions:

- One-dimensional flow: *p(z,t), h(z, t), T(*z, t),...
- Non-participant radiation medium and negligible radiant heat exchange between surfaces.
- Axial heat conduction inside the fluid is neglected.

The semi-integrated governing equations over the above mentioned finite CV, have the following form:

Continuity:

$$[\dot{m}]_i^{i+1} + \frac{\partial m}{\partial t} = 0 \qquad (1\text{-}1)$$

Momentum

$$[\dot{m}_g v_g]_i^{i+1} + [\dot{m}_l v_l]_i^{i+1} + \Delta z \frac{\partial \tilde{m}}{\partial t} = -[p]_i^{i+1} A - \tilde{\tau} P \Delta z - mg \sin\theta \qquad (1\text{-}2)$$

Energy Equations

$$\tilde{\dot{m}}[e_1]_i^{i+1} + [\dot{m}_g(e_g - e_l)]_i^{i+1} + (\tilde{e}_g - \tilde{e}_l)\frac{\partial m_g}{\partial t} + m_g\frac{\partial \tilde{e}_g}{\partial t} + m_l\frac{\partial \tilde{e}_l}{\partial t} - A\Delta z\frac{\partial \tilde{p}}{\partial t} + (\tilde{e}_l - \tilde{e}_l)\frac{\partial m}{\partial t} = \tilde{q}P\Delta z \qquad (1\text{-}3)$$

The terms having ~ above them represent the arithmetic average between properties of two adjacent CVs. The subscript and superscript in the brackets indicate the difference between the quantity *X* at the outlet section and the inlet section. In the governing equations, the evaluation of the shear stress is performed by means of a friction factor *f*. This factor is defined from the expression:

$$\tau = \emptyset \left(\frac{f}{4}\right) \left(\frac{G2}{2p}\right), \qquad (1\text{-}4)$$

Where $\emptyset$ is the two-phase factor multiplier. The one-dimensional model also requires the knowledge of the two-phase flow structure, which is evaluated by means of the void fraction e_g. Finally, heat transfer through the duct wall and fluid temperature are related by the convective heat transfer coefficient *a*, which is defined as:

$$\alpha = \left(\frac{q^{\cdot}}{T_{wall} - T_{fluid}}\right) \qquad (1\text{-}5)$$

The differentiation between the three main regions existing in condensation processes is given by the enthalpy, pressure and vapour quality. These conditions are:

- Liquid region: when $h(p) < h_l(p)$, then $x_g = 0$.
- Two-phase region: when $h_l(p) < h(p) < h_g(p)$, then $0 < x_g < 1$.
- Vapor region: when $h(p) > h_g(p)$, then $x_g = 1$

Where $h_l(p)$ and $h_g(p)$ represent the saturation liquid and gas enthalpy for a given pressure *p*.

1-3-1-2 Heat conduction in the internal tube wall

The conduction equation has been written assuming the following hypotheses: one dimensional transient temperature distribution and negligible heat exchanged by radiation. A characteristic CV is shown in figure 2, where *'P'* represents the central node, *'E* and *'W* indicates its neighbors. The CV-faces are indicated by *'e'*, *'w'*, *'n'* and 's'.

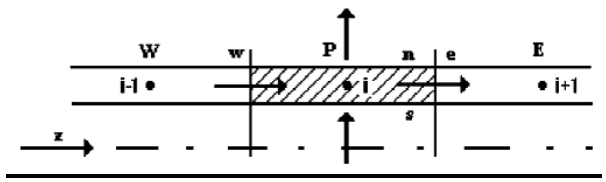

Fig2. Heat fluxes in a control volume of a solid.

Integrating the energy equation over this CV, the following equation is obtained:

$$(\tilde{q}_s P_s - \tilde{q}_n P_n)\Delta z + (\tilde{q}_w - \tilde{q}_e)A = m\frac{\partial \tilde{h}}{\partial t} \qquad (1\text{-}6)$$

Where $q_s^{\sim}$ and $q_n^{\sim}$ are evaluated using the respective convective heat transfer coefficient in each zone, and the conductive heat fluxes are evaluated from the Fourier law, that is:

$$\tilde{q}_e = -\lambda_e(\partial T/\partial z)_e \qquad \tilde{q}_w = -\lambda_w(\partial T/\partial z)_w. \qquad (1\text{-}7)$$

1-3-1-3 Evaluation of empirical coefficients

The mathematical model requires local information about friction factor *f*, convective heat transfer coefficient α and the void fraction ϵ_g. This information is generally obtained from empirical or semi-empirical correlations.

After comparing different empirical correlations presented in the technical literature, we have selected the following to obtain most of the results presented here:

1-3-1-4 Single-phase

In the single-phase regions, the convective heat transfer coefficient is calculated using the Nusselt and the Gnieliski equation, for laminar and turbulent regimes, respectively. The friction factor is evaluated from the expressions proposed by Churchill.

1-3-1-5 Annulus

The friction factor in the annulus is calculated using the expressions corresponding to single-phase flow with the hydraulic diameter. The convective heat transfer is calculated using the Monrad and Pelton correlation developed specifically for flow in annulus.

1-3-1-6 Condensing flow

In the two-phase region, the convective heat transfer coefficient is calculated using the Dobson and Chato correlations that employed two different expressions for the annular and wavy flow regions. The expression proposed by Soliman for the Froude number is taken as a differentiation criterion between annular and wavy condensation. The void fraction is estimated from the semi-empirical equation of Smith. The friction factor is calculated from the same equation as in the case of the single-phase flow using a correction factor (two-phase frictional multiplier) according to Friedel.

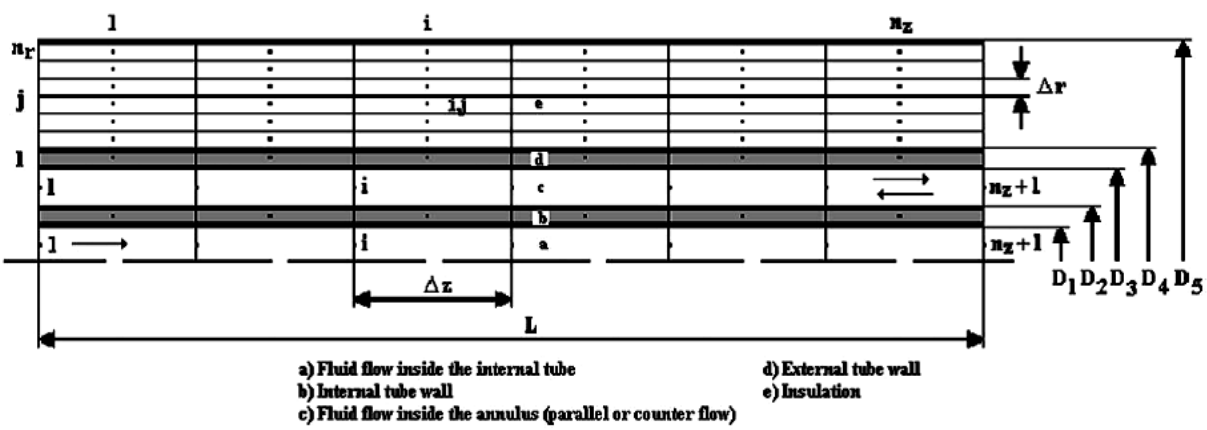

Fig3. Node distribution along the double-pipe heat exchanger

1-3-2 Numerical resolution

1-3-2-1 Spatial and temporal discretization

Fig3. shows the spatial discretization of a double pipe heat exchanger. The discretization nodes are located at the inlet and outlet sections of the CVs in the fluid flow zones, while the discretization nodes are centered in the CVs in the tube wall and insulation. Each one of the fluids has been divided into n_z volumes (i.e. n_z + 1 nodes). The internal tube wall has been discretized into n_z control volumes of length Δz. The external tube and the insulation are discretized into $n_z * n_r$ control volumes of length Δz and width Δz, where $\Delta r = \frac{D_4 - D_3}{2}$ for j = 1 and $\Delta z = \frac{D_5 - D_4}{2*(n_r - 1)}$ for j > 1.

The transitory solution is performed every time step Δt. Depending on the time evolution of the boundary conditions, a constant or variable value of Δt can be selected.

1-3-2-2 Two-phase flow inside ducts

The discretized equations have been coupled in the flow direction. From the known values at the inlet section and guessed values of the wall boundary conditions (obtained from the previous outer iteration), the variable values at the outlet of each CV are iteratively obtained from the discretized governing equations. This solution (outlet values) is the inlet values for the next CV. The procedure is carried out until the end of the tube is reached.

1-3-2-3 Discretization equations

For each CV, a set of algebraic equations is obtained by a discretization of the governing Eqs (1-1)-(1-3)

In the section, mathematical formulation, the governing equations have been directly presented on the basis of the spatial integration over finite CVs. Thus, only their temporal integration is required. The transient terms of the governing equations are discretized using the following approximation:

$$\partial \phi / \partial T \cong (\phi - \phi^{o}) / \Delta t \qquad (1\text{-}8)$$

where ϕ represents a generic dependent variable (f = *h*, *p*, *T*, p,...); superscript 'o' indicates the value of the previous instant.

The averages of the different variables have been estimated by the arithmetic mean between their values at the inlet and outlet sections, that is:

$$\tilde{\phi}_i \cong \bar{\phi}_i \equiv (\phi_i + \phi_{i+1})/2. \qquad (1\text{-}9)$$

Based on the numerical approaches indicated above, the governing Eqs (1-1)-(1-3) can be discretized to obtain the value of the dependent variables (mass flow rate, pressure and enthalpy) at the outlet section of each CV. The final form of the governing equations is given below.

The mass flow rate is obtained from the discretized continuity equation.

$$\dot{m}_{i+1} = \dot{m}_i - \frac{A\Delta z}{\Delta t}(\bar{\rho}_{tp} - \bar{\rho}^{o}_{tp}) \qquad (1\text{-}10)$$

where the two-phase density is obtained from:

$$\rho_{tp} = \epsilon_g\, \rho_g + (1 - \epsilon_l\, \rho_l) \qquad (1\text{-}11)$$

In terms of the mass flow rate, gas and liquid velocities are calculated as,

$$v_g = \left[\frac{\dot{m}x_g}{\rho_g \epsilon_g A}\right] \qquad v_l = \left[\frac{\dot{m}(1 - x_g)}{\rho_l(1 - \epsilon_g)A}\right] \qquad (1\text{-}13)$$

The discretized momentum equation is solved for the outlet pressure,

$$p_{i+1} = p_i - \frac{\Delta z}{A}\left(\Phi\frac{\bar{f}}{4}\frac{\bar{\dot{m}}^2}{2\bar{\rho}_{tp}A^2}P + \bar{\rho}_{tp}Ag\sin\theta + \frac{\bar{\dot{m}} - \bar{\dot{m}}^o}{\Delta t} + \frac{[\dot{m}(x_g v_g + (1 - x_g)v_l)]_i^{i+1}}{\Delta z}\right) \qquad (1\text{-}14)$$

From the energy equation (3) and the continuity equation (1), the following equation is obtained for the outlet enthalpy,

$$h_{i+1} = \frac{2\dot{q}_{\text{wall}} - a\dot{m}_{i+1} + b\dot{m}_i + cA\Delta z/\Delta t}{\dot{m}_{i+1} + \dot{m}_i + \bar{\rho}^{\text{o}}_{\text{tp}} A\Delta z/\Delta t} \tag{1-15}$$

where

$$a = (x_{\text{g}} v_{\text{g}} + (1 - x_{\text{g}}) v_{\text{l}})^2_{i+1} + g \sin\theta \Delta z - h_i \tag{1-16}$$

$$b = (x_{\text{g}} v_{\text{g}} + (1 - x_{\text{g}}) v_{\text{l}})^2_{i} - g \sin\theta \Delta z + h_i \tag{1-17}$$

$$c = 2(\bar{p}_i - \bar{p}^{\text{o}}_i) - \bar{\rho}^{\text{o}}_{\text{tp}}(h_i - 2\bar{h}^{\text{o}}_i) - (\bar{\rho}\bar{v}^2_i - \bar{\rho}^{\text{o}} v^{\text{o}^2}_i) \tag{1-18}$$

Temperature, mass fraction and thermophysical properties are evaluated using matrix functions of the pressure and enthalpy, refilled with the refrigerants properties evaluated using spline interpolation or by fitting polynomials on the unknown data.

$$T = f(p, h); \quad x_{\text{g}} = f(p, h); \quad \rho = f(p, h); \ldots$$

The above mentioned conservation equations of mass, momentum and energy together with the thermophysical properties, are applicable to transient two-phase flow. Situations of steady flow and/or single-phase flow (liquid or gas) are particular cases of this formulation.

1-3-2-4 Boundary conditions

- *Inlet conditions:* the boundary conditions for solving a step by step method directly are the inlet mass flux (m_{in}), pressure *(p_{in})* and temperature *(T_{in})* or mass fraction (x_{gin}) in the cases of inlet two-phase flow. From any of these values (temperature or mass fraction) and the pressure, enthalpy (our independent variable) is obtained. Other boundary conditions such as *($m_{_\ in}$, p_{out})* or (p_{in}, p_{out}) or (p_{in}, m_{out}) can be solved using a Newton or House-Holder_Broyden algorithm.
- *Solid boundaries:* the wall temperature profile in the tube or the heat flux through the tube wall in each CV must be given. These boundary conditions are expressed in the energy equation in this compact form:

$$\dot{q}_{\text{wall}} = (1-\beta)\dot{q}_{\text{wall}} + \beta\alpha(T_{\text{wall}} - T_{\text{fluid}}) \tag{1-19}$$

1-3-2-5 Heat conduction in the internal tube wall

The following equation has been obtained for each node of the grid:

$$a_i T_{\text{wall},i} = b_i T_{\text{wall},i+1} + c_i T_{\text{wall},i-1} + d_i \tag{1-20}$$

Where a, b, c and d are:

$$a_i = \frac{\lambda_{\text{w}} A}{\Delta z} + \frac{\lambda_{\text{e}} A}{\Delta z} + (\alpha_{\text{s}} P_{\text{s}} + \alpha_n P_n)\Delta z + \frac{A\Delta z}{\Delta t}\rho c_{\text{p}} \tag{1-21}$$

$$b_i = \frac{\lambda_{\text{e}} A}{\Delta z} \tag{1-22}$$

$$c_i = \frac{\lambda_{\text{w}} A}{\Delta z} \tag{1-23}$$

$$d_i = (\alpha_{\text{s}} P_{\text{s}} \bar{T}_{\text{s}} + \alpha_n P_n \bar{T}_n)\Delta z + \frac{A\Delta z}{\Delta t}\rho c_{\text{p}} T^0_{\text{wall},i} \tag{1-24}$$

The coefficients mentioned above are applicable for $2 \leq i \leq n_z$-1; for i = 1 and $i = n_z$ adequate coefficients are used to take into account the axial heat conduction or temperature boundary conditions. The set of heat conduction discretized equations is solved using fully implicit over entire equations or fully explicit method for each CV.

1-3-2-6 Heat conduction in the external tube and insulation

The following equation has been obtained for each node of the grid:

$$\begin{aligned} a_{\text{P}} T_{\text{wall},i,j} = {} & a_{\text{E}} T_{\text{wall},i+1,j} + a_{\text{W}} T_{\text{wall},i-1,j} + a_{\text{N}} T_{\text{wall},i,j+1} \\ & + a_{\text{S}} T_{\text{wall},i,j-1} + d_{\text{P}} \end{aligned} \tag{1-25}$$

$$a_{\text{S}} = \frac{\lambda_{\text{s}} P_{\text{s}} \Delta z}{\Delta r}; \qquad d'_{\text{P}} = \frac{A\Delta z}{\Delta t}\rho c_{\text{P}} \tag{1-26}$$

$$a_{\text{P}} = a_{\text{W}} + a_{\text{E}} + a_{\text{N}} + a_{\text{S}} + d'_{\text{P}}; \;\; d_{\text{P}} = d'_{\text{P}} T^0_{\text{wall},i,j} \tag{1-27}$$

The coefficients mentioned above are applicable for $2 \leq i \leq n_z$-1 and $2 \leq j \leq n_r$-1; for the nodes in the extremes (see Fig. 3) the following considerations have been applied:

- For $j = 1$ forced convection is considered in the south face, tube thermal conductivity in east and west faces and insulation thermal conductivity in north face, all these evaluated to the mean temperature between the nodes that separated them.
- For $j = n_r$ natural convection with the ambient is considered (using the correlation developed by Raithby and Hollands) and also the conduction through the insulation external part of thick equal to Dr=2, with thermal conductivity evaluated to the node temperature.
- For $i = 1$ and $i = n_z$ adequate coefficients are used to take into account the axial heat conduction or temperature boundary conditions.

1-3-2-7 Numerical algorithm

At each time step solution process is carried out on the basis of a global algorithm that solves in both segregated and a conjoint manner the flow inside the tube, the flow inside the annulus and the heat conduction in the tubes and insulation. The coupling between the four main subroutines has been performed iteratively each time step following the procedure in the explicit and implicit codes:

- For *fluid flow inside the internal tube,* the equations are solved considering the tube wall temperature distribution as boundary condition, and evaluating the convective heat transfer in each CV.
- For *fluid flow inside the annulus,* the same process is carried out considering both wall temperatures (internal tube wall and external tube wall).
- In the *internal tube wall,* the temperature distribution is re-calculated using the fluid flow temperature and the convective heat transfer coefficients evaluated in the preceding steps.
- In the *external tube and insulation,* the temperature distribution is re-calculated using the fluid flow temperature and the convective heat transfer coefficients evaluated in the annulus and the external ambient.

The governing equations corresponding to a steady state situation are the same equations shown above without considering the temporal derivative terms. This situation can be solved using a pseudo transient calculation with a guessed initial condition (for example, fluids at rest and uniform temperature in the whole domain). In transient situations, the initial conditions must be completely specified (i.e. the complete distribution of the variables in the whole domain). Sometimes these initial conditions are obtained from a steady state solution.

1-4 Used correlations

Heat transfer coefficient

In the single-phase regions, the convective heat transfer coefficient is calculated using the Nusselt and the Gnieliski equations, for laminar and turbulent regimes, respectively which are represented below:

Nusselt equation (laminar, Const.flux)	**Nu = 4.364**	(1-28)
Gnieliski equation (Turbulent)	$Nu = \dfrac{(f/8)(Re-1000)Pr}{1+12.7(f/8)^{1/2}(Pr^{2/3}-1)}$	(1-29)

Gnieliski equation is to be used with following equation for friction factor proposed by Filonenko:

$$f = (1.82\log_{10}Re - 1.64)^{-2}. \qquad (1\text{-}30)$$

The outside heat transfer coefficient h_o is computed from the Monrad and Pelton's equation for turbulent flow in annuli,

$$Nu = 0.020Re^{0.8}Pr^{1/3}(D_2/D_1)^{0.53} \qquad (1\text{-}31)$$

, in which D_1 and D_2 are the inner and outer diameter of the annulus respectively.

Void fraction model

There are two kinds of void fraction models. One is to determine the void fraction based on slip ratio, and the other is to calculate the void fraction directly. The relationship between the void fraction and the slip ratio is as follows.

$$\alpha = \frac{1}{1 + \left(\frac{1}{x} - 1\right) S \frac{\rho_g}{\rho_f}} \tag{1-32}$$

Smith model

$$S = K + (1 - K)\left[\frac{\frac{1}{P.I._1} + K\left[\frac{1-x}{x}\right]}{1 + K\left[\frac{1-x}{x}\right]}\right]^{\frac{1}{2}} \tag{1-33}$$

Where

$$P.I._1 = \frac{\rho_g}{\rho_f} \tag{1-34}$$

K is entrainment ratio and K = 0.4 is recommended.

Premoli model

$$S = 1 + F_1\left[\frac{y}{1 + yF_2} - yF_2\right]^{\frac{1}{2}} \tag{1-35}$$

$$F_1 = 1.578 Re_f^{-0.19}\left(\frac{\rho_f}{\rho_g}\right)^{0.22} \tag{1-36}$$

$$F_2 = 0.0273 We_f Re_f^{-0.51}\left(\frac{\rho_f}{\rho_g}\right)^{-0.08} \tag{1-37}$$

$$y = \frac{x\rho_f}{(1 - x)\rho_g} \tag{1-38}$$

$$Re_f = \frac{GD_i}{\mu_f} \tag{1-39}$$

$$We_f = \frac{G^2 D_i}{\sigma \rho_f} \tag{1-40}$$

One of the most accurate two-phase pressure drop correlations is that of Friedel (1979). It was obtained by optimizing an equation for Φ_{fo}^2 using a large data base of two-phase pressure drop measurements

$$\Phi_{fo}^2 = A_1 + 3.24\frac{A_1 A_2}{Fr^{0.045} we^{0.035}} \quad (1\text{-}41)$$

Where $A_1 = (1-x)^2 + x^2\left(\frac{\rho_f f_{go}}{\rho_g g_{go}}\right)$ (1-42)

$$A_2 = x^{0.78}(1-x)^{0.224} \quad (1\text{-}43)$$

$$A_3 = \left(\frac{\rho_f}{\rho_g}\right)^{0.91}\left(\frac{\mu_g}{\mu_g}\right)^{0.19}\left(1-\frac{\mu_g}{\mu_f}\right)^{0.7} \quad (1\text{-}44)$$

$$Fr = \frac{G^2}{gD\bar{\rho}} \quad (1\text{-}45)$$

$$We = \frac{G^2 D}{\rho\sigma} \quad (1\text{-}46)$$

Where f_{go} and f_{go} are the friction factors and G is total mass velocity as all vapor and all liquid, respectively. D is the equivalent diameter, $\sigma$is the surface tension and ρ is the homogeneous density.

1-5 Assumptions

1. Axis symmetrical over entire heat exchanger:

The gravity is the only factor which makes this assumption to be controversial but gravity can be ignored here since the flows have high speed, this assumption is logical in high speed of flow because in high speed, the terms associated with gravity force can be neglected. This means that the symmetrical assumption will be more plausible in cases that the flow rate is high rather than low, therefore in these situations, one dimensional flow can be premised more confidently : P(z,t), h(z,t), T(z,t) ….

2. Axial heat conduction inside the fluid and any heat radiation are disregarded.

This assumption can be viewed as the ramification of the previous one.

3. The enthalpy of single phase water is only function of temperature. $h(p,T) = f(T)$

This assumption, though inaccurate, is acceptable because the impact of pressure on the enthalpy of water is infinitesimal and can easily be disregarded.

4. Viscosity of saturated vapor is constant.

This is a pretty valid assumption since the viscosity of saturated vapor ranges from 14e-3 to 16e-3 centipoises; hence the constant value of 15e-3 centipoises was selected.

5. Thermal conductivity of water and vapor and pipe are constant.

Although not very precise, this assumption is fairly acceptable, the thermal conductivity is a function of temperature but it's variation is not extreme, therefore for the sake of simplicity the value of thermal conductivity for water, saturated vapor and pipe has been set to **0.585**, **2.77, 55** W/m/c respectively. Chrome steel is chosen for the inner pipe because it shows less variation in thermal conductivity and also is a very stable metal. The type of pipe gets its importance, when it has two dimensions.

6. Water is considered incompressible in range 0°-100°.

Since the variation in density of water, when temperature changes, is small, the impact of this assumption is trifling; hence the density of water is specified to 990 kg/m3.

7. Roughness of the pipe is set to $1.5 * 10^{-6}$.
8. The condensed water will remain as annular flow.
9. For calculating the convection heat transfer coefficient in the inner pipe, Gnieliski correlation and for calculating the convection heat transfer coefficient in the outer pipe, Monrad and Pelton correlation is used along the pipe.
10. The properties of two phase flow are often calculated using steam quality or void.
11. In the inner pipe, the lateral convection of pipe with surrounding environment is neglected.

1-6 Explicit methods

Unlike our implicit algorithm, our explicit codes use a step by step method for solving the equations of each grid nodes. Also, the effect of superheated steam and heat transfer with environment is only studied through explicit codes and there is no implicit code for this condition. Nevertheless, Countercurrent flows and boundary value problems are investigated by implicit codes and explicit codes can't support them.

1-6-1 Explicit codes flowchart

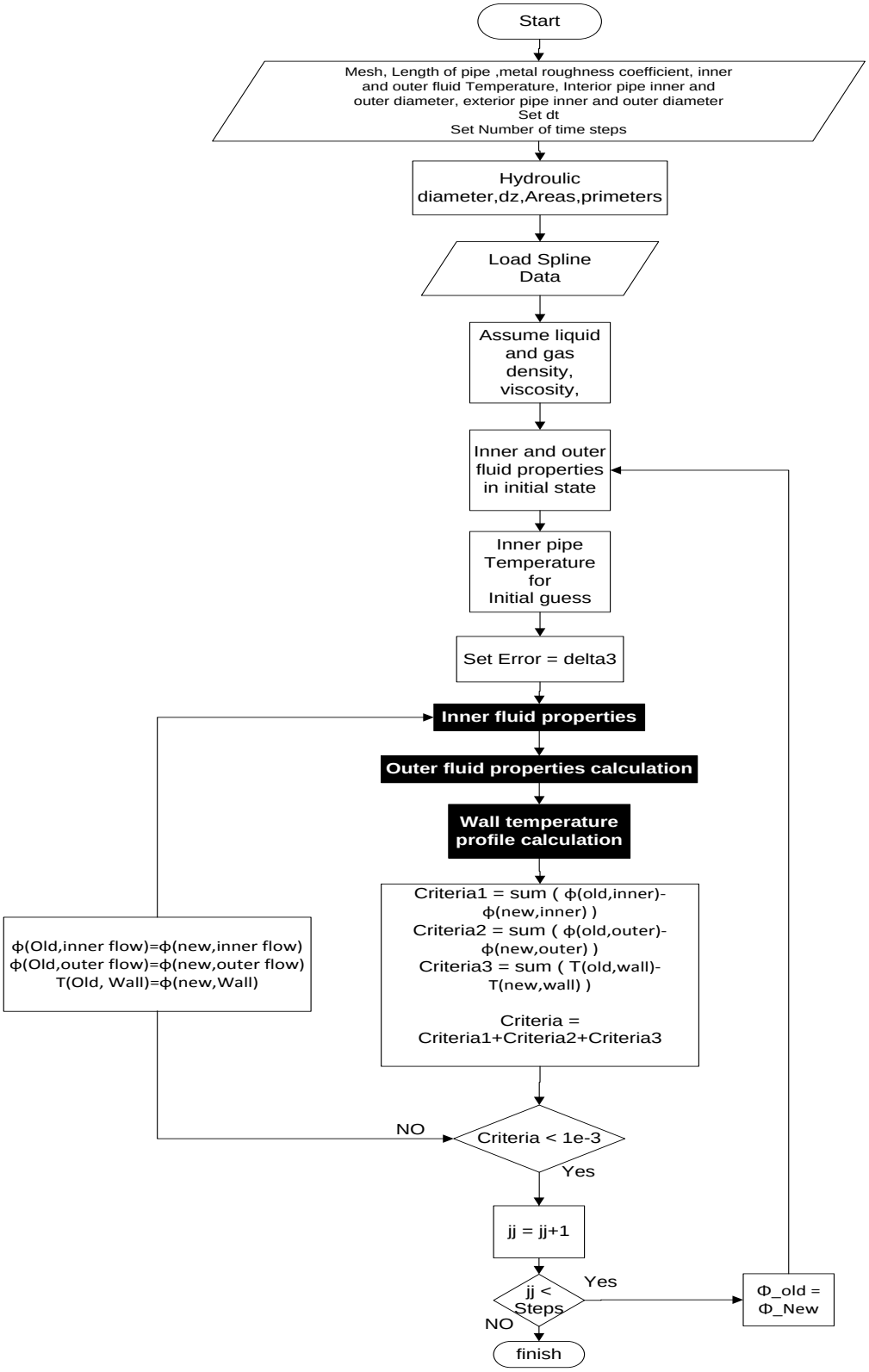

Flowchart 1- The main part of unsteady state codes.

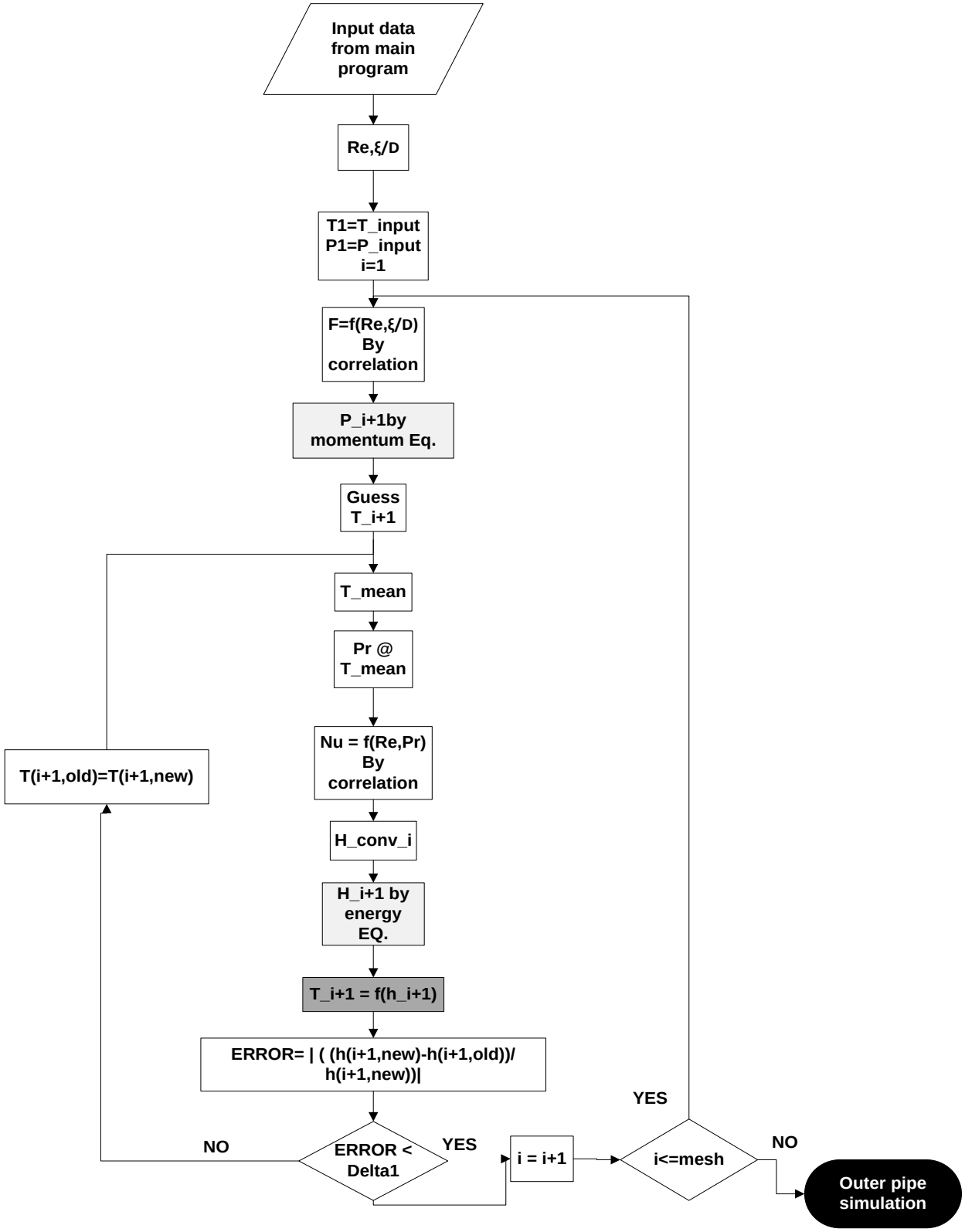

Flowchart 2- Simulating the inner pipe (subcooled water) by appending its equations.

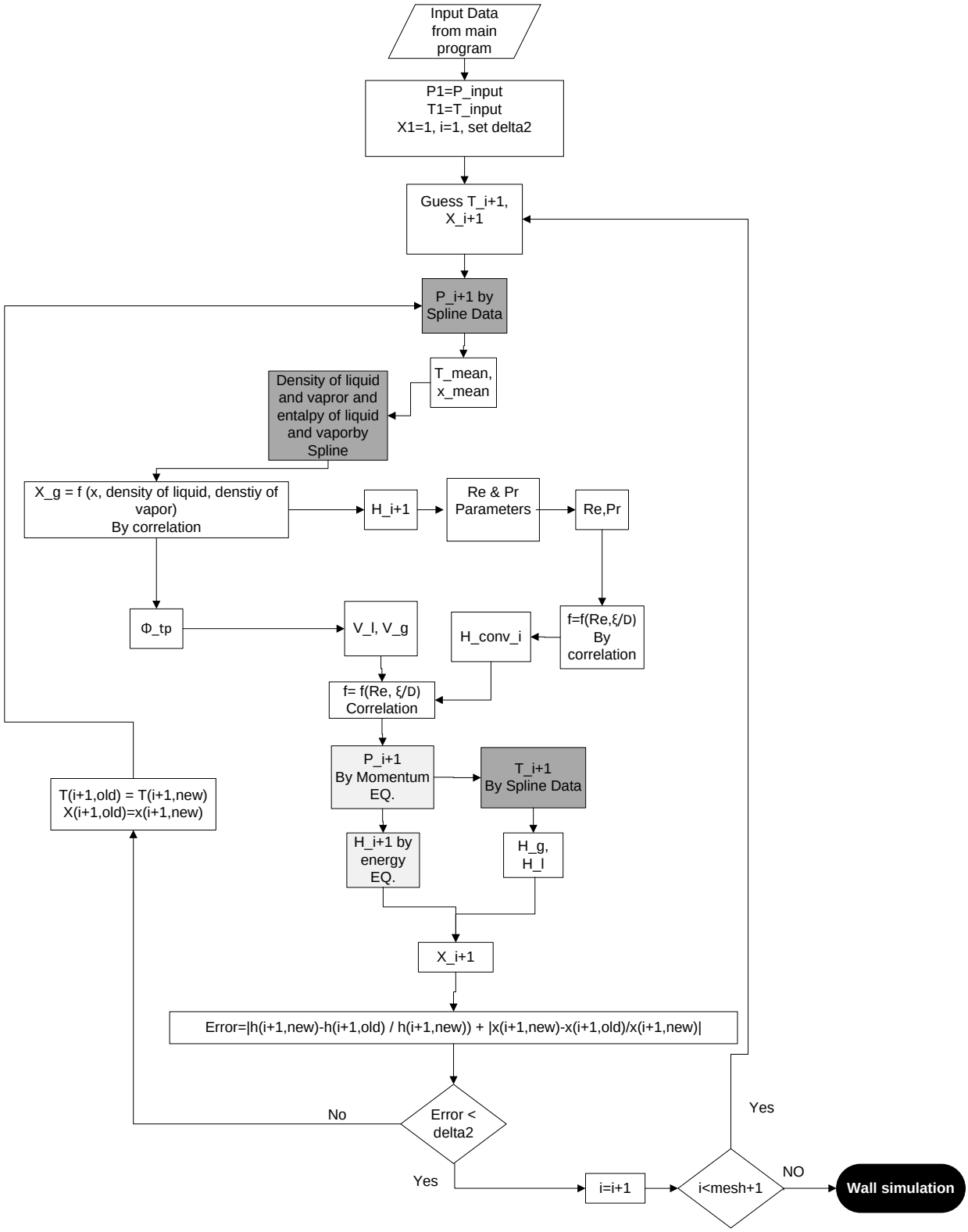

Flowchart 3- Simulation of outer pipe (steam)

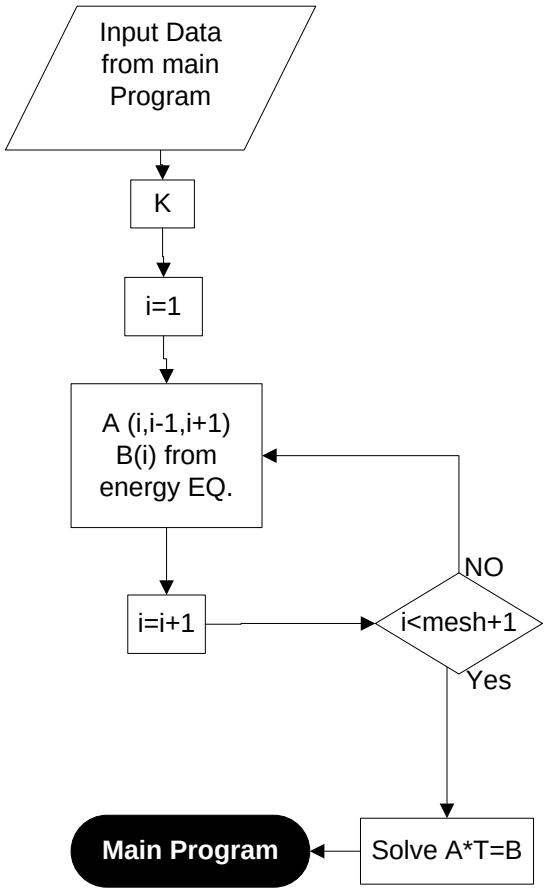

Flowchart 4- assembling the equations of inner pipe wall (one dimensional method)

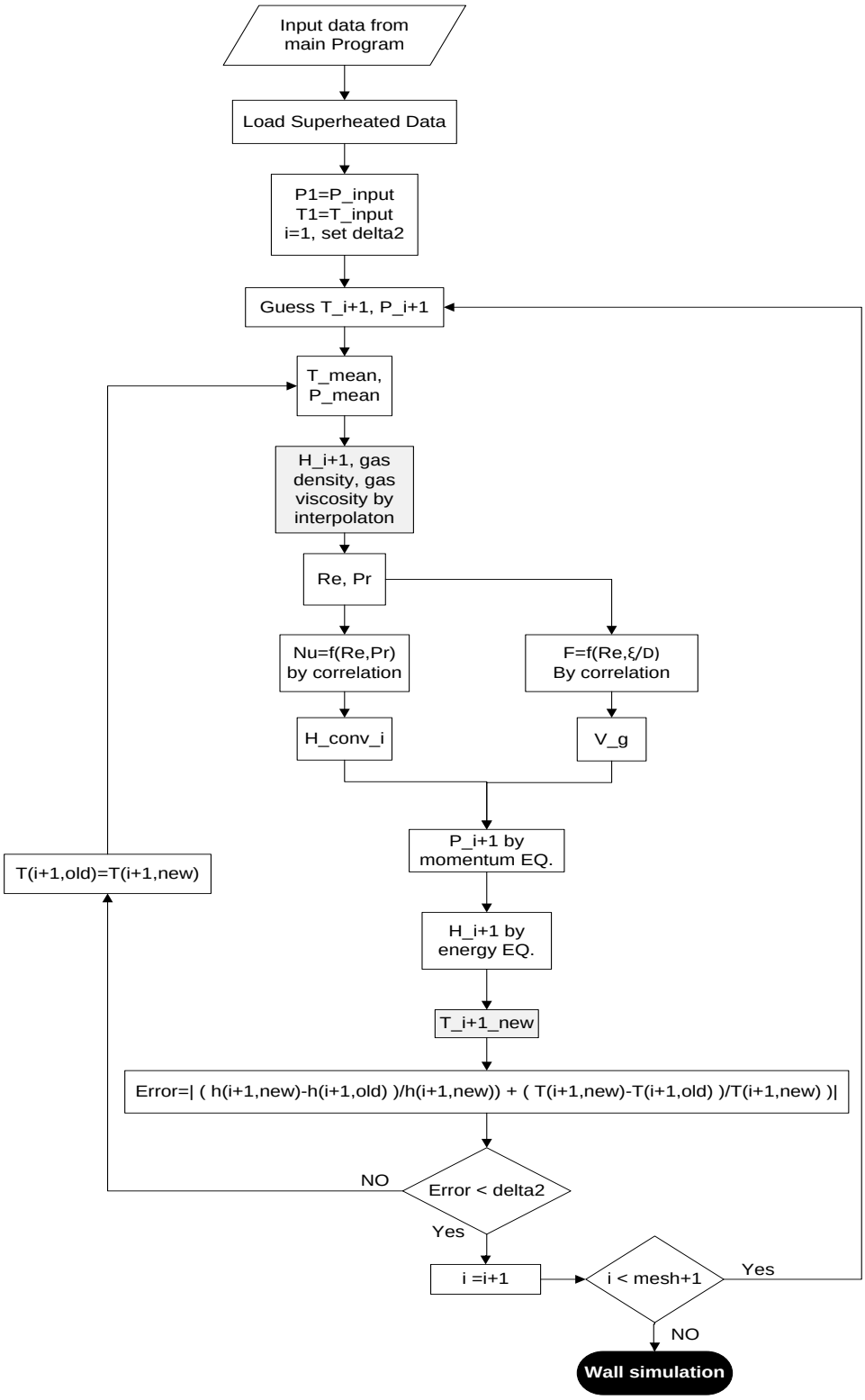

Flowchart 5- superheat vapor changes the outer pipe simulation algorithm. Others parts remain the same.

1-6-2 Explicit codes structure

- All the convergence criteria in these codes are set to 10^{-5} .
- The initial temperature of inner pipe wall is evaluated by assuming uniform temperature for the fluids and solving energy equations then this value is assigned to all the wall grids. This procedure is tagged with "%% initial guess for inner wall".
- There are several important structures in each program which holds the information of each layer. "inner_f" records all the information of inner fluid, "outer_f" is for outer fluid and "inner_w, outer_w" structure saves the information of inner and outer pipe walls, respectively.
- In order to reduce the time, the piece wise polynomials of saturated vapor table are generated separately using our own spline codes and then they are stored in .mat matrixes which will be loaded at the beginning of the program. The value of these piecewise polynomials will be returned using Matlab build in function "*ppval*".
- Variables which have prefixed with "all", refer to a specific property at two adjacent meshes and between the meshes.
- All the variables that have a prefix "TEMP" are used for keeping the previous track of specific variable that is going to be rewritten.
- All the variables which have the suffix of "mean" indicate the value between two adjacent meshes in sub cooled water or steam. Recall that the arrangement of meshes is explained in the literature review.
- The pulse in the quality of steam is set to "0.001".
- The "TimeStruc" structure is for keeping track of previous time properties.
- The converging criterion is set on the difference of enthalpies of both steam and liquid of all grids plus the temperature of inner pipe wall for two consecutive time steps.

1-7 Implicit methods

The implicit algorithm is not a step by step method, but rather a general solver like method which assembles all the equations of the system altogether and then treats it in a single jacobian matrix at each time step.

1-7-1 Unsteady implicit flowcharts

NOTE: flowcharts of counter-current flows and Crank-Nicholson method are ignored due to their similar structures.

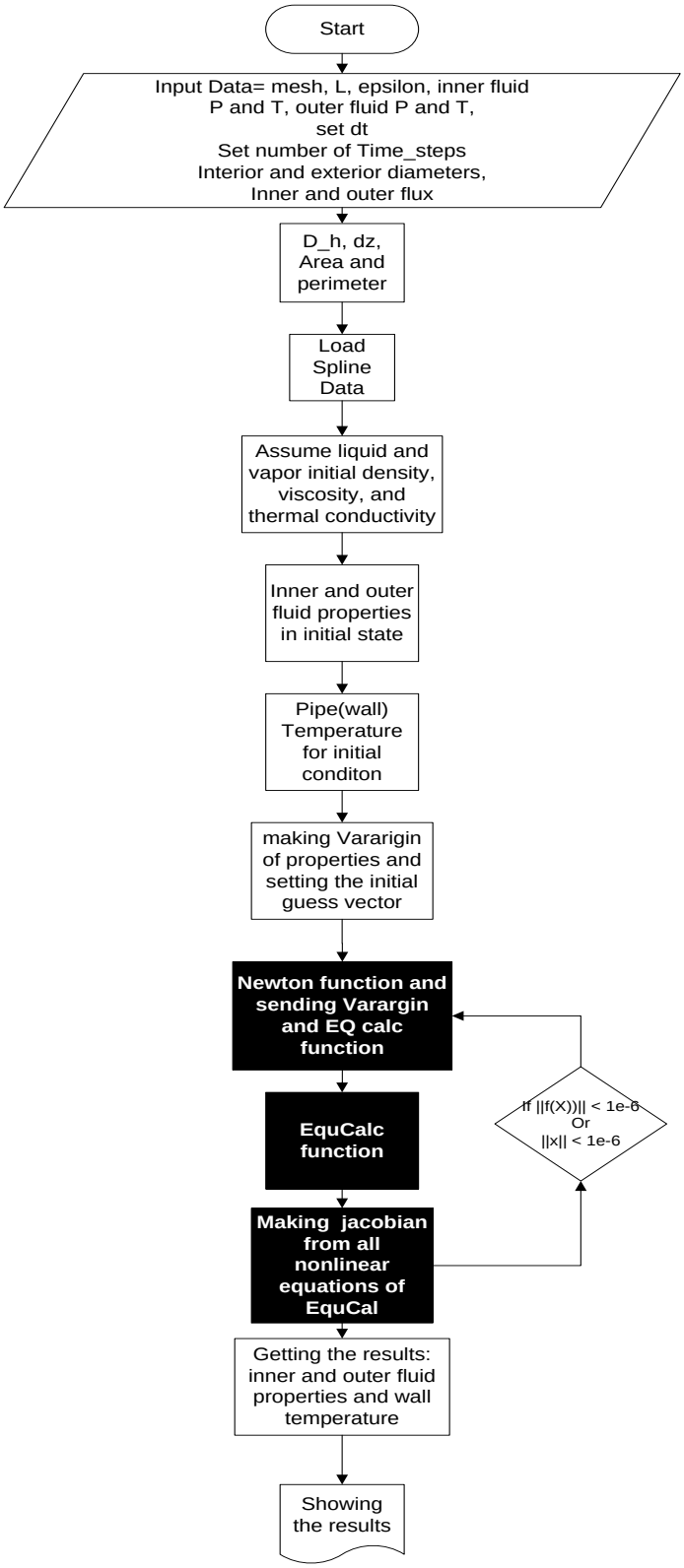

Flowchart 6- Structure of main.m file in the implicit codes.

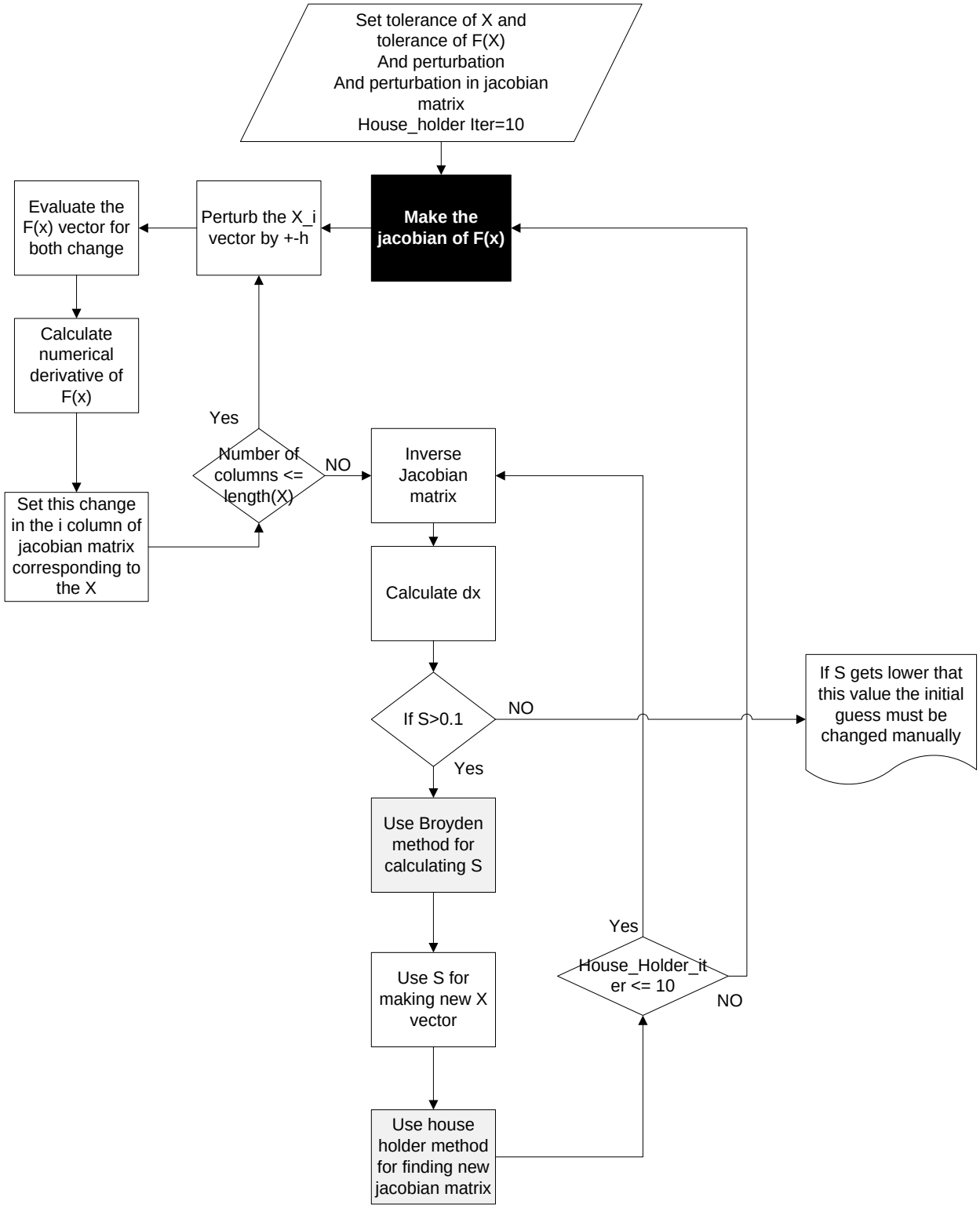

Flow chart 7- Newton function and its sub function jacobian which includes House Holder Broyden method.

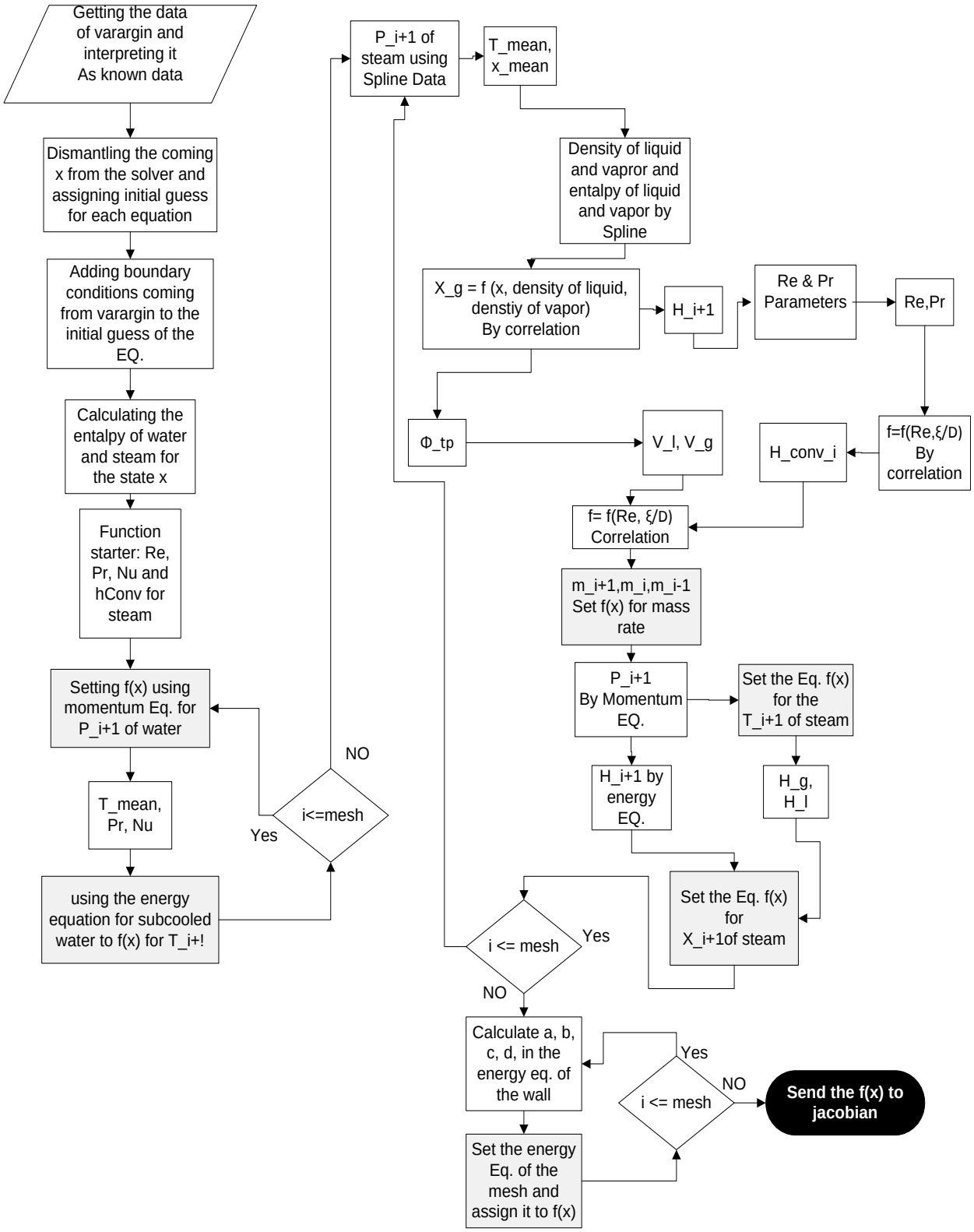
Getting the data of varargin and interpreting it As known data
Dismantling the coming x from the solver and assigning initial guess for each equation
Adding boundary conditions coming from varargin to the initial guess of the EQ.
Calculating the entalpy of water and steam for the state x
Function starter: Re, Pr, Nu and hConv for steam
Setting f(x) using momentum Eq. for P_i+1 of water
T_mean, Pr, Nu
using the energy equation for subcooled water to f(x) for T_i+!
i<=mesh
Yes
NO
P_i+1 of steam using Spline Data
T_mean, x_mean
Density of liquid and vapror and entalpy of liquid and vapor by Spline
X_g = f (x, density of liquid, denstiy of vapor) By correlation
H_i+1
Re & Pr Parameters
Re,Pr
f=f(Re,ξ/D) By correlation
H_conv_i
Φ_tp
V_l, V_g
f= f(Re, ξ/D) Correlation
m_i+1,m_i,m_i-1 Set f(x) for mass rate
P_i+1 By Momentum EQ.
Set the Eq. f(x) for the T_i+1 of steam
H_i+1 by energy EQ.
H_g, H_l
Set the Eq. f(x) for X_i+1of steam
i <= mesh
Yes
NO
Calculate a, b, c, d, in the energy eq. of the wall
Set the energy Eq. of the mesh and assign it to f(x)
i <= mesh
Yes
NO
Send the f(x) to jacobian

Flow chart 8- Structure of function "EquCalc".

1-7-2 Implicit codes structure

- The convergence criteria of Newton-Householder-Broyden method is set on both x and f(x) to be 10^{-6} *and* 10^{-6} respectedly.
- *"EquCalc"*, *"Newton"* and subfuncion *"jacobian"* in *"newton"* are the most important functions in the implicit codes.
- For the sake of beauty and order of codes, memory management functions of *"varargin"*,*"feval"and "nargin"* are implemented.
- All the information of main function will be sent to the *"EquCalc"* function using *"varargin"*.
- Introduced global variables are responsible for keeping track of some final results of structures in the function "EquCalc".
- In order to reduce the time, the piece wise polynomials of saturated vapor table are generated separately using our own spline codes and then they are stored in .mat matrixes which will be loaded at the beginning of the program. The value of these piecewise polynomials will be returned using Matlab build in function "*ppval*".
- The equations of all grids are assembled using following variables and arrangement: (for steady state the $F(M_Steam_i)$ doesn't participate.)

$$\begin{bmatrix} F(P_water_i)=0 \\ F(T_water_i)=0 \\ F(M_steam_i)=0 \\ F(P_steam_i)=0 \\ F(T_steam_i)=0 \\ F(T_pipe_i)=0 \end{bmatrix} \quad \text{When} \quad i=0:n-1$$

- The "TimeStruc" structure is for keeping the track of previous time properties.
- The "TempTime" is a cell which is used for keeping the track of "TimeStruc" structures of all time steps. This is the final result of simulation and will be saved at the end of program. The loading data for each unsteady state GUI is "TempTime" which contains all the simulation.

1-8 Results

The provided codes are categorized into separated folders, each devoted to a particular study. For each case, the specified condition aims at featuring work analysis rather than extra privilege.

1-8-1 steady state study of heat exchanger:

In this case, we are going to investigate all the properties of heat exchanger in its steady state condition. Following conditions are set for the model. The number of mesh for each layer is set to 20.

Water flux (kg/m2/s)	Steam flux (kg/m2/s)	Water T (c)	Water P (kpa)	Steam T (c)	Length (m)
250	80	22	1000	180	7

Inner pipe inner D (m)	Inner pipe outer D (m)	Outer pipe inner D (m)	Outer pipe (m)
8e-3	10e-3	14e-3	16e-3

Solution)

Table 1. Results of various methods for steady state condition.

water temperature(c)				water pressure(kpa)				water convection coefficient		
Explicit	Newton	HHB		Explicit	Newton	HHB		Explicit	Newton	HHB
22	22	22		1000	1000	1000		87.2966	87.2966	87.2966
24.1164	24.1166	24.1166		999.9	999.9	999.9		87.3085	87.3085	87.3085
26.2122	26.213	26.213		999.9	999.9	999.9		87.3203	87.3203	87.3203
28.276	28.2778	28.2778		999.8	999.8	999.8		87.3319	87.3319	87.3319
30.3108	30.314	30.314		999.7	999.7	999.7		87.3434	87.3434	87.3434
32.3185	32.3235	32.3235		999.7	999.7	999.7		87.3547	87.3547	87.3547
34.2984	34.3055	34.3055		999.6	999.6	999.6		87.3658	87.3658	87.3658
36.2495	36.2591	36.2591		999.5	999.5	999.5		87.3767	87.3768	87.3768
38.1721	38.1846	38.1846		999.5	999.5	999.5		87.3875	87.3876	87.3876
40.0672	40.0829	40.0829		999.4	999.4	999.4		87.3981	87.3982	87.3982
41.9356	41.9548	41.9548		999.3	999.3	999.3		87.4086	87.4087	87.4087
43.7776	43.8007	43.8007		999.3	999.3	999.3		87.4189	87.419	87.419
45.5935	45.6208	45.6208		999.2	999.2	999.2		87.429	87.4292	87.4292
47.3834	47.4153	47.4153		999.1	999.1	999.1		87.439	87.4392	87.4392
49.148	49.1848	49.1848		999.1	999.1	999.1		87.4488	87.4491	87.4491
50.8875	50.9295	50.9295		999	999	999		87.4585	87.4588	87.4588
52.6024	52.6499	52.6499		998.9	998.9	998.9		87.4681	87.4684	87.4684
54.2928	54.3461	54.3461		998.9	998.9	998.9		87.4775	87.4778	87.4778

55.959	56.0184	56.0184		998.8	998.8	998.8		87.4868	87.4871	87.4871
57.6012	57.667	57.667		998.7	998.7	998.7		**87.4959**	**87.4963**	**87.4963**
59.2183	**59.2909**	**59.2909**		**998.7**	**998.7**	**998.7**				

Steam temperature ©				Steam pressure (Kpa)				Outer fluid convection coefficient		
Explicit	Newton	HHB		Explicit	Newton	HHB		Explicit	Newton	HHB
180	180	180		1002.6	1002.6	1002.6		877.9328	879.0741	879.0741
179.9855	179.9865	179.9865		1002.3	1002.3	1002.3		867.9168	871.236	871.236
179.9767	179.9786	179.9786		1002.1	1002.1	1002.1		858.0353	863.4679	863.4679
179.9703	179.9733	179.9733		1001.9	1002	1002		848.261	855.7487	855.7487
179.9654	179.9693	179.9693		1001.8	1001.9	1001.9		838.5959	848.0815	848.0815
179.9613	179.9661	179.9661		1001.7	1001.8	1001.8		829.0414	840.4689	840.4689
179.9578	179.9635	179.9635		1001.6	1001.8	1001.8		819.5987	832.9132	832.9132
179.9548	179.9614	179.9614		1001.6	1001.7	1001.7		810.2685	825.4166	825.4166
179.9521	179.9595	179.9595		1001.5	1001.7	1001.7		801.0515	817.9809	817.9809
179.9496	179.9579	179.9579		1001.4	1001.6	1001.6		791.948	810.608	810.608
179.9474	179.9565	179.9565		1001.4	1001.6	1001.6		782.9583	803.2993	803.2993
179.9454	179.9553	179.9553		1001.3	1001.6	1001.6		774.0825	796.0563	796.0563
179.9435	179.9542	179.9542		1001.3	1001.5	1001.5		765.3205	788.8802	788.8802
179.9417	179.9532	179.9532		1001.3	1001.5	1001.5		756.6722	781.7721	781.7721
179.9401	179.9523	179.9523		1001.2	1001.5	1001.5		748.1372	774.7329	774.7329
179.9385	179.9514	179.9514		1001.2	1001.5	1001.5		739.7153	767.7637	767.7637
179.937	179.9507	179.9507		1001.1	1001.5	1001.5		731.4058	760.865	760.865
179.9356	179.95	179.95		1001.1	1001.4	1001.4		723.2083	754.0374	754.0374
179.9343	179.9493	179.9493		1001.1	1001.4	1001.4		715.122	747.2816	747.2816
179.933	179.9487	179.9487		1001.1	1001.4	1001.4		**707.1144**	**740.5712**	**740.5712**
179.9318	**179.9482**	**179.9482**		**1001**	**1001.4**	**1001.4**				

Condensed liquid				inner pipe temperature		
Explicit	Newton	HHB		Explicit	Newton	HHB
0.0029	0.0029	0.0029		**168.3571**	**168.3716**	**168.3716**
0.0087	0.0087	0.0087		168.4499	168.492	168.492
0.0144	0.0144	0.0144		168.4753	168.5446	168.5446
0.02	0.02	0.02		168.5022	168.5983	168.5983
0.0256	0.0256	0.0256		168.5301	168.6525	168.6525
0.0311	0.0311	0.0311		168.5587	168.7071	168.7071
0.0365	0.0365	0.0365		168.5877	168.7617	168.7617
0.0419	0.0419	0.0419		168.6171	168.8162	168.8162

0.0472	0.0473	0.0473		168.6467	168.8705	168.8705
0.0525	0.0526	0.0526		168.6765	168.9248	168.9248
0.0578	0.0578	0.0578		168.7066	168.9788	168.9788
0.0629	0.063	0.063		168.7369	169.0328	169.0328
0.068	0.0681	0.0681		168.7674	169.0866	169.0866
0.0731	0.0732	0.0732		168.7982	169.1402	169.1402
0.0781	0.0782	0.0782		168.8291	169.1937	169.1937
0.0831	0.0831	0.0831		168.8603	169.2471	169.2471
0.088	0.088	0.088		168.8917	169.3003	169.3003
0.0929	0.0929	0.0929		168.9232	169.3534	169.3534
0.0977	0.0977	0.0977		168.955	169.4064	169.4064
0.1024	0.1025	0.1025		**168.8987**	**169.3745**	**169.3745**

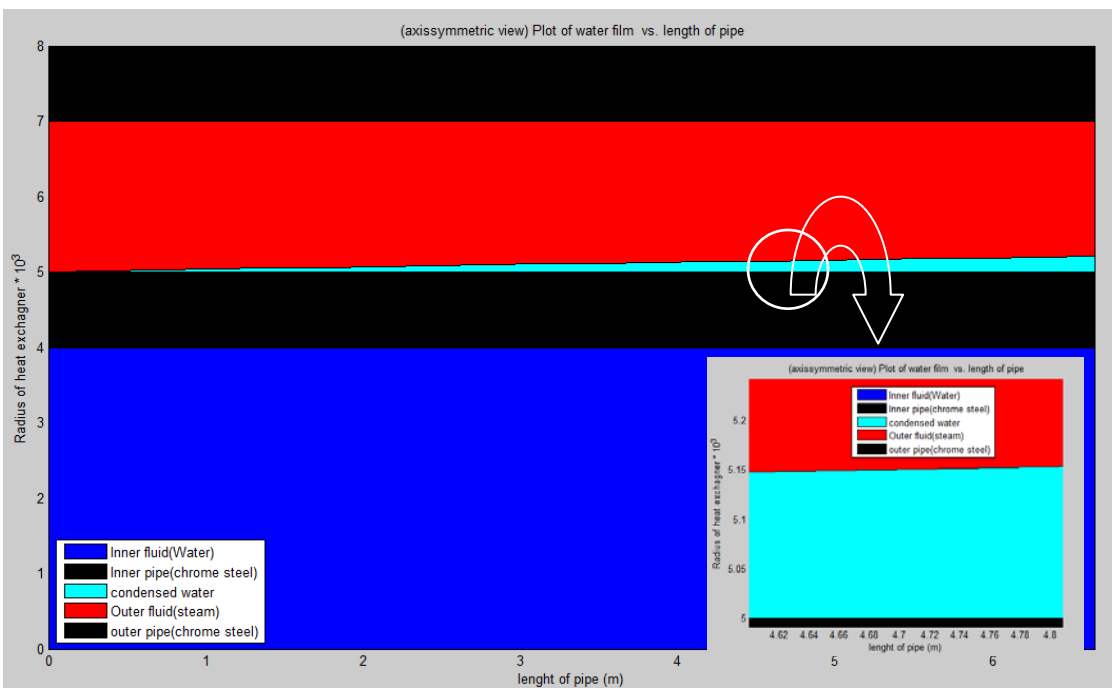

Fig4 .Schematic illustration of steady state results in Matlab. Use zoom object for detailed view.

1. As we proceed further along the pipe, the amount of condensed liquid in the outer pipe goes up, therefore, because of difference between the velocity of condensed liquid and steam, concealment of pipe perimeter by condensate water and also reduction in amount

of steam, the heat transfer coefficient of steam decreases, this is manifested in the obtained data.

2. With the assumption of constant water viscosity and thermal conductivity in the inner pipe, as the temperature increases, Cp increases; therefore, the increase in Pr and Nu and as a result convection heat transfer coefficient (hConv) is expected. The attained results give evidence for this statement.

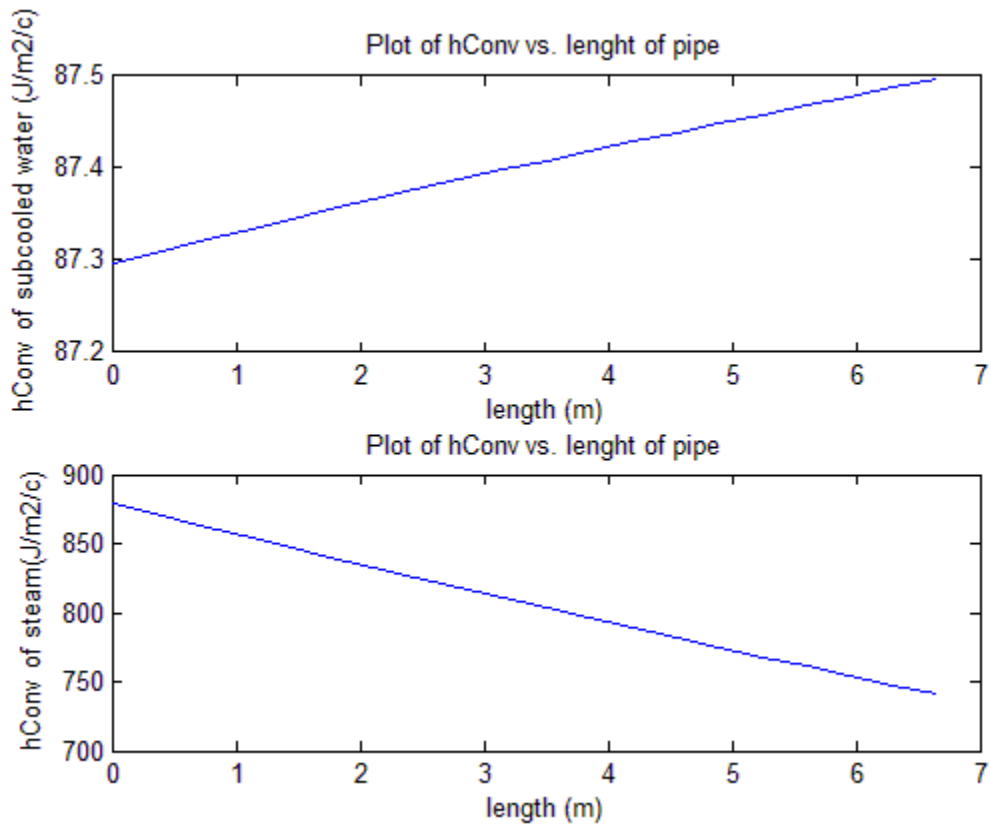

Fig5. Curves of convection heat transfer coefficient for inner and outer fluids.

3. We always expect the subcooled water temperature to rise but the very important point is that this rising in temperature decreases along its profile so its plot shows curvature like behavior. There are two theoretical reasons for this statement. The first is the reduction of

convection heat transfer coefficient, which was explained above, and the second reason is the reduction in the difference between fluids and pipe wall temperature.

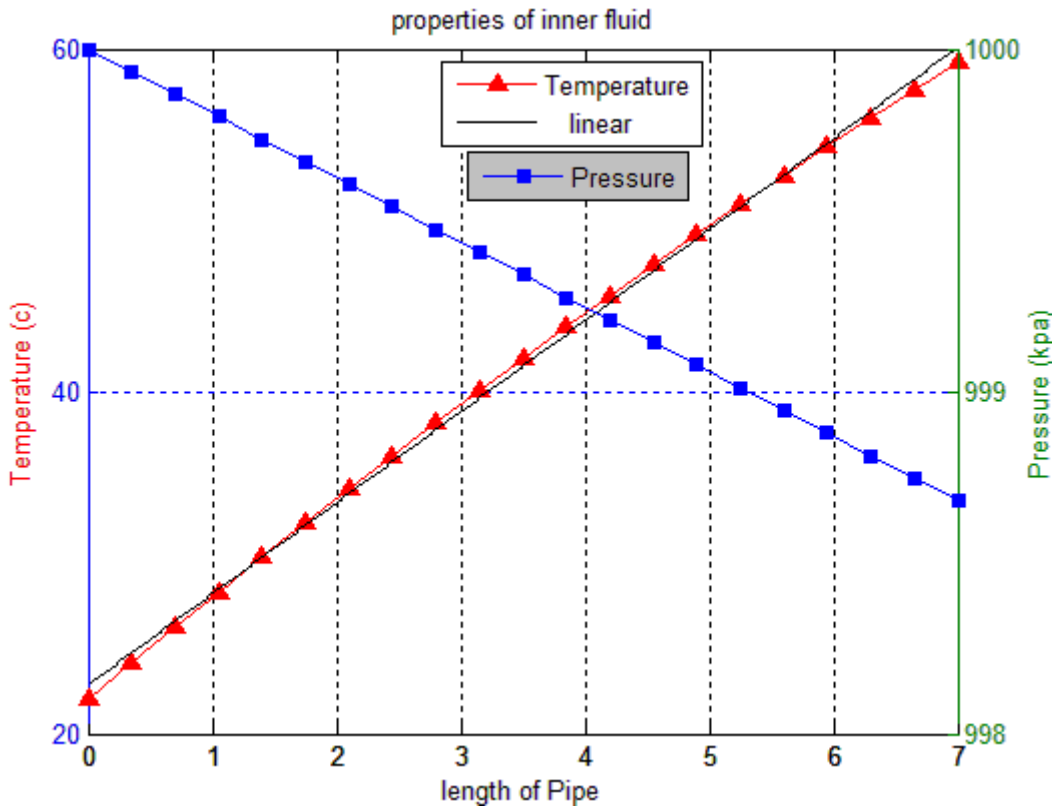

Fig6. Water temperature and pressure profile in its steady state in steady state condition.

4. The rate of increasing water temperature decreases and as a result heat transfer between steam and water decreases, hence, we expect other parameters increasing rate also decreases, such as quality and steam temperature.

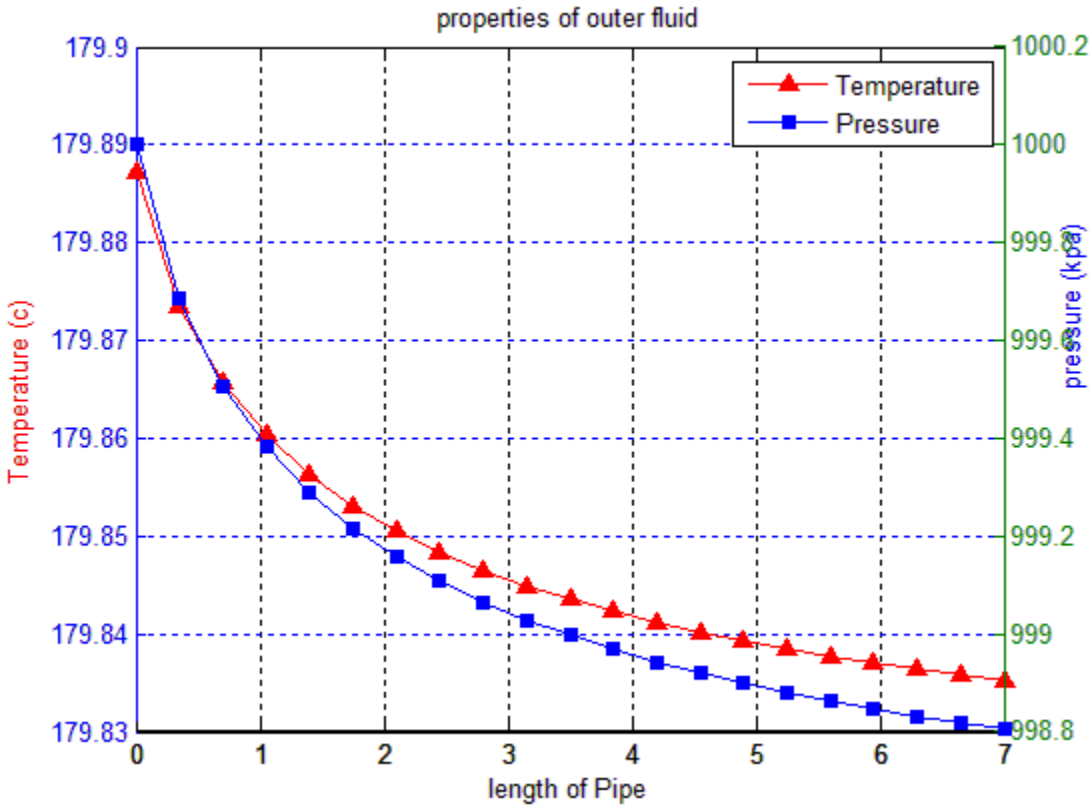

Fig7. Steam temperature and pressure profile in its steady state condition.

5. The temperature of wall, in this case, goes up along the pipe because the steam temperature doesn't change intensively here and yet, the temperature of water increases, so the temperature of inner pipe wall also increases but notice should be given that this is not always the case. This assertion is presented in all data except the first and last data. These data are shown with red color. This disharmony can be attributed, confidently, to the overlooked lateral heat transfer of wall with environment. This neglecting represents itself in the coefficient matrix of inner pipe wall which contains no expression for lateral heat transfer.

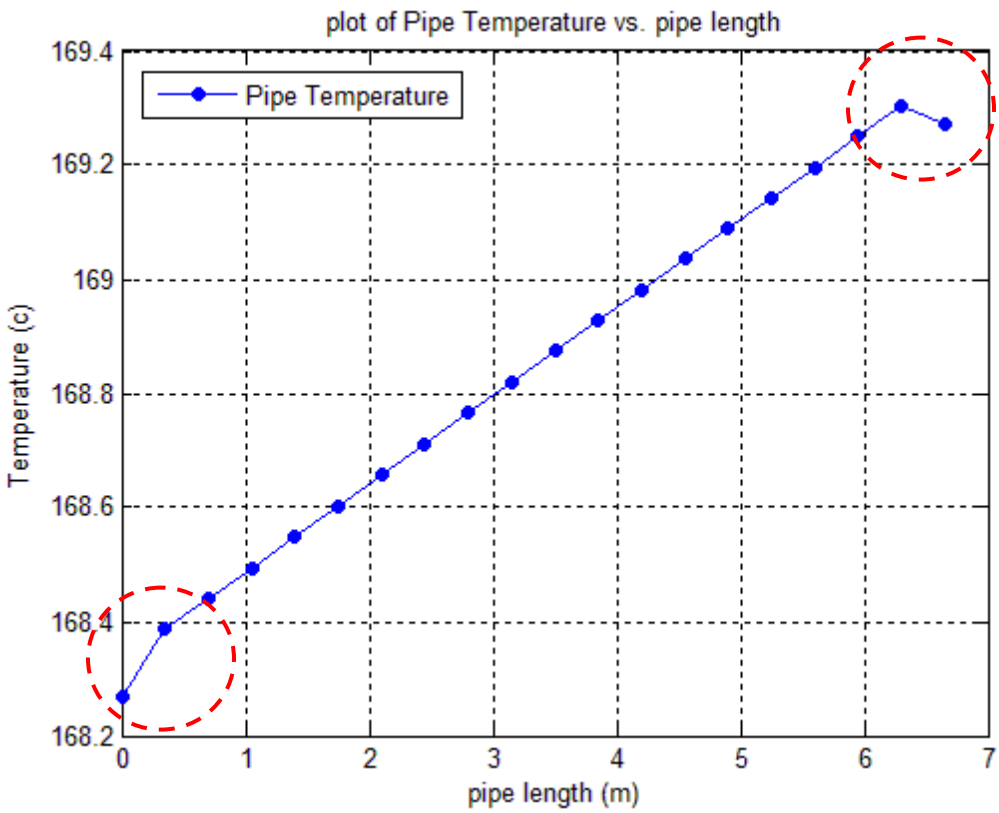

Fig8. Temperature of pipe wall, the red circles, as it was explained, shows the effect of neglecting lateral heat transfer.

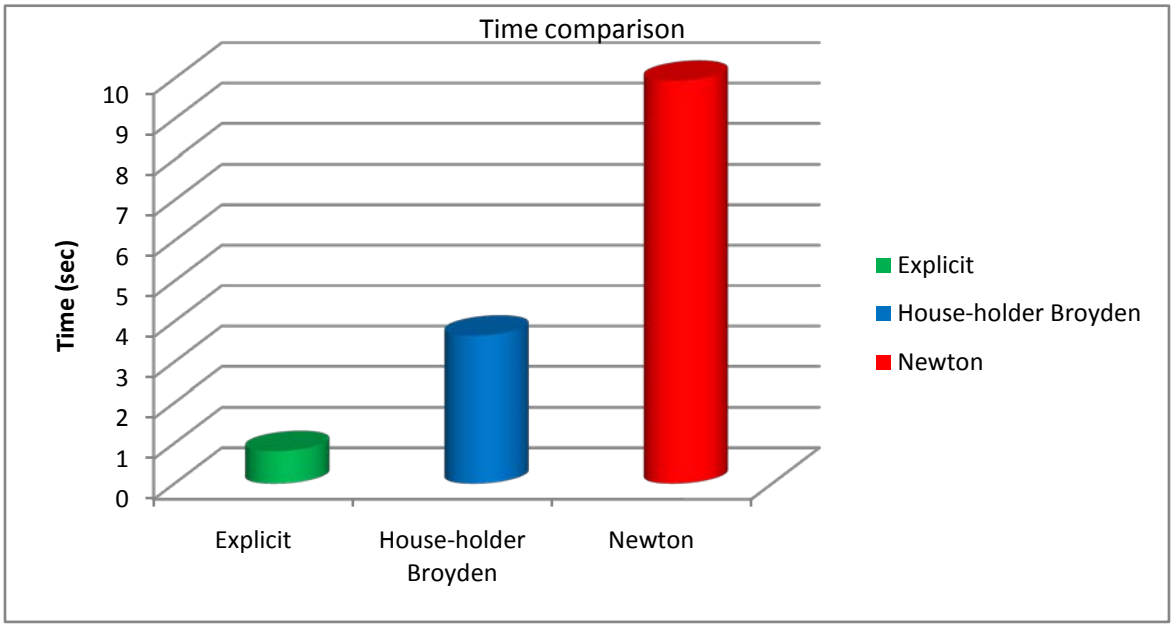

Fig9. Comparing the time of convergence between different methods.

1-8-2 Study the effect of various parameters on steady state results:

In this case, the impact of changing different parameters of heat exchanger on the profile of subcooled water temperature and pressure and steam temperature, pressure and quality is investigated. For this purpose, we set a default condition and then change one variable to see the results. The number of mesh for each layer is set to 20.

Water flux (kg/m2/s)	Steam flux (kg/m2/s)	Water T (c)	Water P (Kpa)	Steam P (Kpa)	Length (m)
300	180	22	500	500	5

Inner pipe inner D (m)	Inner pipe outer D (m)	Outer pipe inner D (m)	Outer pipe (m)
8e-3	10e-3	14e-3	16e-3

Default Angle (degree)
0

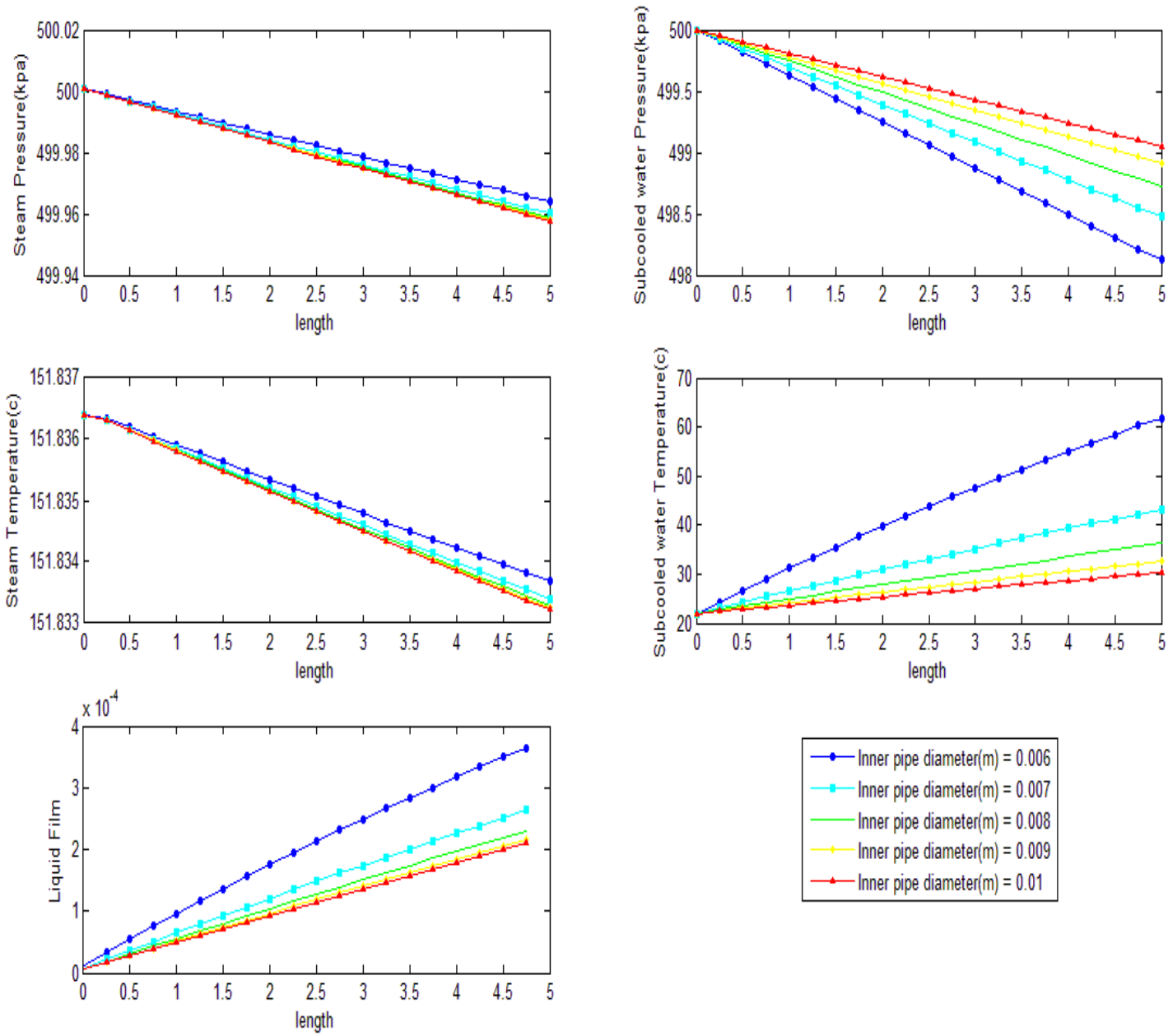

Fig10. Effect of Inner pipe diameter on the heat exchanger steady state condition

Increasing the inner pipe diameter, at constant fluxes, means the increase in flow rate of water, reduction in the outer diameter and, thus, decline in the flow rate of steam. At this circumstances, the amount of heat, transferred to water, have to scatter in more water, so the temperature of water is expected to increase less. Yet, reciprocally, the reduction in steam flow rate causes its temperature and pressure to decrease more. The worst scenario is that the heat transferred to water will remain constant, although this is won't then this reduction in the temperature of steam will be accompanied with an insignificant reduction in the amount of liquid condensate.

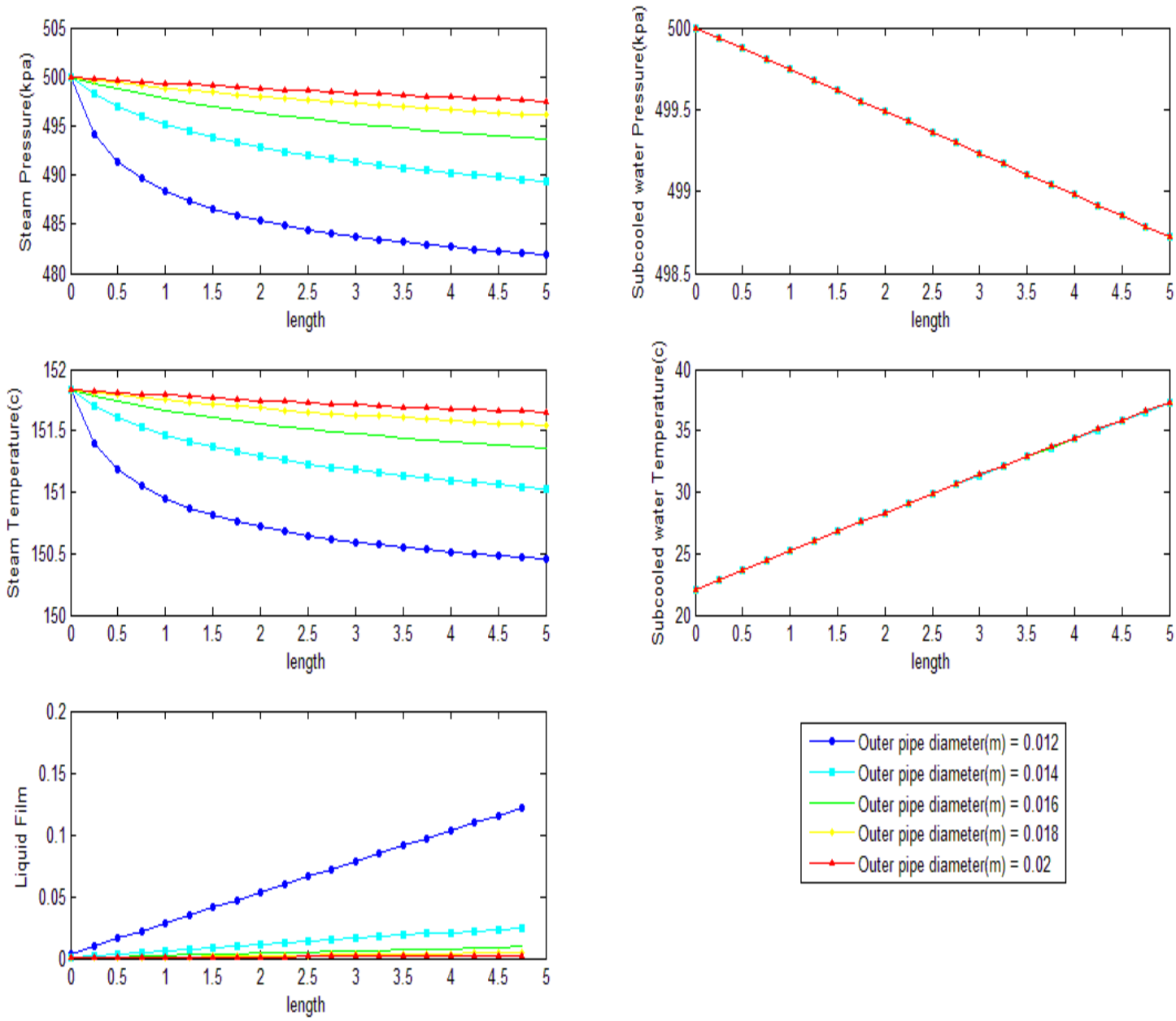

Fig11. Effect of Outer pipe diameter on heat exchanger steady state condition

Increasing the outer pipe diameter, at constant fluxes, boosts the amount of steam, so for a specific heat taken from steam, the amount of produced condensate diminishes. On the other hand, outer pipe enlarging evokes reduction in pressure drop and consequently decline in temperature of steam. Nevertheless, since the amount of heat transferred to water is not function of outer pipe diameter (assuming no heat transfer with environment), the temperature of water doesn't change intangibly and remains approximately unvaried.

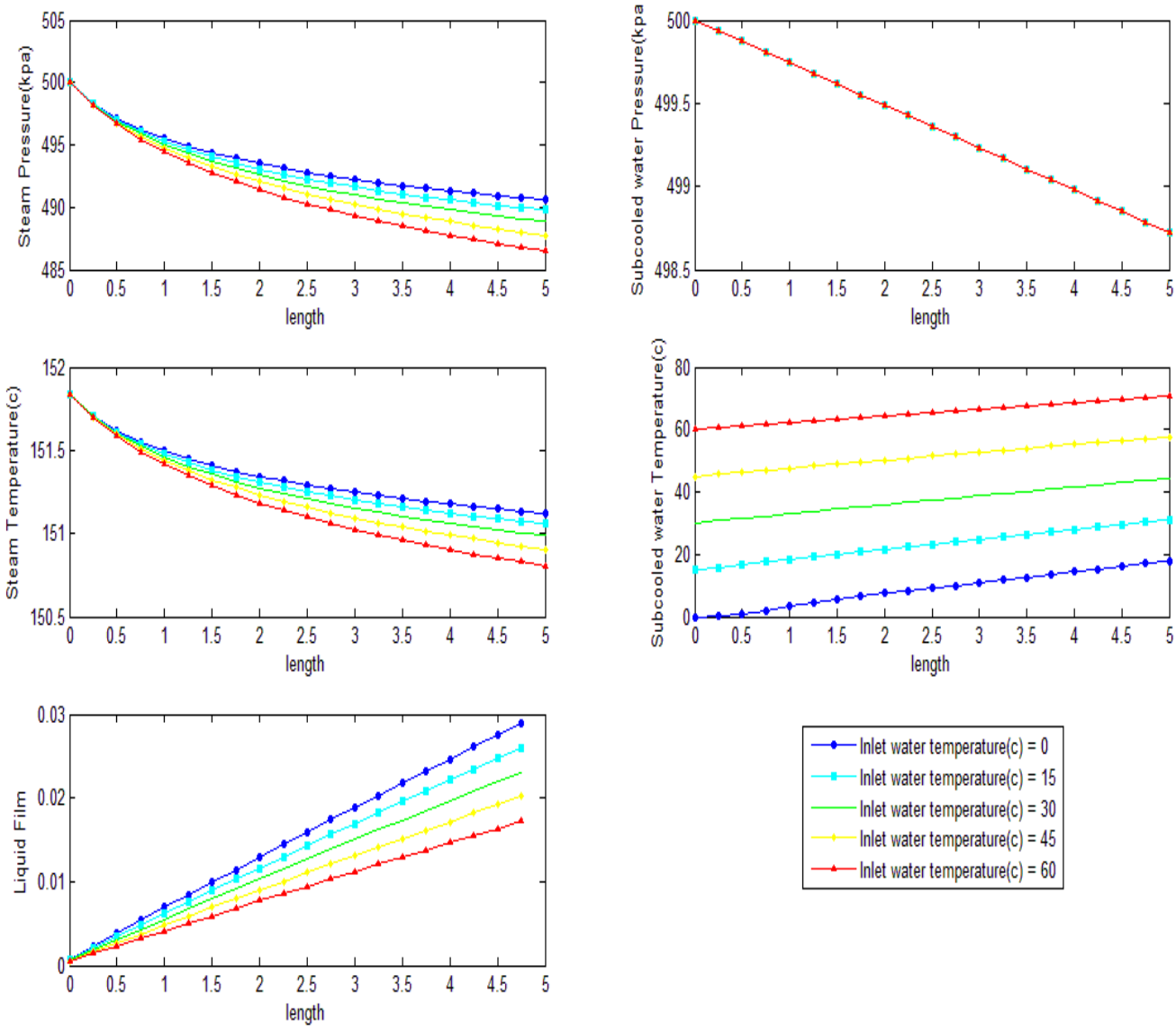

Fig12. Effect of Inlet subcooled water temperature on heat exchanger steady state condition

Plot of this case are very similar to that of water flux, and here, because of increasing temperature, constant convection heat transfer coefficient and reduction in temperature difference, the temperature of pipe wall increases and consequently, the amount of condensate reduces.

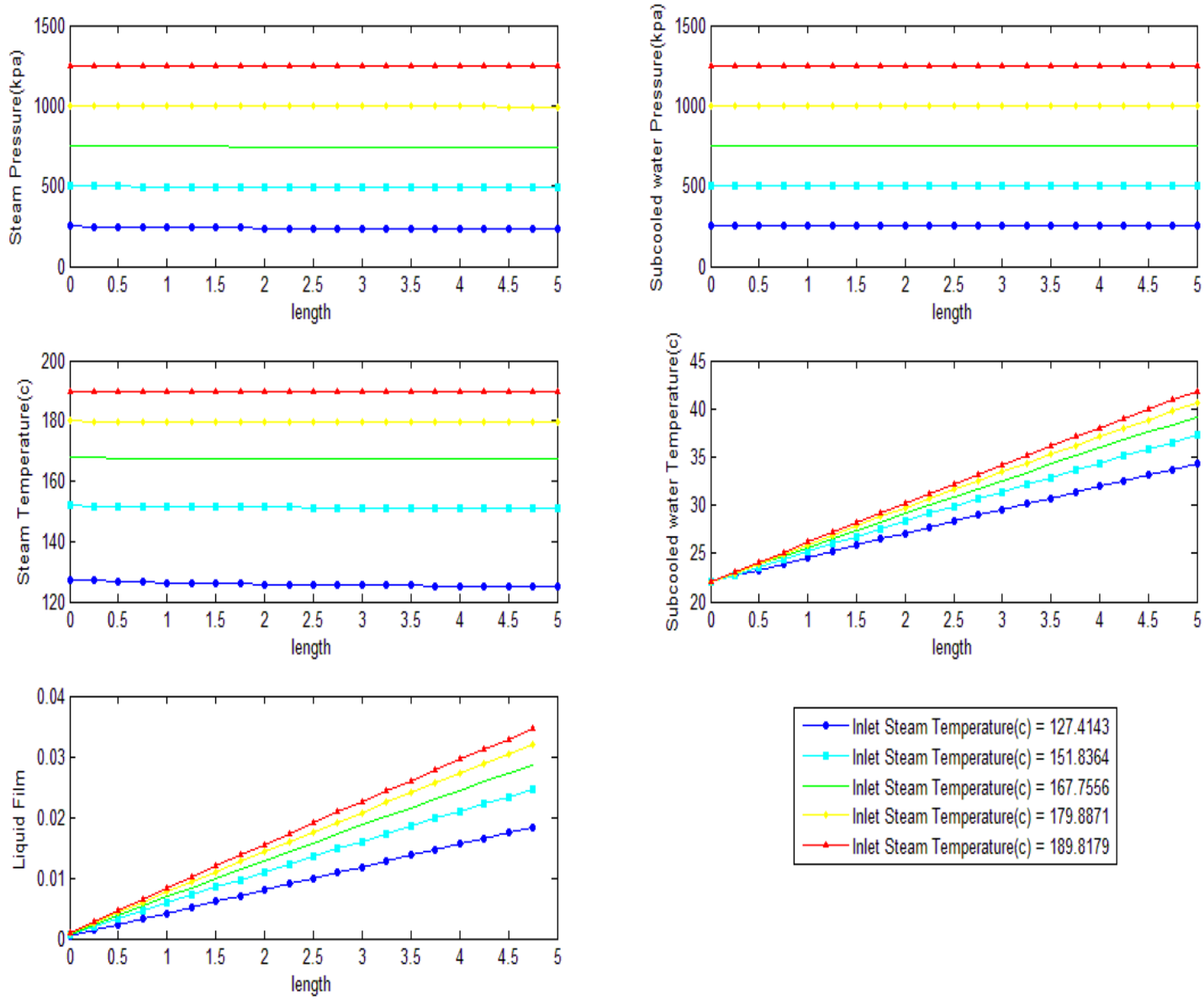

Fig13. Effect of Inlet saturated steam temperature on the heat exchanger steady state condition

If the steam temperature increases, the difference between temperature of steam and subcoolded water increases and also its convection coefficient grows, therefore, the transferred heat to water goes up and its temperature rises, also, as the flow rate and other parameters are constant, steam looses more energy; thus, we expect more condensation in the outer pipe.

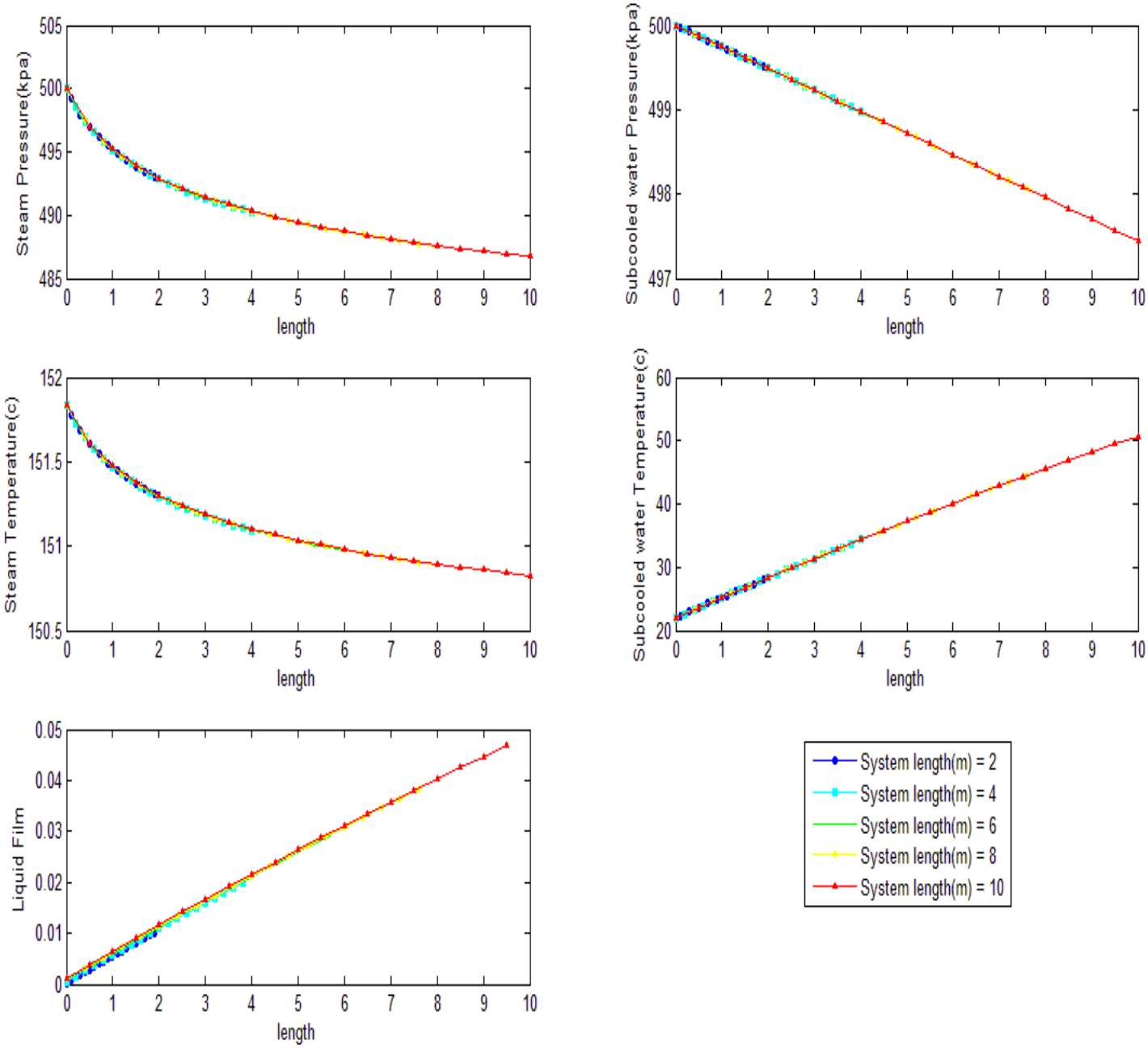

Fig14. Effect of heat exchanger's length on its steady state condition

Obviously, pressure of subcooled water drops in linear trend by enlarging the heat exchanger's length but unlike water, steam figures show a curve like trend. This is due to uprising condensation of saturated steam, which reduces the heat convection coefficient of outer fluid; however the energy that subcooled water gains, remains the same. The important point is that by increasing the length of pipe, because the amount of condensation increases, the rate of change in all qualities declines.

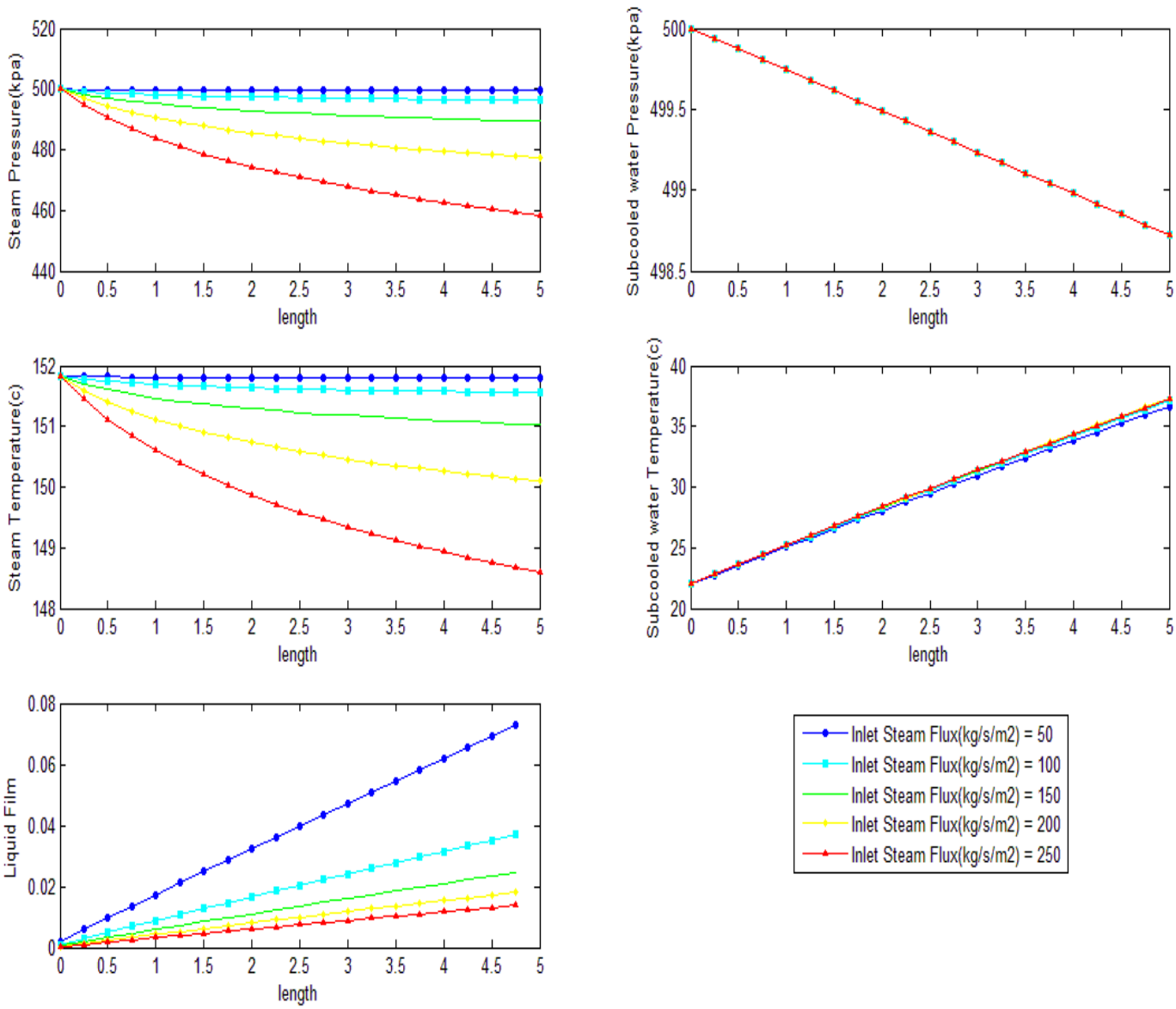

Fig15. The impact of Inlet saturated steam flux on various data in steady state condition

By increasing the flux of steam, its pressure drop goes up and thus, its temperature drop grows. On the other hand, both, Re number and convection heat transfer coefficient increases, therefore, the temperature of inner pipe wall rises but it has no significant effect on the heat transferred to water. Therefore the temperature of water won't increase considerably; however, because of high temperature in wall, the amount of produced condensate diminishes.

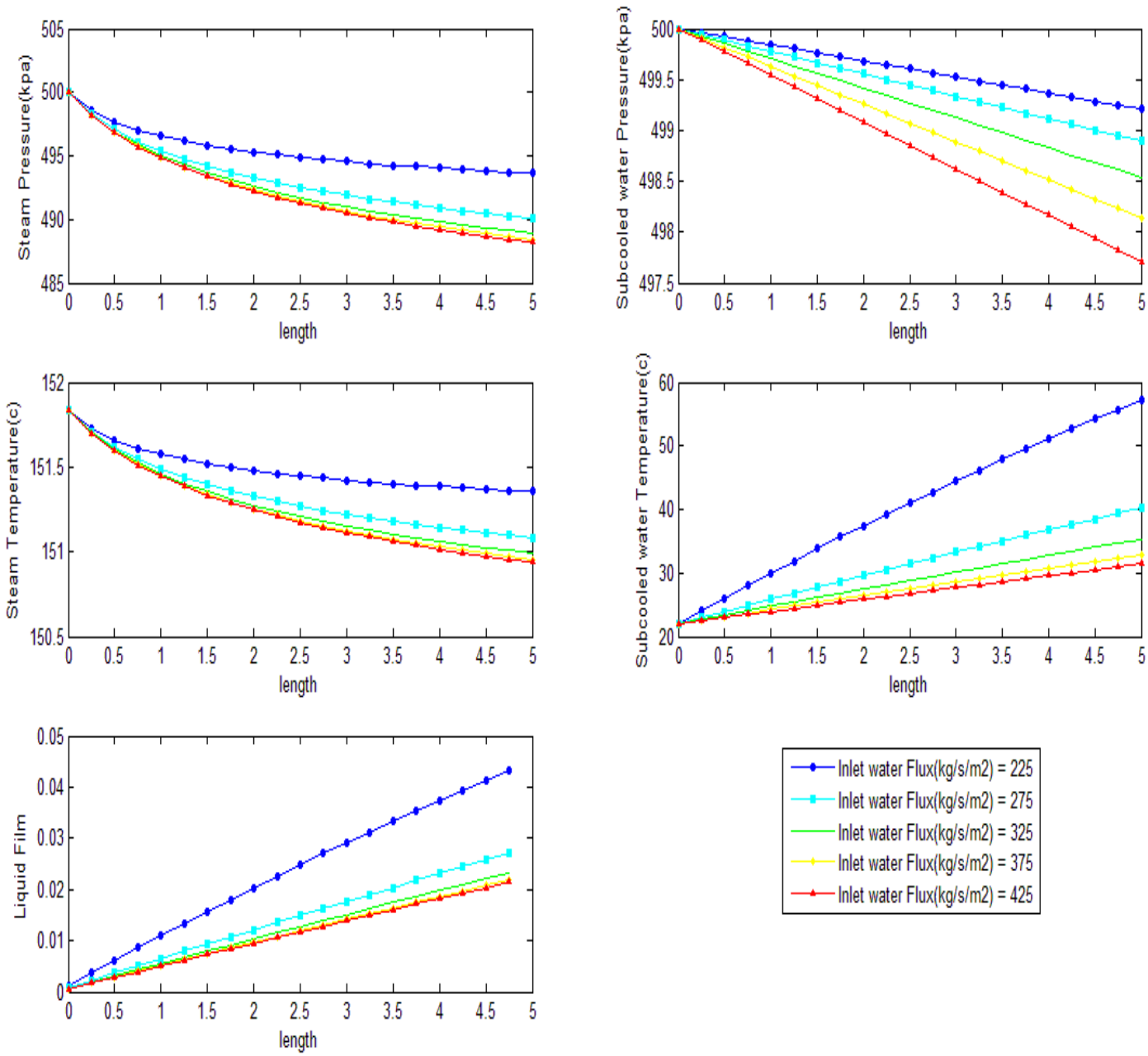

Fig16. Effect of Inlet water flux on various data in steady state condition

Increasing in flux of water means increase in its flow rate. This augment in the flow rate, intensifies pressure drop of subcooled water, yet, the heat transferred to water will be distributed in more water, hence, reduction in the temperature of water will be mitigated.

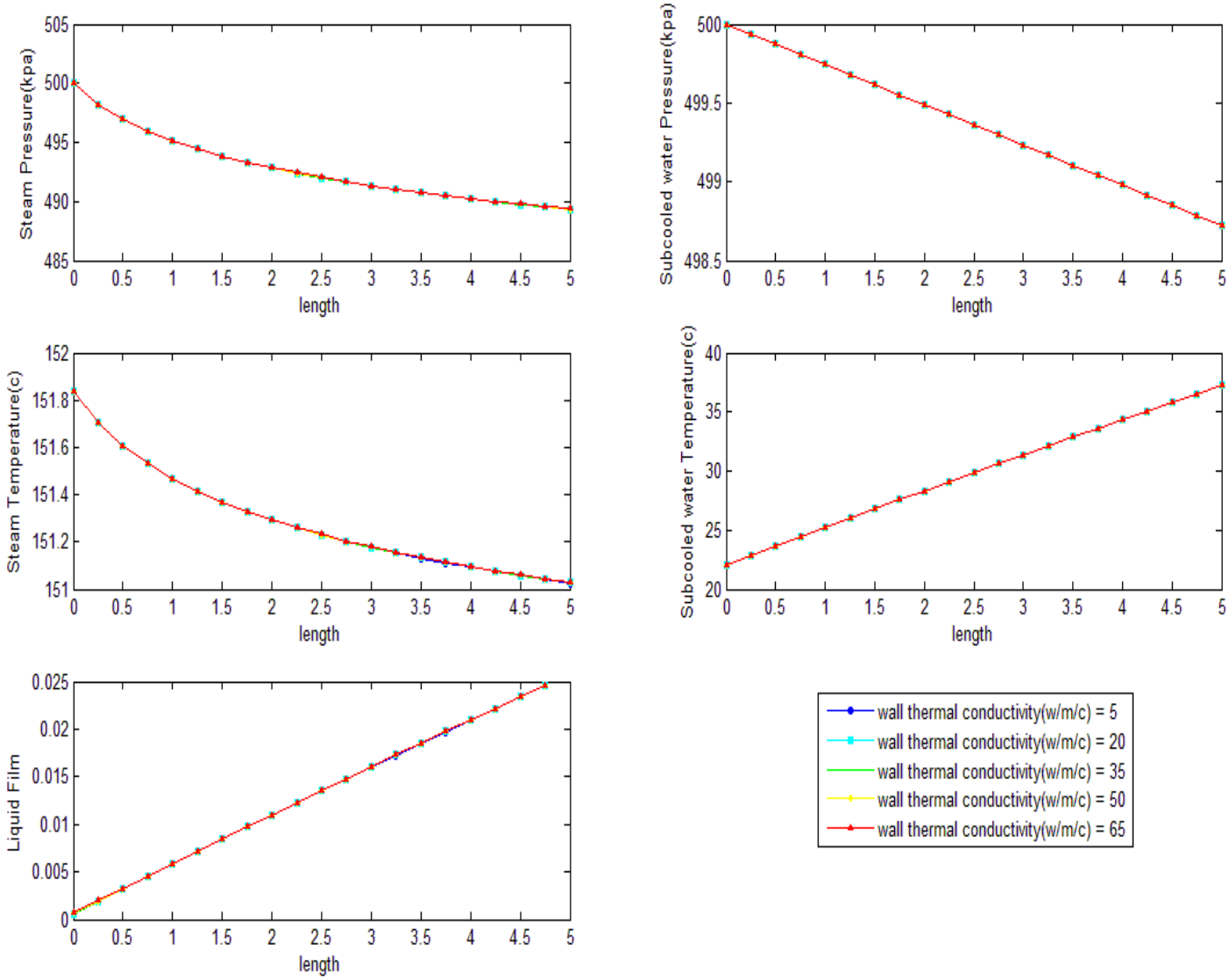

Fig17. Effect of having one dimensional wall on steady state condition

Clearly, because we have assumed that inner pipe wall is one dimensional and no heat convection with environment happens, the energy that inner pipe wall gains from steam, it also gives to the water. In the assumption of one block center point for the inner pipe wall, practically, the heat transfer between inner pipe water and steam happens directly. This means that metal type and thickness of it won't affect the results, we have gone deep into details for this subject in the environment case analysis.

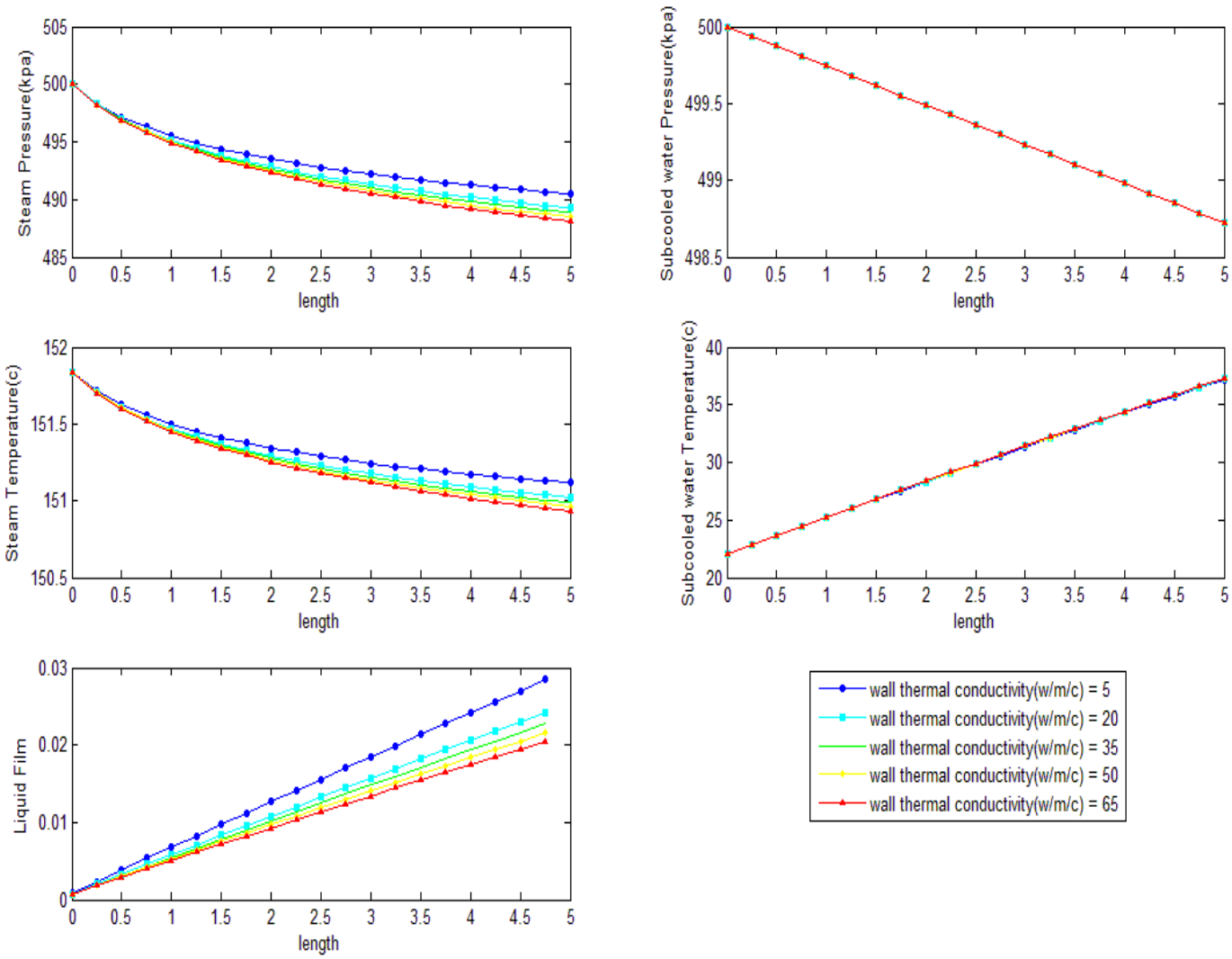

Fig18. Effect of two dimensional walls on various results in steady state condition

As the thermal conductivity of pipe increases, its thermal resistivity decreases and it's ceil and bottom temperature get close. On the other hand, since convection heat transfer coefficient of steam is far more than that of water, it is expected that the temperature of pipe wall be closer to steam temperature (in common conditions). Therefore, the increase in pressure drop and temperature and also, reduction in produced condensate is witnessed.

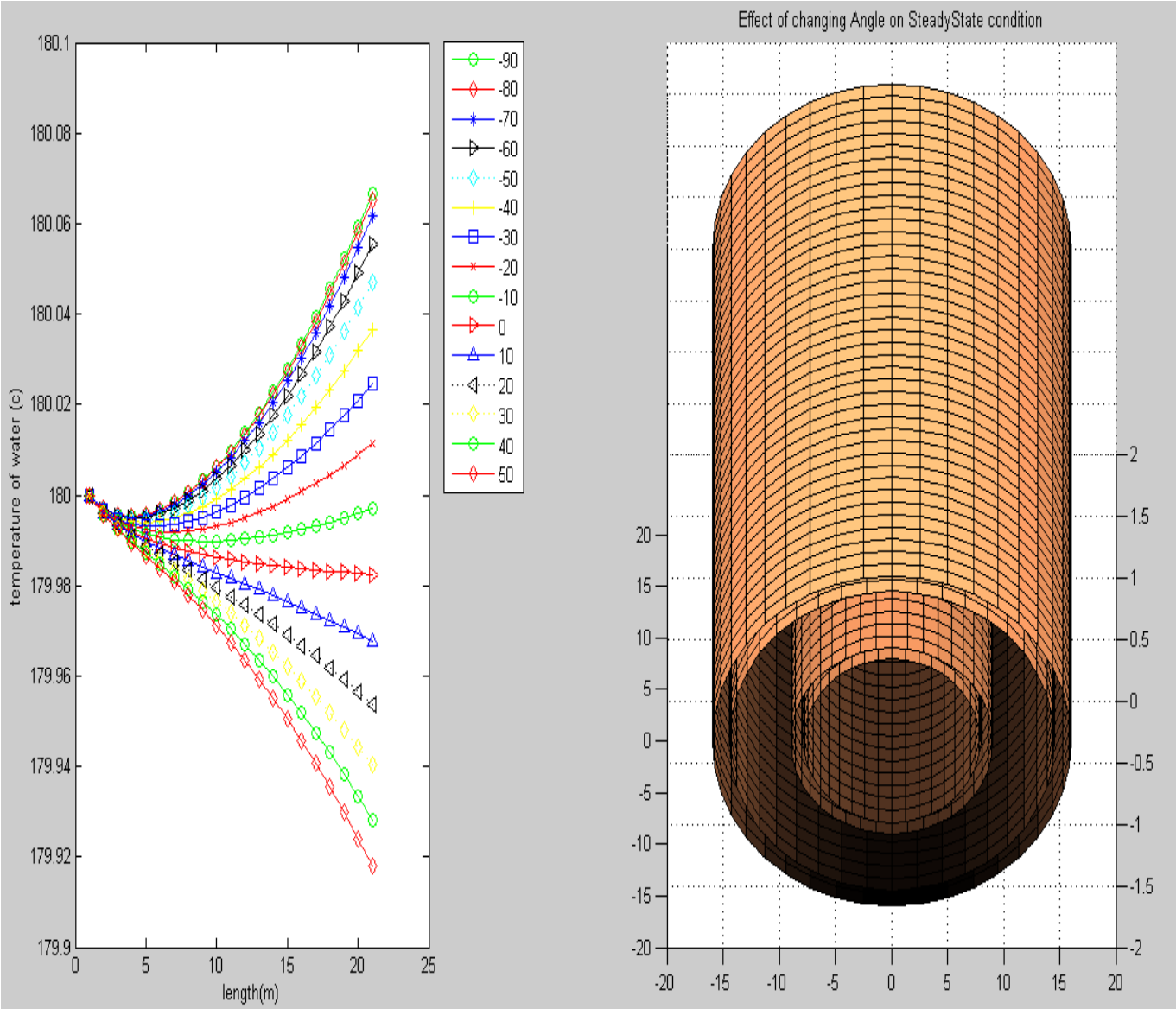

Fig19. Effect of changing angle of heat exchanger on water temperature along the pipe

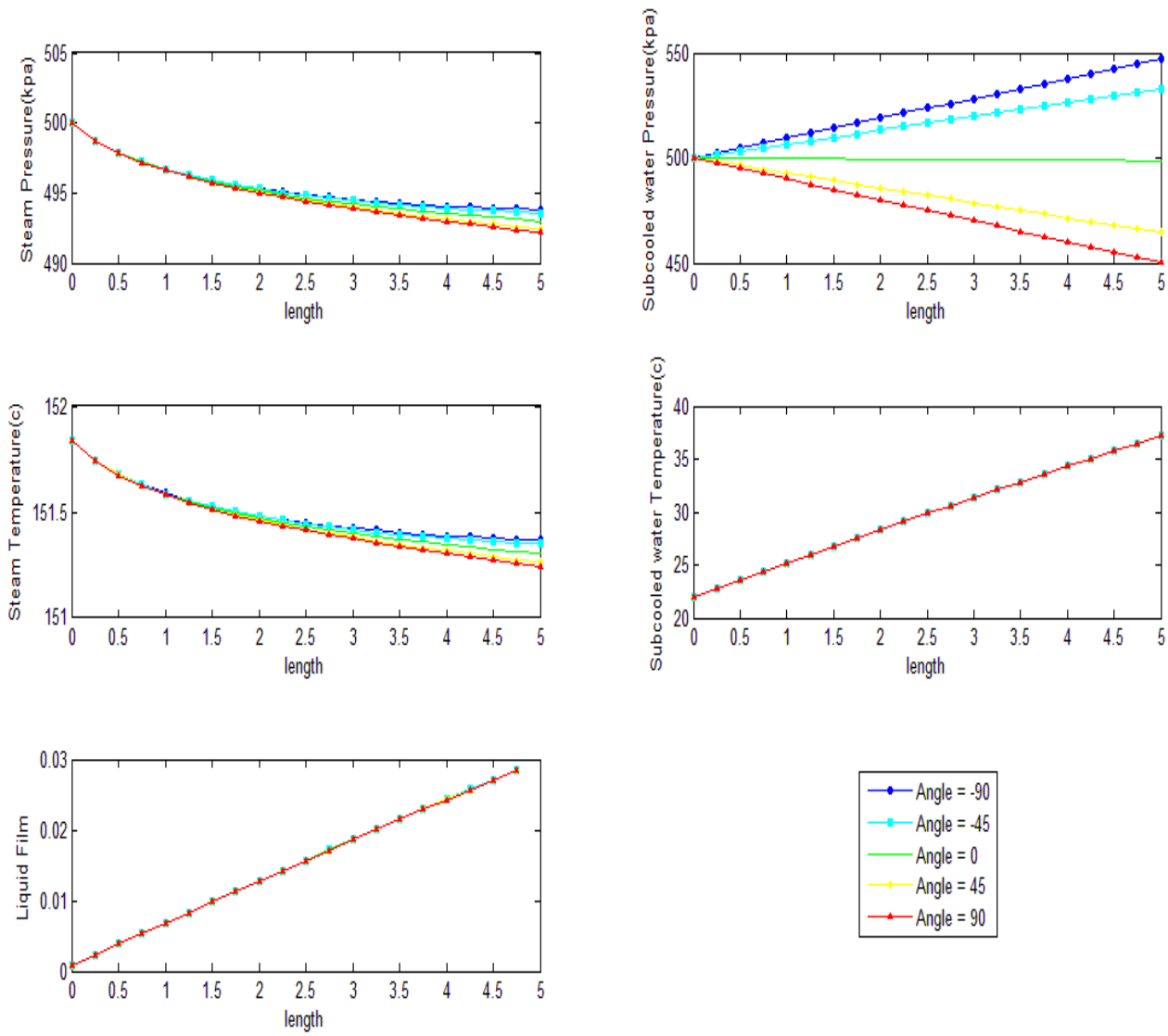

Fig20. Effect of changing angle of heat exchanger on various parameters in S.S condition

Along the outer pipe, accumulation of pressure drop caused by friction and, also, changing in pressure due to angle variation is witnessed. However, these factors collaborate when angle is positive which makes pressure drop even more, but nullify each other's effect when angle is negative which mitigates the pressure drop. So the outlet pressure is anticipated to be higher, equal, or less than the inlet pressure for both steam and water. The attained results prove these statements. However, although this pressure drop in steam, accompanies temperature drop in it, but little change in quality of steam, induces no further growth in the temperature of water. The results, also, show these concepts. Increasing the inlet temperature of steam means increasing its pressure and hence, growth in its convection coefficient and more difference between its temperature and temperature of water. Therefore, the amount of heat transfer to water augments which ends up in more liquid condensate.

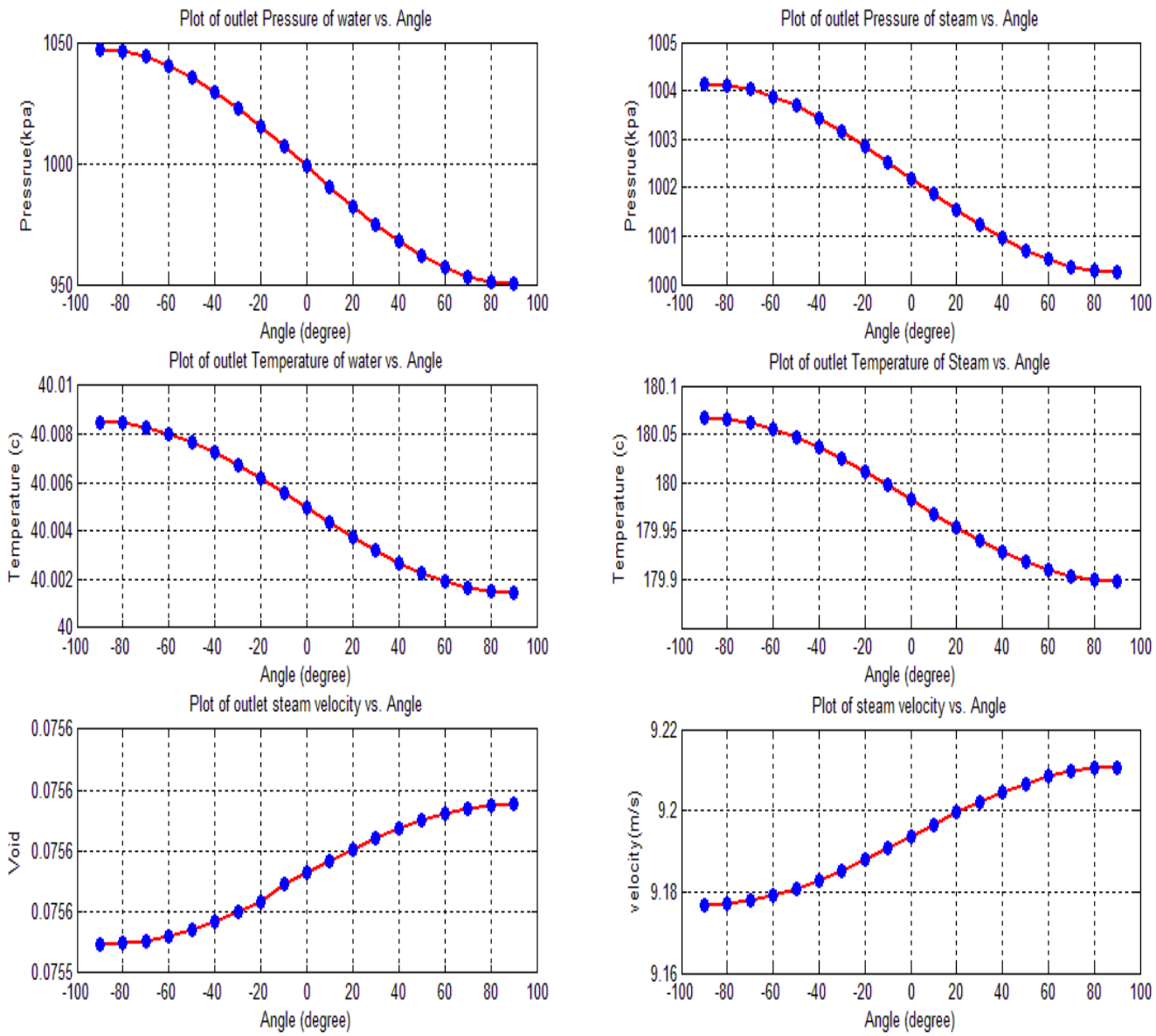

Fig21. Effect of changing angle of heat exchanger on various parameters in outlet section

Any variation in angle will be, conspicuously, registered to subcooled water pressure. Also, pressure drop, though with less intensity, occurs in the steam. This variation in angle doesn't change water temperature tangibly, but steam temperature profile shows variation in harmony with its pressure drop, so we expect the water temperature to be increased but in an intangible manner, which has happened here.

1-8-3 Study of unsteady state behavior of Co-current flows:

In all previous cases, the steady state condition was explored in details. In this case, some obvious differences exist. The most important one is the advent of time in the equations, which requires knowing the properties of the fluids in the previous time.

The objective of this case is to investigate the unsteady state behavior of heat exchanger. For attaining this aim, two different initial conditions are considered and the animated results are explained. Heat transfer with environment is neglected in this case.

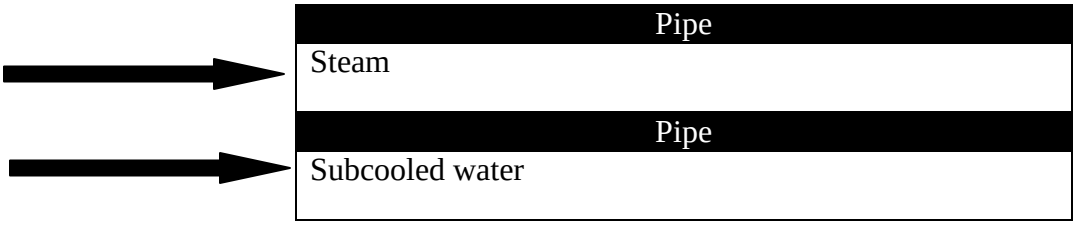

1. In the program after the initial condition is set, the equations will be solved for the specified Δt and the acquired answers will be stored in a structure ("TimeStruc"). Therefore, the properties of the fluids which are needed in the next interval in the equations can be retrieved from this structure.
2. For setting the initial condition of unsteady state two assumptions have been made:
   A. Uniform condition: in this condition, it is assumed that the temperature of all the grids in the inner and outer pipe fluids is equal to its inlet fluid temperature and also, the fluids are static, initially.
   B. Pulsed steady state: in this condition, it is assumed that the system, after a while however, has reached the steady state condition, therefore, all profiles such as temperature, pressure and liquid condensate film is determined. The pulse is set on an important parameter like steam or water flux. We have set the pulse to be on the water flux and the steady state answer of this system, which will be an unsteady state initial condition for the actual problem, is used for simulating the problem.
3. In the explicit method, choosing the appropriate Δt is very crucial for convergence and the chosen Δt is constrained to the governing equations and the method which is used for

discritizing them. Furthermore, if the conduction is supposed to be considered, the predicament, even, gets worse and not every Δt can be utilized.

4. Because the behavior of equations for diverse initial and boundary conditions and even, various solving methods are different, seeking for a suitable Δt and Δz can be, sometimes, cumbersome. Similarly, implicit method leads to singularity and ill condition matrixes if jacobian matrix is not handled properly.

1-8-3-1 case study

Water flux (kg/m2/s)	Steam flux (kg/m2/s)	Water T (c)	Water P (kpa)	Steam T (c)	Length (m)
350	150	10	1000	180	7

Inner pipe inner D (m)	Inner pipe outer D (m)	Outer pipe inner D (m)	Outer pipe (m)
8e-3	10e-3	14e-3	16e-3

Number of mesh for each layer	Time intervals
100	0.3 seconds

Solution)

For unsteady cases, animations of the simulation are provided in .mat matrixes which will be loaded at the beginning of the provided GUI associated with that case.

Run Time for explicit method for 100 mesh	Run Time for Implicit method for 20 mesh	Runtime for Crank-Nicholson method for 20 mesh
310.067164	436.507468	490.255809

As we know, fluids convey pressure pulse too quickly through them, therefore its interval is too short and this is less than selected Δt in the programs. The provided animations advocate this concept very well.

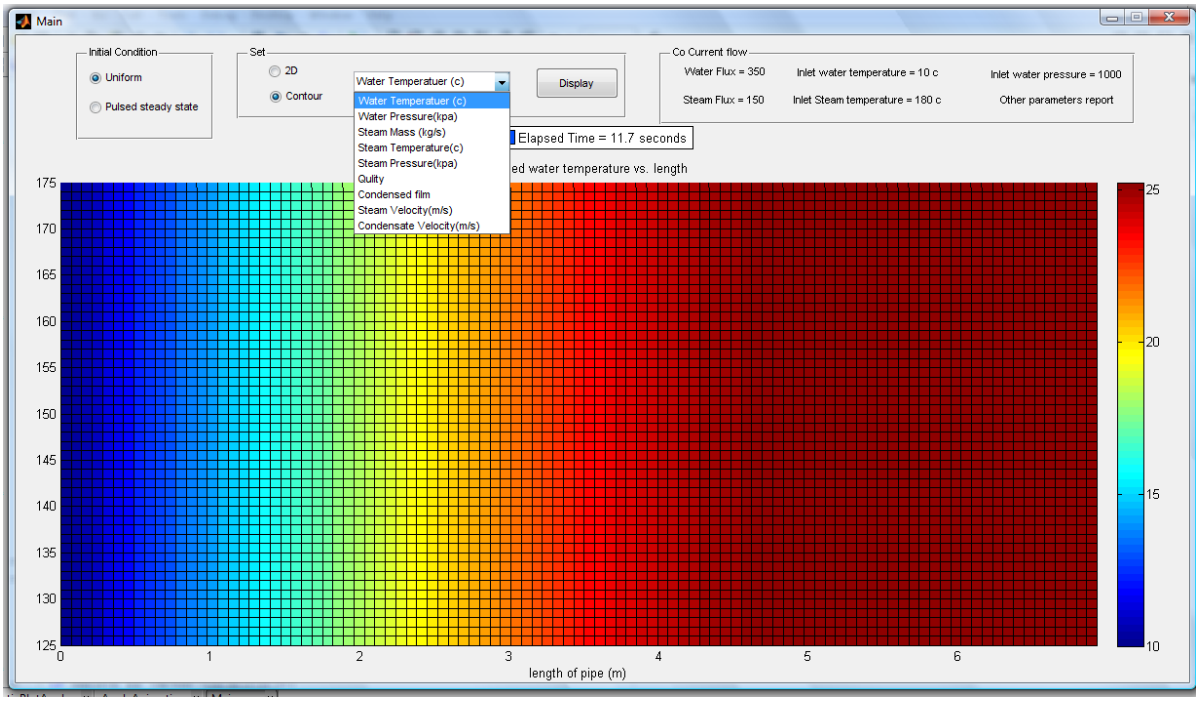

Fig22. The moving effect of water temperature for uniform initial condition after 11.7 seconds.

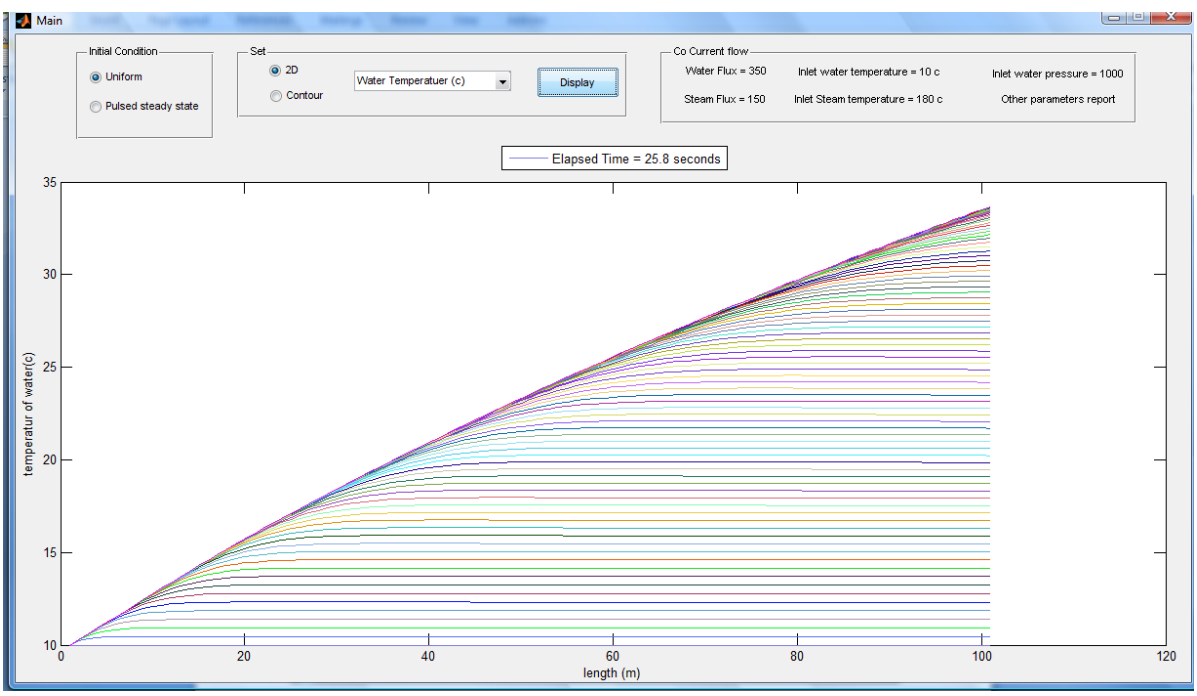

Fig23. After some moments, the steady state is reached. ***The blinking*** *line shows the steady state situation.*

Time of reaching steady state is the time when no parameter will change afterwards. Determining this time for various parameters of the animations is possible. For this purpose, a

zoom object is added to the GUI which can be used for pursuing the unsteady state curves of 2D graphs. It is obvious that the pressure will be pioneer in reaching steady state condition. The mass flow rate of steam, liquid condensate, steam temperature and water temperature are the next properties, respectively.

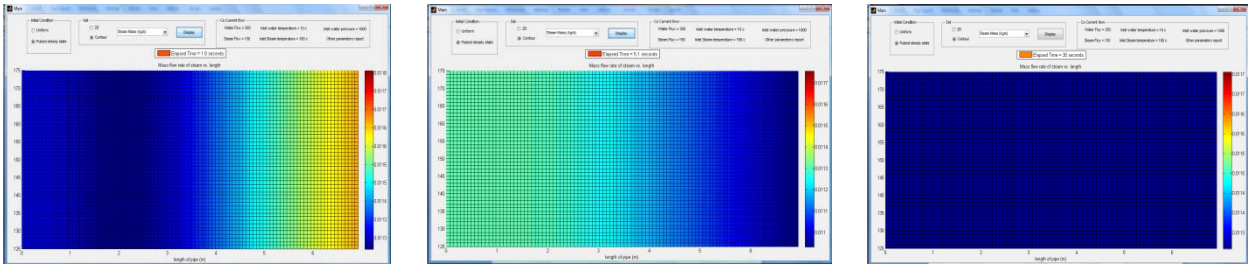

Fig24. Left to right. Moving front of steam mass flow after 1.8, 5.1 and 30 seconds. Final figure shows the steady state. Note that the steady state happens after 21 seconds for pulsed initial condition.

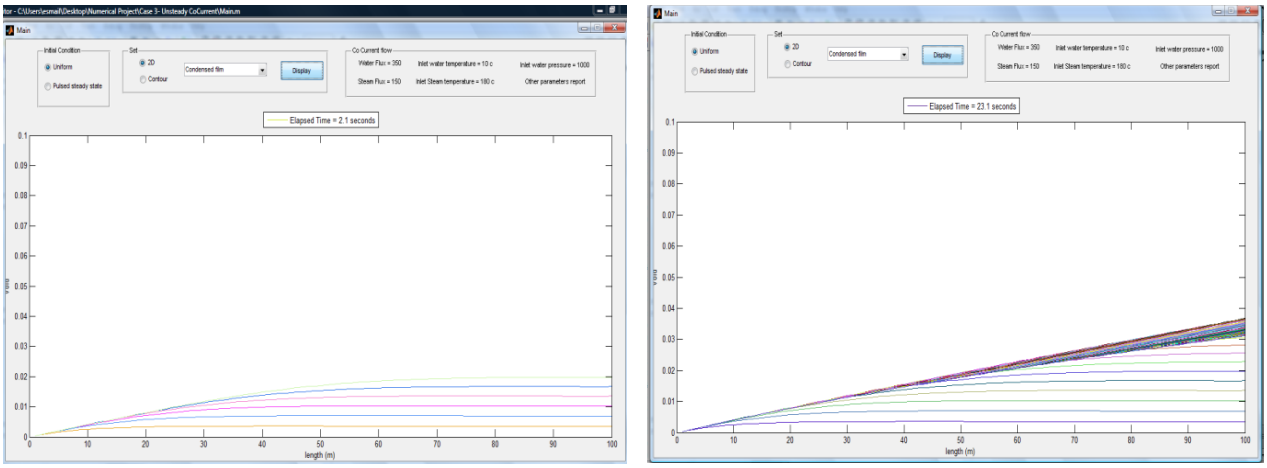

Fig25. Liquid film after 2.1 and 23.1 seconds (steady state) for uniform initial condition. Like some other properties, liquid film shows forth and back behavior. This behavior isn't detected for water temperature during working on the project.

As the animations represent, the initial condition has an extreme impact on the time and trend of reaching the steady state condition, although the final conditions (steady state), as we expect, are identical.

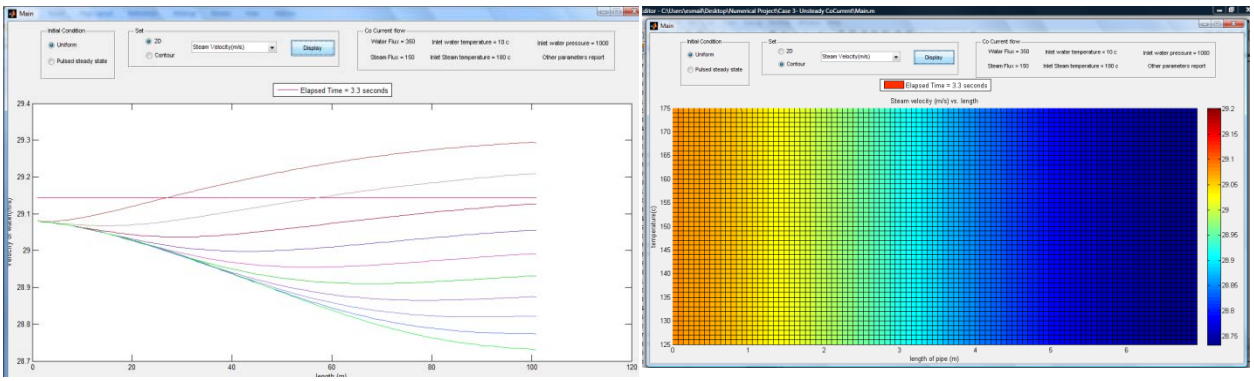

Fig26. 2D and contour plots of steam velocity after 3.3 seconds (uniform initial condition).

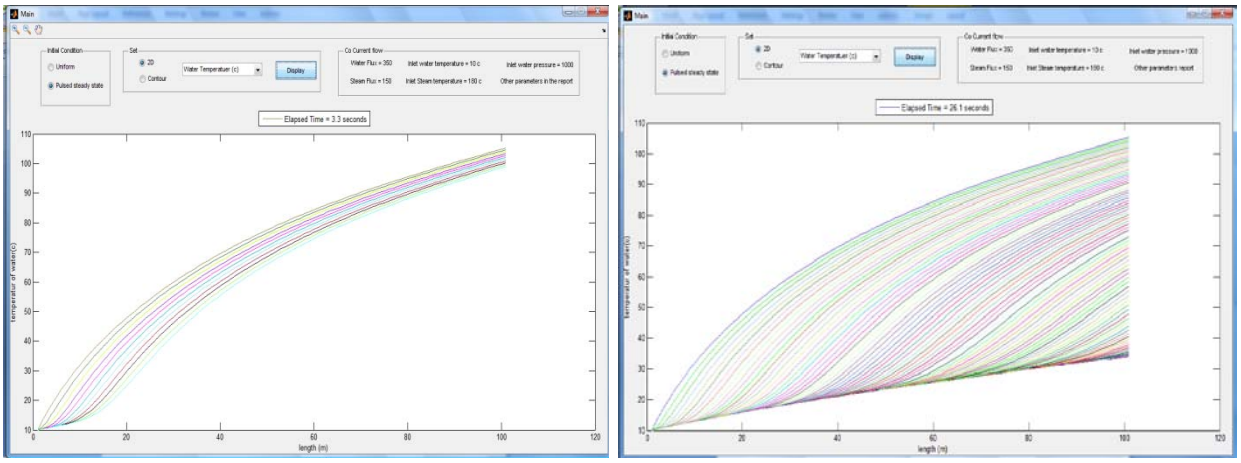

Fig27. The reaction of water temperature towards its stable state after applying pulse. The left figure is captured after 3.3 seconds and the right one, after steady state.

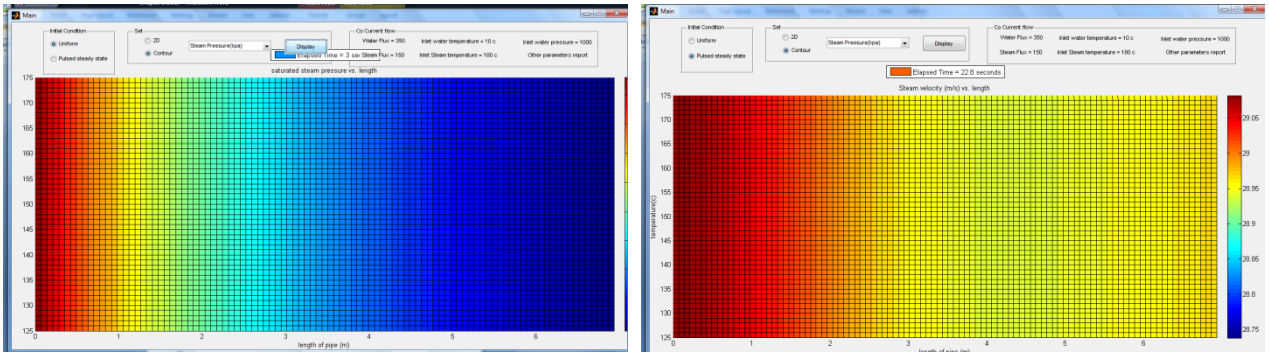

Fig28. Profile of steam pressure after 3 seconds (left) and after steady state (right). Some of the properties are particularly more evident in counter plots.

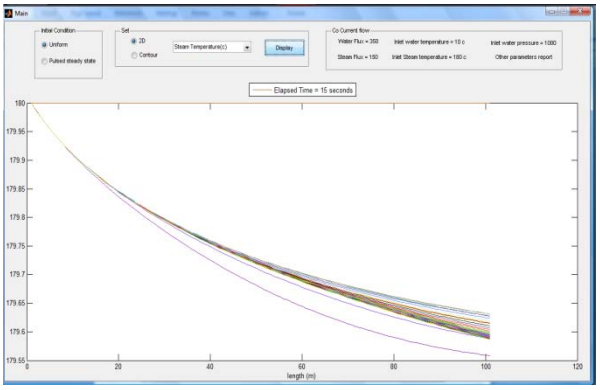

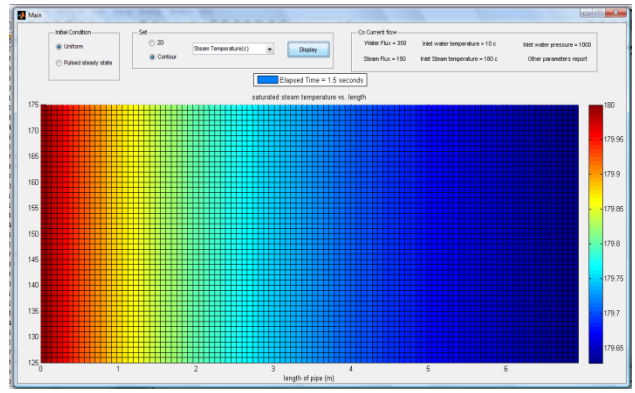

Fig29. Both plots shows steam temperature after 15 seconds (uniform initial condition).

Table 2. Results of unsteady after 10.1 seconds for Uniform Initial Condition

Explicit Method			Implicit Method			Crank-Nicholson Method		
Water T	Gas Quality	Wall T	Water T	Gas Quality	Wall T	Water T	Gas Quality	Wall T
10	1	168.9659	10	1	174.636	10	1	174.7015
11.5225	0.9964	169.4437	11.0926	0.9976	174.6212	11.0929	0.9976	174.7338
13.0564	0.9931	169.6748	12.2238	0.995	174.5691	12.2245	0.995	174.7559
14.5545	0.9899	169.8971	13.3739	0.9925	174.5252	13.3755	0.9925	174.7802
15.9843	0.9868	170.1038	14.5242	0.99	174.4873	14.5269	0.99	174.8055
17.3453	0.9839	170.2965	15.6566	0.9875	174.4535	15.6606	0.9875	174.8297
18.6492	0.9811	170.4762	16.7622	0.9851	174.4228	16.7678	0.9851	174.852
19.8975	0.9784	170.6418	17.8333	0.9827	174.3941	17.8407	0.9827	174.8715
21.0665	0.9757	170.7834	18.8464	0.9803	174.3657	18.8559	0.9803	174.8869
22.0921	0.9731	170.8863	19.7567	0.978	174.3354	19.7686	0.978	174.8965
22.8931	0.9706	170.9364	20.5042	0.9757	174.301	20.5185	0.9757	174.8983
23.424	0.9681	170.9314	21.0361	0.9733	174.2611	21.0531	0.9733	174.8911
23.7114	0.9656	170.8831	21.3408	0.971	174.2157	21.3605	0.971	174.8752
23.834	0.9631	170.8088	21.462	0.9687	174.1666	21.4844	0.9687	174.8521
23.8719	0.9606	170.7226	21.4781	0.9664	174.1163	21.503	0.9664	174.8244
23.8767	0.9581	170.6322	21.461	0.9641	174.0663	21.4884	0.9641	174.7937
23.8713	0.9556	170.5407	21.448	0.9618	174.0173	21.4777	0.9618	174.7611
23.8638	0.9531	170.4489	21.4439	0.9595	173.9692	21.4759	0.9595	174.7266
23.856	0.9505	170.3571	21.4421	0.9572	173.9218	21.4763	0.9572	174.6903
23.8484	0.948	170.2644	21.4392	0.9549	173.8212	21.4755	0.9548	174.633
23.8398	**0.9453**		**21.435**	**0.9525**		**21.474**	**0.9525**	

In the first case, it was showed that the steady state condition is completely irrelevant of the used method. This indisputable concept was tested for all implicit, explicit and Crank-Nicholson method in the unsteady state condition to see whether after some interval, when system is still in its unsteady state condition, the answers are different or similar. The outcomes of this study are prepared in following table. All the reported properties are measured after 10.5 seconds for identical initial conditions.

1-8-3-2 comparison

Table 3. Results of unsteady after 10.1 seconds for pulsed Steady-State Initial Condition

Explicit Method			Implicit Method			Crank-Nicholson Method		
Water T	Gas Quality	Wall T	Water T	Gas Quality	Wall T	Inner T	Gas Quality	Wall T
10	1	168.9659	10	1	174.636	10	1	173.6721
11.5225	0.9964	169.4437	11.0926	0.9976	174.6212	11.0912	0.9976	174.1065
13.0564	0.9931	169.6748	12.2239	0.995	174.5691	12.2244	0.995	174.4221
14.5545	0.9899	169.8971	13.3741	0.9925	174.5252	13.3752	0.9925	174.6865
15.9844	0.9868	170.1039	14.5259	0.99	174.4874	14.5283	0.99	174.9024
17.3461	0.9839	170.2971	15.6669	0.9875	174.4544	15.6685	0.9875	175.0795
18.6573	0.9811	170.4808	16.8084	0.9851	174.4263	16.8041	0.9851	175.2235
19.948	0.9784	170.6652	17.9991	0.9827	174.4048	17.9735	0.9827	175.3412
21.2872	0.9757	170.8687	19.3355	0.9803	174.3938	19.2578	0.9803	175.4392
22.7977	0.9732	171.1189	20.9681	0.978	174.3982	20.7907	0.978	175.5254
24.6239	0.9707	171.4325	23.0559	0.9757	174.422	22.731	0.9757	175.606
26.8333	0.9684	171.8006	25.6717	0.9735	174.4652	25.1815	0.9734	175.6852
29.3588	0.9663	172.1905	28.7307	0.9712	174.5229	28.108	0.9712	175.7618
32.0437	0.9643	172.5678	32.0159	0.9691	174.5871	31.3343	0.969	175.8312
34.7327	0.9624	172.9126	35.2689	0.967	174.6503	34.6085	0.9669	175.8873
37.3325	0.9607	173.2195	38.3163	0.9649	174.7087	37.7221	0.9648	175.9263
39.8122	0.959	173.492	41.1227	0.963	174.7621	40.5979	0.9628	175.9475
42.1725	0.9575	173.7349	43.7308	0.961	174.8116	43.2591	0.9608	175.9524
44.4227	0.956	173.9533	46.1874	0.9591	174.8584	45.7553	0.9589	175.9434
46.5729	0.9547	174.1507	48.5162	0.9572	174.849	48.1184	0.957	175.8733
48.632	**0.9533**		**50.729**	**0.9554**		**50.362**	**0.9552**	

1. As it was expected, the data of the table show that the answers of unsteady state are different for a specific time below before the steady state time.

2. The data of the table also indicate that for various numerical methods, the answers of unsteady state are different for a specific time before steady state time.

3. Comparing the results of the table, we can understand that explicit method has rapid changes relative to the explicit and semi-implicit methods.

4. We expect that the changes in the Crank-Nicholson method to be between the explicit and implicit method. The data of the table show this anticipation, very well.

For the steady state condition, it was explained that co-current and counter-current flows has little differences in their outcomes, and their answers are close to each other, however they have opposite trends, which are more conspicuous in the condensation process. However, in the counter-current flows, the quality of steam remains at x=1 along the pipe for a relatively more distance. This has some undesirable consequences in handling the jacobian matrix as it depend on the initial and boundary conditions, severely. Therefore, cautious should be taken, not to implement any initial conditions. However, unlike uniform initial condition, the pulsed steady state method is, often, promising for counter-current flows. This is the reason no animated results is reported for unsteady counter-current flows.

1-8-4 Simulating Counter-Current flows:

The aim of this case is to represent the counter current flows in the heat exchanger. For attaining this objective the following condition is considered in the heat exchanger. The outer pipe is isolated.

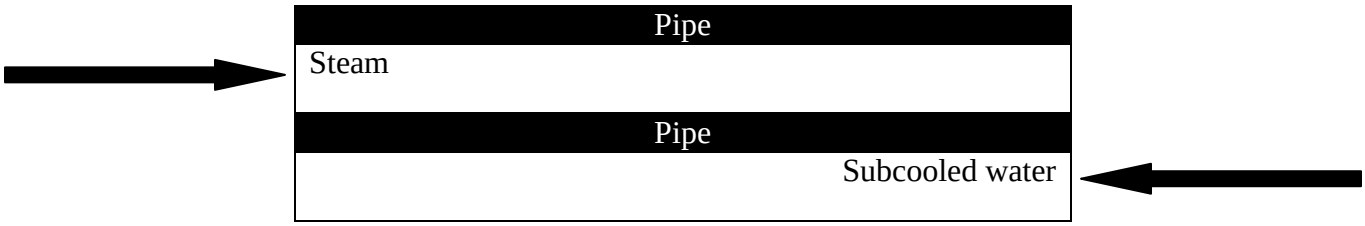

Water flux (kg/m2/s)	Steam flux (kg/m2/s)	Water T (c)	Water P (kpa)	Steam T (c)	Length (m)
300	300	22	1000	180	7

Inner pipe inner D (m)	Inner pipe outer D (m)	Outer pipe inner D (m)	Outer pipe (m)
8e-3	10e-3	14e-3	16e-3

Number of mesh for each layer	Time intervals
20	0.3 seconds

For unsteady cases, animations of the simulation are provided in .mat matrixes which will be loaded at the beginning of the provided GUI associated with that case, however, it may be of primary interest to show the steady state solution of counter current flows and then see the animated results for unsteady state.

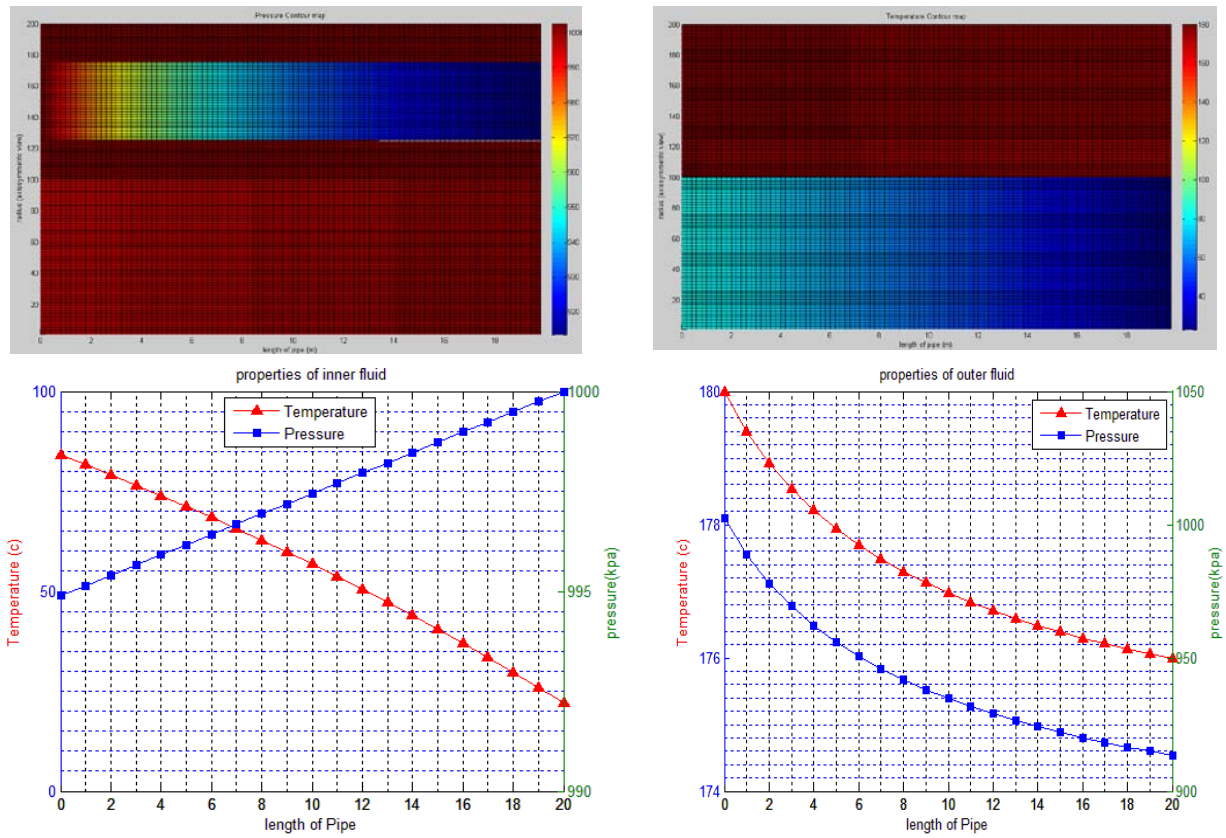

Fig 30. Steady state results of the problem. Figure above-left shows the distribution of pressure in entire heat exchanger. The black color represents the pipe. The above-left figure shows the temperature distribution in entire heat exchanger. Note that steam temperature doesn't change very much relative to that of water. Contrary to it, water pressure change is very low relatively. The wall temperature, however, is more affected by steam temperature and hence gets black color.

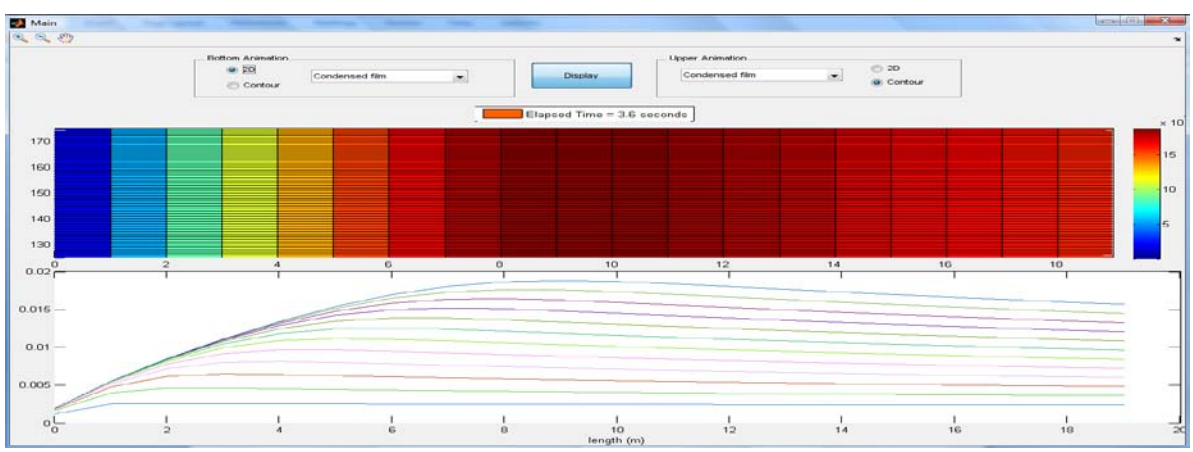

Fig31. These plots, both 2D and contour, represent the progress of liquid film. The first is captured after 3.6 seconds and the latter after 17.7 seconds. The time of steady state for the fluid is about 62 seconds, although various properties may have different steady times.

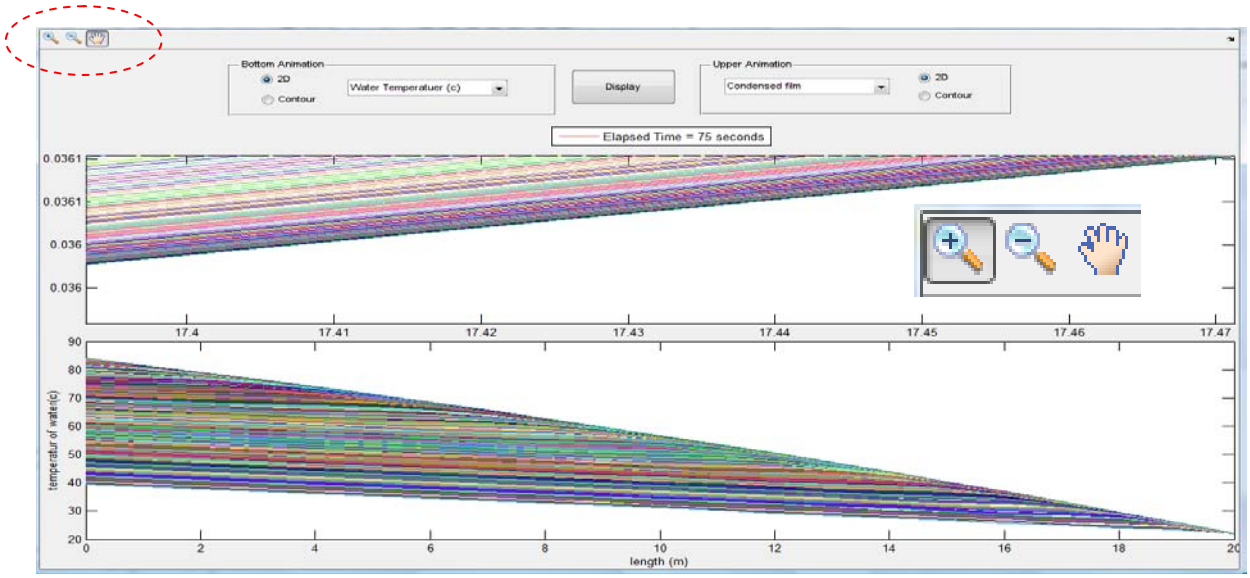

Fig32. Pursuing the lines by zoom objects is required in order to estimate the exact steady state time. The first figure is zoomed on the condensate film lines and the second shows water temperature (Both in steady state).

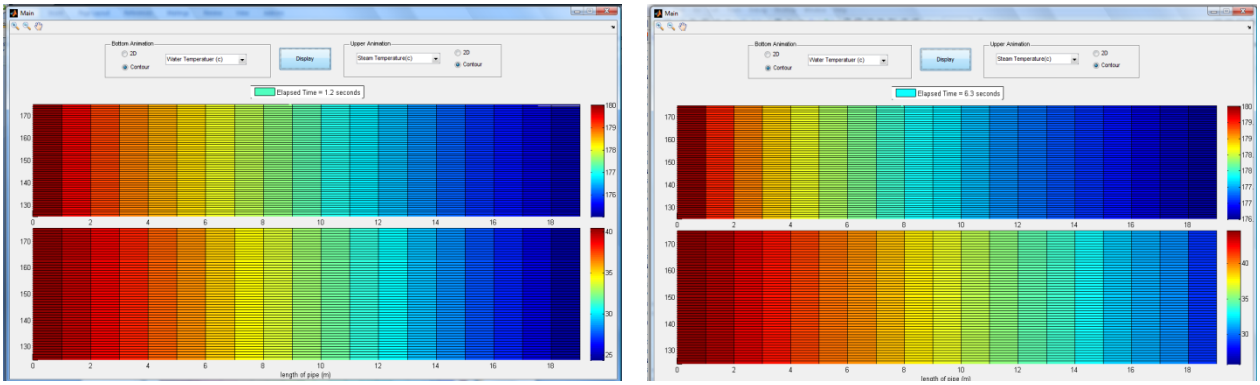

Fig 33. Water temperature (lower) vs. steam temperature(upper) at 1.2 and 6.3 seconds.

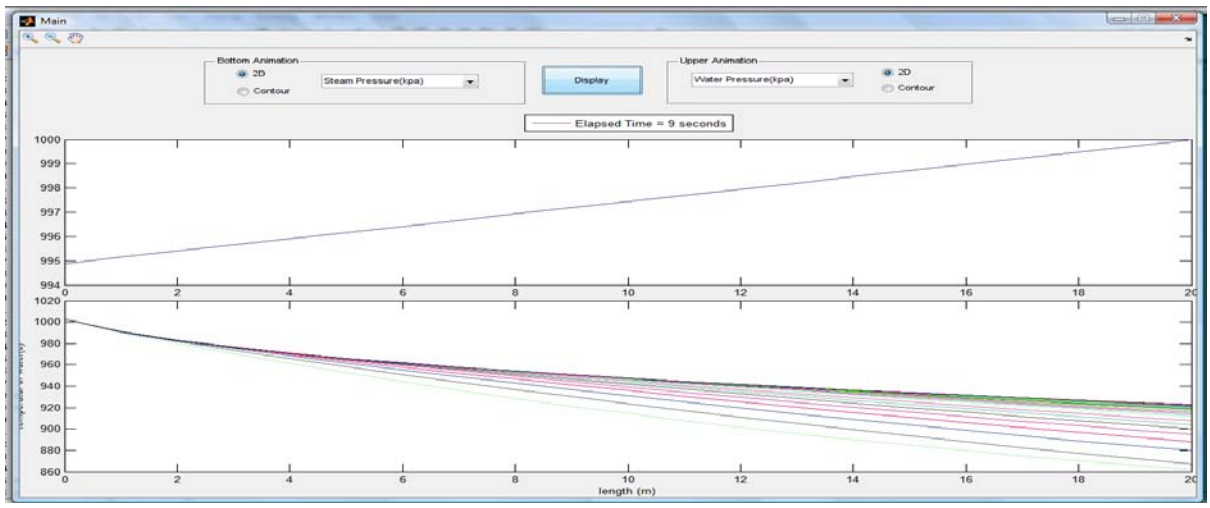

Fig34. Water pressure (upper) vs. steam pressure (lower) at 9 seconds. As it was explained, as it was explained, fluids convey the effect of pressure quickly through themselves.

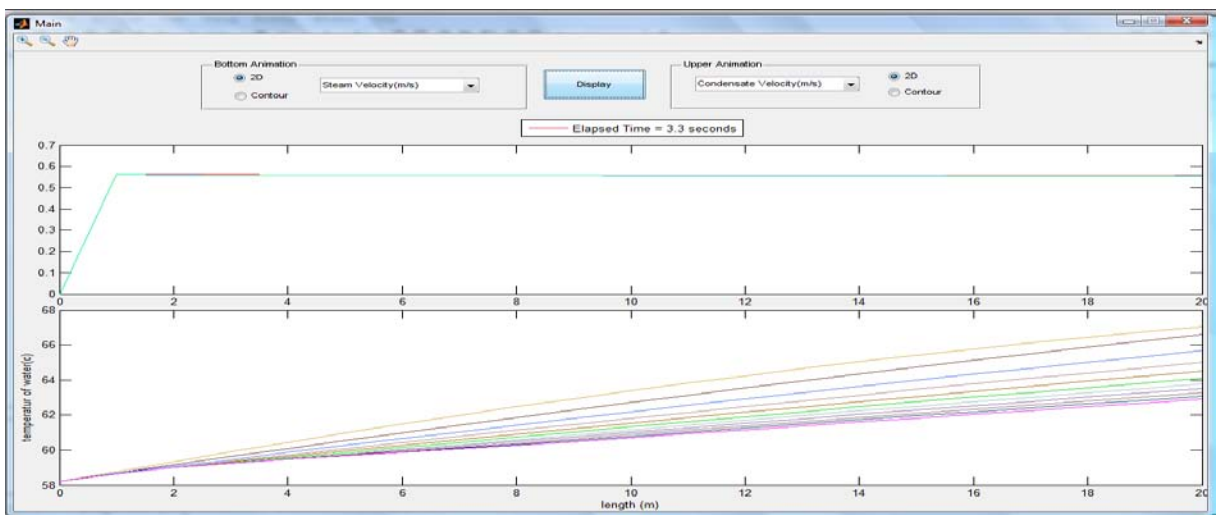

Fig35. Liquid film velocity (upper) vs. steam velocity (lower) at 3.3 seconds.

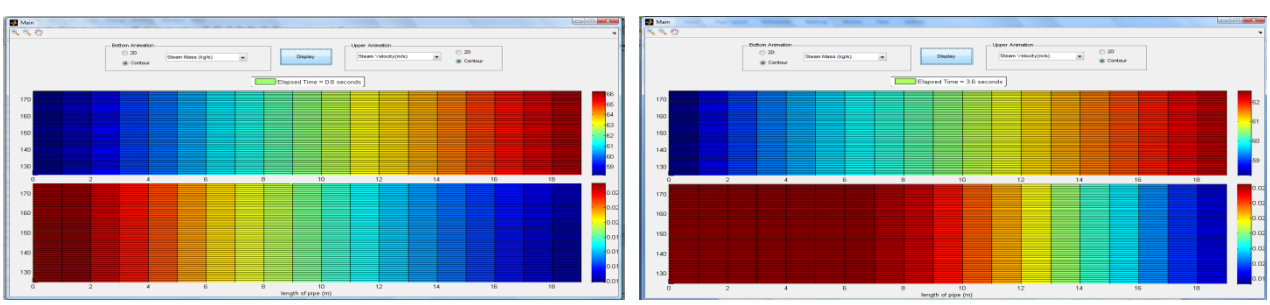

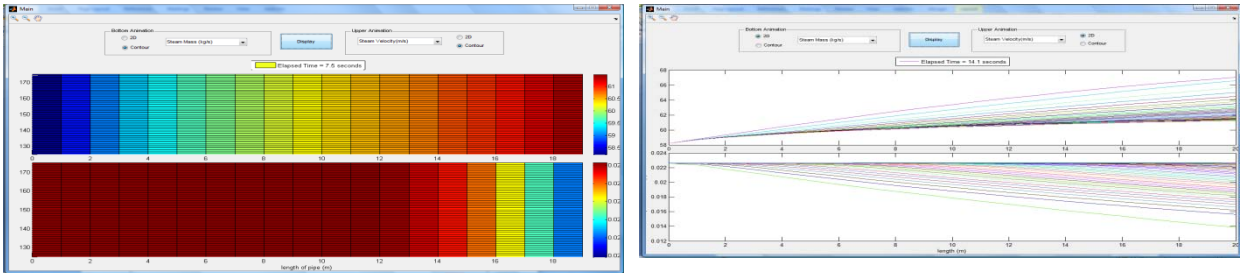

Fig 36. Steam mass flow (upper) vs. Steam velocity (lower). These plots are captured at 0.5, 3.6, 7.5 and 14.1seconds respectively.

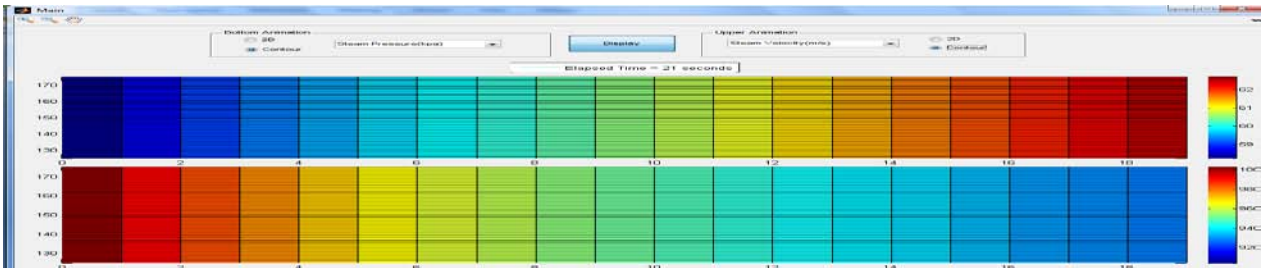

Fig 37. Steam pressure vs. steam velocity at 21 seconds.

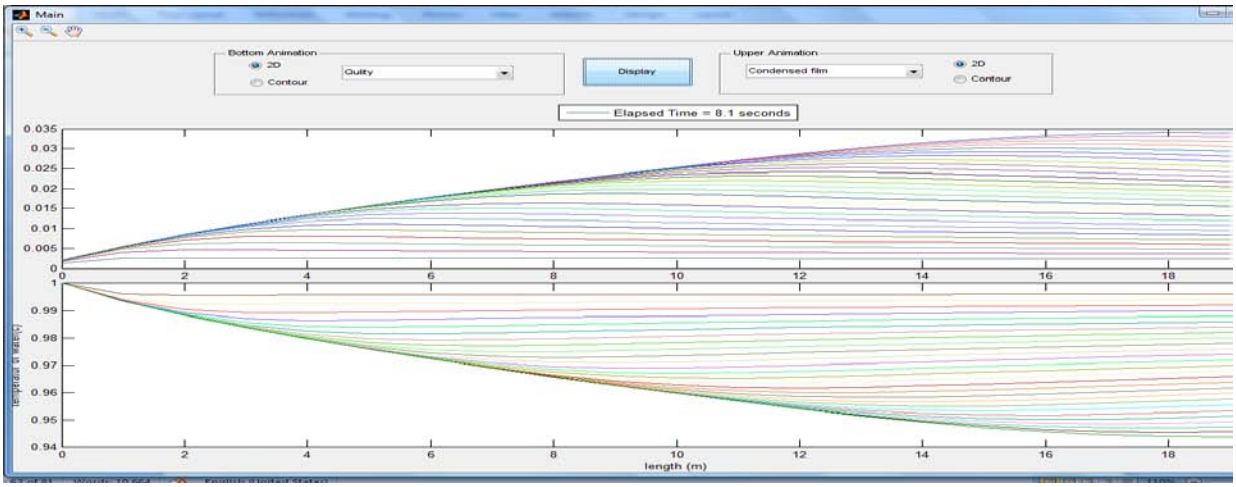

Fig38. Quality (lower) vs. condensate film (upper) at 8.1 sec.

Table 4. Comparison between co-current and counter-current flow. Note that the data of the problem are set as the default data.

Water flux=220 Steam flux=60 Kg/s/m2				Water flux=260 steam flux=120 Kg/s/m2				Water flux=300 steam flux=200 Kg/s/m2			
Liquid Film		Inner Temperature		Liquid Film		Inner Temperature		Liquid Film		water Temperature	
Co	Counter	Co	Counter	Co	Countr	Co	Counter	Co	Counter	Co	Counter
0.016	0.0045	**22**	**134.9836**	0.0049	0.0025	**22**	**98.9393**	0.0024	0.0015	**22**	**82.5324**

0.0472	0.0138	32.0497	132.2079	0.0146	0.0077	27.2578	96.2327	0.0073	0.0046	25.8215	80.1565
0.0768	0.0239	41.3815	129.2385	0.024	0.0131	32.3375	93.4312	0.012	0.0077	29.5472	77.7258
0.1048	0.0346	50.0361	126.0618	0.0332	0.0187	37.2429	90.5306	0.0166	0.0109	33.18	75.2366
0.1313	0.0463	58.0647	122.6625	0.0421	0.0245	41.9747	87.5264	0.0212	0.0143	36.7203	72.6857
0.1563	0.0588	65.5068	119.0244	0.0507	0.0305	46.5421	84.4151	0.0256	0.0177	40.1684	70.0714
0.1799	0.0723	72.411	115.1304	0.0591	0.0368	50.9504	81.1932	0.03	0.0212	43.5293	67.3927
0.2022	0.0868	78.8151	110.9637	0.0672	0.0433	55.2051	77.8568	0.0342	0.0248	46.8051	64.6477
0.2233	0.1025	84.7573	106.5047	0.0751	0.0501	59.3101	74.4005	0.0383	0.0286	49.9978	61.834
0.2432	0.1195	90.2755	101.7325	0.0827	0.0572	63.2693	70.8191	0.0424	0.0324	53.1098	58.949
0.2619	0.1378	95.4004	96.6269	0.0902	0.0645	67.0889	67.1105	0.0464	0.0363	56.1428	55.9904
0.2796	0.1577	100.1634	91.1659	0.0974	0.0721	70.7751	63.271	0.0502	0.0404	59.098	52.9568
0.2964	0.1792	104.5932	85.3248	0.1044	0.0801	74.3323	59.2946	0.054	0.0445	61.977	49.847
0.3122	0.2025	108.7144	79.0817	0.1111	0.0884	77.7626	55.1753	0.0577	0.0488	64.7819	46.6595
0.3271	0.2279	112.5512	72.4094	0.1177	0.097	81.0714	50.9098	0.0613	0.0532	67.5154	43.392
0.3412	0.2554	116.1265	65.2825	0.1241	0.1059	84.2642	46.4946	0.0649	0.0577	70.1797	40.0427
0.3545	0.2855	119.4603	57.678	0.1303	0.1153	87.3452	41.9247	0.0683	0.0624	72.7764	36.6097
0.3671	0.3182	122.5706	49.5663	0.1363	0.125	90.3178	37.1956	0.0717	0.0672	75.3063	33.0887
0.379	0.3541	125.4747	40.9299	0.1421	0.1352	93.1856	32.2985	0.075	0.0721	77.7705	29.4799
0.3903	0.3936	128.1885	31.7436	0.1477	0.1457	95.9524	27.2342	0.0782	0.0771	80.1712	25.784
		130.725	**22**			**98.6219**	**22**			**82.5106**	**22**

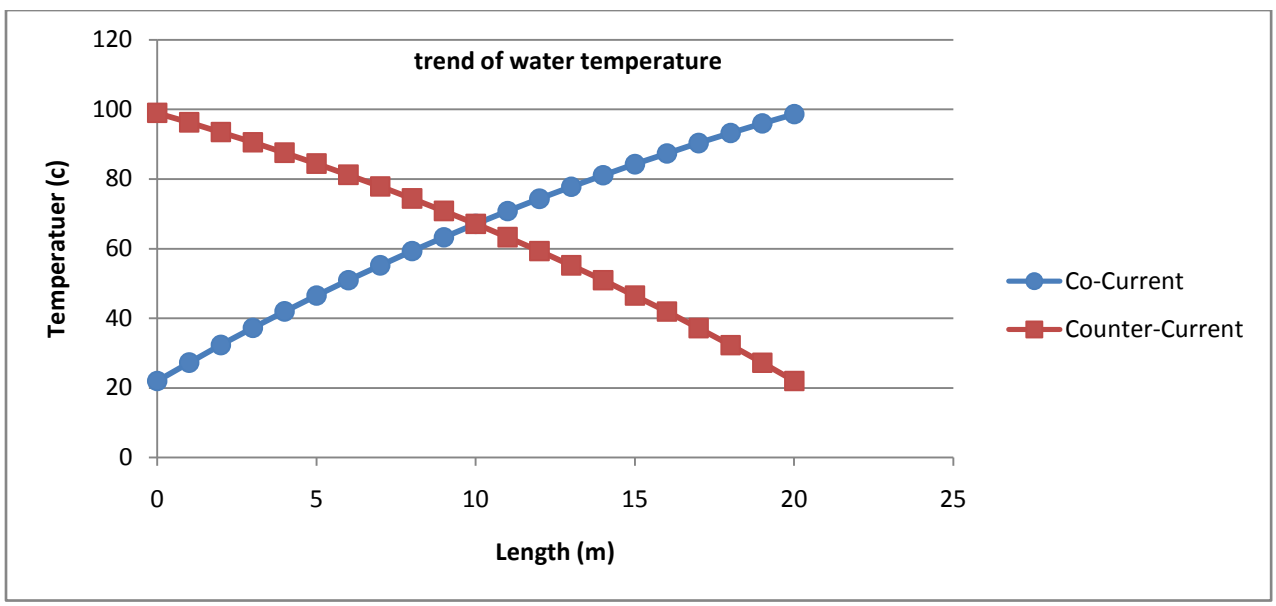

Fig39.Plot of temperature of water for co-current and counter-current. The inlet temperature of water for both is equal but the direction of inlet water differs.

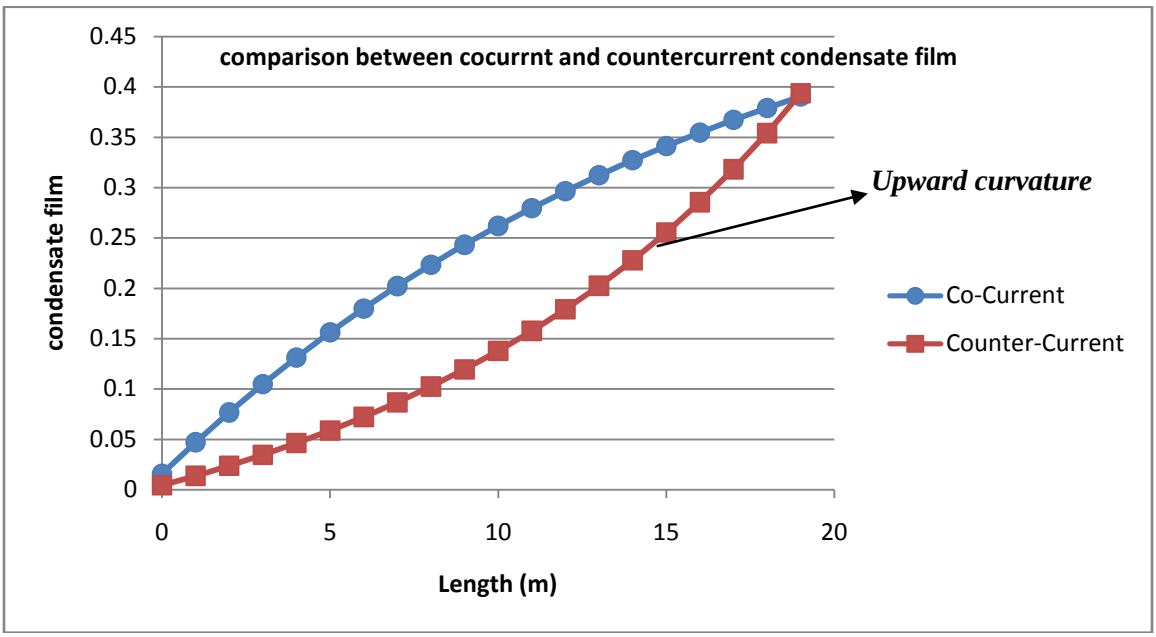

Fig40. The fantastic plot of liquid film for both co-current and counter-current. Note that for all the plots, the results and reasons are explained in the context.

1-8-5 Study of Super-heat entrance:

Here the assumption of saturated vapor entrance will be replace by the assumption of super heat entrance. Super heat vapor is differs from saturated vapor in the sense that its properties are function of both temperature and pressure.

1-8-5-1 without conduction

This example is devoted to present how superheat vapor entrance would influence different parameters. In this example, it is assumed that the pipe length is small so no saturated vapor would be produced at the end of heat exchanger

Inner pipe inner D (m)	Inner pipe outer D (m)	Outer pipe inner D (m)	Outer pipe (m)
9.5e-3	11e-3	14.5e-3	16e-3

Water flux	Steam flux	Water T	Water P	Steam T	Steam P	Length

(kg/m2/s)	(kg/m2/s)	(c)	(kpa)	(c)	(kpa)	(m)
180	90	22	500	400	500	3

1. It is expected that due to high velocity of superheated steam relative to water, its pressure drop, also, be greater.
2. On the other hand, due to specific heat capacity of steam and because of no phase alteration, it is expected that steam temperature drop be more than water temperature increasing, let alone steam flow rate intensifies this justification further.
3. As the data of the below table represent, the steam viscosity variation is significant and it, first, decreases, and then rises, hence, Re number and consequently convection heat transfer coefficient, primarily increases and then decreases. Reduction in temperature difference between water and steam and, in addition, increasing in gas viscosity provides adequate grounds for decreasing the rate of temperature drop in steam, heat transferred from steam and as a result rate of temperature increasing in water.
4. Due to less reduction of steam temperature relative to its pressure, steam density is in direct influence of its temperature, rather than its pressure, and increases along the pipe. This rationalizes the reduction in steam velocity, which data, also, proclaims.
5. Another beautiful point, in this example, is that by changing the trend of rectifying the temperature of steam for the next iteration and by powering the ratio of enthalpies, convergence time will decrease.

Power of steam T	1	2	3
Time sec	36.65	17.74	11.51

Table 5. Results for inlet superheat vapor without conduction. No saturated steam will be produced in this length.

Water Pressure	Water Temperature	Steam Pressure	Steam Temperature	Gas Velocity	Gas Viscosity*10^4
500	22	500	400	55.53	0.2404
499.9896	25.2274	498.947	381.8431	54.1377	0.2339
499.9792	28.2923	497.9207	365.0019	52.8455	0.2278
499.9688	31.19	496.9216	349.0693	51.6197	0.2221
499.9583	33.9311	495.9489	333.9151	50.4504	0.2166

499.9479	36.5202	495.0002	319.594	49.343	0.2115
499.9375	38.965	494.0742	306.0577	48.2945	0.2066
499.9271	41.2741	493.1715	293.2778	47.2796	0.202
499.9167	43.4553	492.2911	281.2048	46.2998	0.1976
499.9063	45.5151	491.43	269.8034	45.374	0.1935
499.8959	47.4601	490.5868	259.0309	44.499	0.1893
499.8854	49.2978	489.7628	248.8691	43.6732	0.182
499.875	51.0353	488.9574	239.3829	42.9014	0.1752
499.8646	52.6783	488.1702	230.4065	42.1707	0.1693
499.8542	54.2303	487.3977	221.9263	41.4806	0.1663
499.8438	55.6956	486.6381	213.9163	40.8292	0.1634
499.8334	57.079	485.8907	206.3479	40.2142	0.1607
499.823	58.3849	485.1545	199.2248	39.6347	0.1581
499.8125	59.6184	484.4287	192.6615	39.0912	0.1558
499.8021	60.7841	483.7128	186.461	38.5786	0.1535
499.7917	61.8858	483.0061	180.6021	38.0951	0.1514
499.7813	62.927	482.3081	175.0727	37.6399	0.1879
499.7709	63.8811	481.5287	170.0317	37.236	0.307
499.7605	64.7607	480.6818	165.3913	36.8743	0.4151
499.75	65.5783	479.7857	161.0904	36.5474	0.5138
499.7396	66.3359	478.8519	156.962	36.2386	0.6069

1-8-5-2 with conduction

Due to low temperature difference between inner pipe wall and saturated steam, no tangible conduction is expected. Nevertheless, when superheat steam enters the pipe, the conduction between steam and inner pipe wall can play an effective role.

For steady state, we have:

$$[mh]_z - [mh]_{z+\delta z} = q_{Conv} \tag{1-47}$$

Now if we take into account the conduction, then equation yields:

$$\left[-kA\frac{\partial T}{\partial z}\right]_z - \left[-kA\frac{\partial T}{\partial z}\right]_{z+\delta z} + [mh]_z - [mh]_{z+\delta z} = q_{Conv} \tag{1-48}$$

This after discritizing, gives:

$$h_{i+1} = h_i + \frac{h_{Conv,i} P \Delta z (T_{wall,i} - T_{mean}) + \frac{kA}{\Delta z}(T_{i+1} - 2T_i + T_{i-1})}{m_i} - 0.5(V_{i+1}{}^2 - V_i^2) \qquad (1\text{-}49)$$

This modified equation is used in the program algorithm.

Below table uses previous data as its default data, so the effect of considering and not considering conduction in rendered.

Table 6. Comparing the results with and without conduction assumption for various flux rates.

Steam Temperature Comparison					
Steam flux=135 kg/s/m2,L=1 m		**Steam flux=45 kg/s/m2,L=1 m**		**Steam flux=15 kg/s/m2,L=1 m**	
Without Conduction	*With Conduction*	*Without Conduction*	*With Conduction*	*Without Conduction*	*With Conduction*
600	600	600	600	600	600
592.9662	592.9721	582.4101	582.4163	562.5583	562.5719
586.9717	586.9761	567.3027	567.3088	530.2644	530.2827
581.076	581.08	552.6961	552.7028	499.9734	499.9955
575.2586	575.2623	538.5018	538.509	470.8296	470.8505
569.5183	569.5215	524.7061	524.714	443.1765	443.2078
563.8539	563.8567	511.2951	511.3071	416.7995	416.8223
558.2646	558.267	498.2304	498.2317	391.9016	391.9348
552.7494	552.7514	485.3132	485.3156	368.336	368.3642
547.3074	547.3089	472.7666	472.7698	346.199	346.2335
541.9377	541.9387	460.5698	460.5738	325.3203	325.35
536.6392	536.6398	448.6941	448.7043	305.7574	305.7841
531.4111	531.4112	437.0249	437.0232	287.4522	287.4833
526.2524	**526.252**	425.6911	425.6902	270.3203	270.3483
521.1622	**521.1613**	414.6895	414.6894	254.3002	254.3367
516.1395	**516.138**	404.0109	404.0157	239.4058	239.4365
511.1798	**511.1813**	393.5823	393.5896	225.4637	225.489
506.2893	**506.2902**	383.4224	383.4184	212.4372	212.47
501.4632	**501.4514**	373.5699	373.5668	200.272	200.3021
496.6331	**496.622**	364.0122	364.0141	189.1822	189.2129
491.8363	**491.8252**	354.749	354.7523	178.7648	178.7945
487.1026	**487.0915**	345.7407	345.7462	169.6681	169.6948
482.4307	**482.4196**	336.9782	336.9853	162.3742	162.4034
477.8188	**477.8078**	328.4818	328.4808	155.9922	156.0214
473.2493	**473.2383**	320.2078	320.2086	150.2176	150.2441
467.964	**467.9548**	310.9914	310.9964	144.1274	144.1532

It is expected that due to conduction heat transfer from points with high temperature to the points with less temperature, the temperature of pipe be greater than when we have no conduction. The ratio of conduction to convection heat transfer increases when the flow rate of steam decreases. The data associated with less flux of steam for the inlet section of pipe, where the heat transfer is maximum due to high temperature difference, clearly, indicate that the temperature of points are more when conduction is considered. This is more obvious for steam flux of 15 kg/m/s2. In high flow rates and in the final data, however, some data challenge this general concept, this is due to the method used for calculating conduction, and however, these are negligible.

The important conclusion of this simulation is that in fluids, the prevailing mechanism of heat transfer is convection and even in low fluxes, the impact of conduction is insignificant.

1-8-5-3 General form of inlet superheat vapor

In this example, it is assumed that the reformation to saturated vapor happens.

Water flux (kg/m2/s)	Steam flux (kg/m2/s)	Water T (c)	Water P (kpa)	Steam T (c)	Steam P (kpa)	Length (m)
300	60	22	500	300	500	12

Inner pipe inner D (m)	Inner pipe outer D (m)	Outer pipe inner D (m)	Outer pipe (m)
8e-3	10e-3	14e-3	16e-3

Table 7. Table of results for reformation of superheat to saturated vapor

Subcooled water			Superheat →saturated vapor				
P (kpa)	T (c)	HConv (j/m2/s)	P (kpa)	T (c)	Quality	Liquid drop	HConv(j/m2/s)
500	22	65.265	500	300	1	0	
499.8773	25.0528	65.2823	498.911	278.4774	1	0	619.2393
499.7547	27.8463	65.2981	497.8677	258.8887	1	0	628.8911
499.632	30.3981	65.3126	496.8698	241.1181	1	0	643.9972
499.5094	32.7336	65.3258	495.9169	224.9415	1	0	664.018
499.3867	34.8673	65.3378	494.9976	210.2041	1	0	673.9094
499.2641	36.8152	65.3488	494.1086	196.7853	1	0	682.8748
499.1414	38.5951	65.3588	493.2467	184.797	1	0	691.35
499.0188	40.2232	65.3679	492.4094	173.8333	1	0	699.3488

498.8961	41.6659	65.3759	491.4074	164.0869	1	0	474.3452
498.7735	42.9552	65.3834	490.2795	155.4325	1	0	373.2805
498.6508	44.2185	65.3907	**489.4872**	**151.0375**	**0.9974**	**0.0008**	**605.5456**
498.5282	45.4417	65.3979	489.1521	151.0118	0.989	0.0041	605.0161
498.4055	46.6508	65.4049	488.9671	150.9976	0.9807	0.0091	604.3592
498.2828	47.8458	65.4119	488.8428	150.988	0.9725	0.0141	603.6712
498.1602	49.0271	65.4188	488.7511	150.981	0.9644	0.0191	602.958
498.0375	50.1948	65.4256	488.6798	150.9755	0.9563	0.024	602.2186
497.9149	51.349	65.4324	488.6222	150.9711	0.9484	0.0289	601.4543
497.7922	52.49	65.439	488.5747	150.9675	0.9406	0.0338	600.6662
497.6696	53.6179	65.4456	488.5346	150.9644	0.9328	0.0386	599.8557
497.5469	54.7326	65.4521	488.5003	150.9618	0.9251	0.0433	599.0239
497.4243	55.8345	65.4585	488.4707	150.9595	0.9176	0.048	598.1718
497.3016	56.9236	65.4648	488.4448	150.9575	0.9101	0.0527	597.3007
497.179	57.9999	65.4711	488.422	150.9558	0.9027	0.0574	596.4114
497.0563	59.0637	65.4773	488.4018	150.9542	0.8954	0.062	595.5051
496.9337	60.1144		488.3839	150.9528	0.8881	0.0666	594.5796

It was explained, in the previous example, why the convection heat transfer coefficient of water increases and why the rate of water temperature increasing decreases, which data, also, confirms.

In the data, it is witnessed that the convection heat transfer coefficient decreases, which is expected.

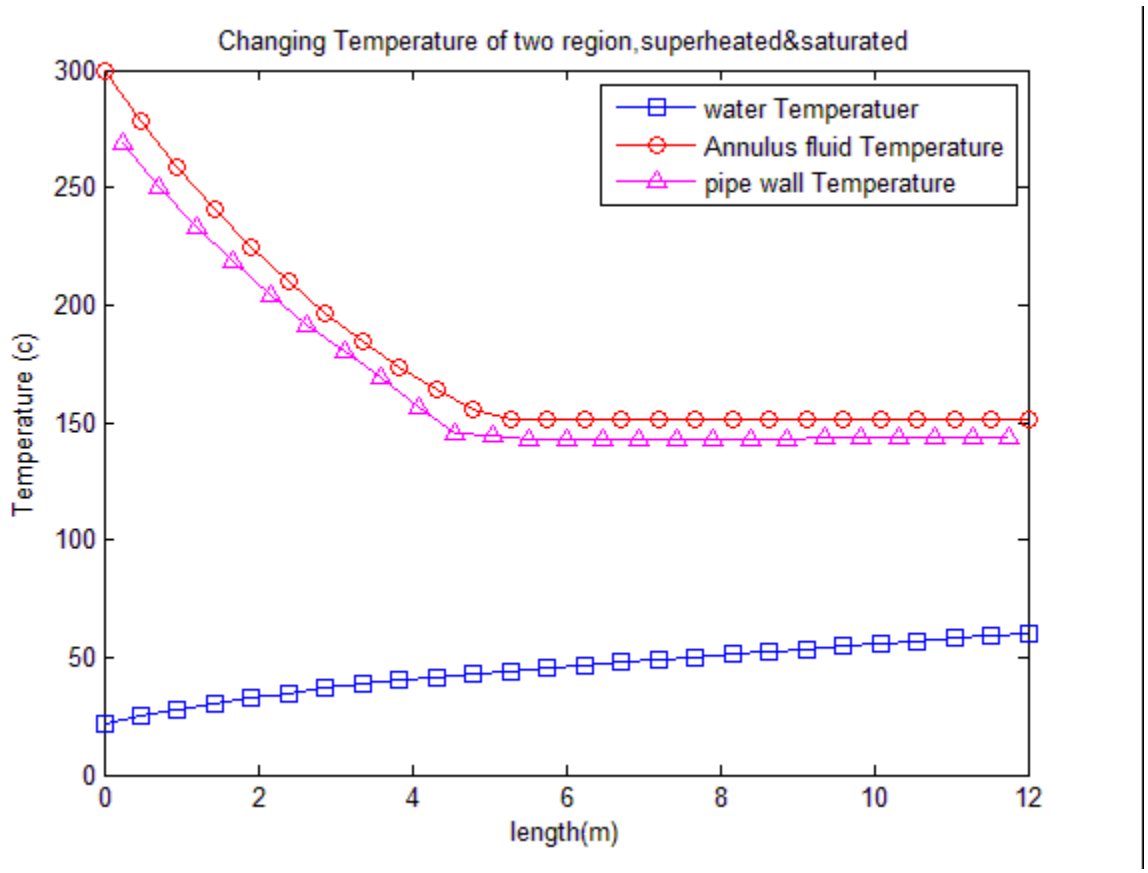

Fig41. Changing temperature of steam where superheated vapor enters the heat exchanger.

The data for the outer pipe demonstrate two different trends, which implies the change of one phase steam into two phase flow. In the one phase region, temperature drop, due to less specific heat capacity of steam, is considerable and its convection heat transfer coefficient, which is in direct influence of its viscosity, is variable. However, as soon as the steam has reached its saturated temperature, the drops of water began to emerge. These drops release significant amount of latent heat and resist any further quick reduction in steam temperature and provide adequate reasons for having two different curve trends.

Having two different curve trends for the steam, the temperature of pipe wall, which is in relation to the heat transfer coefficient of steam, will, also, be affected the same.

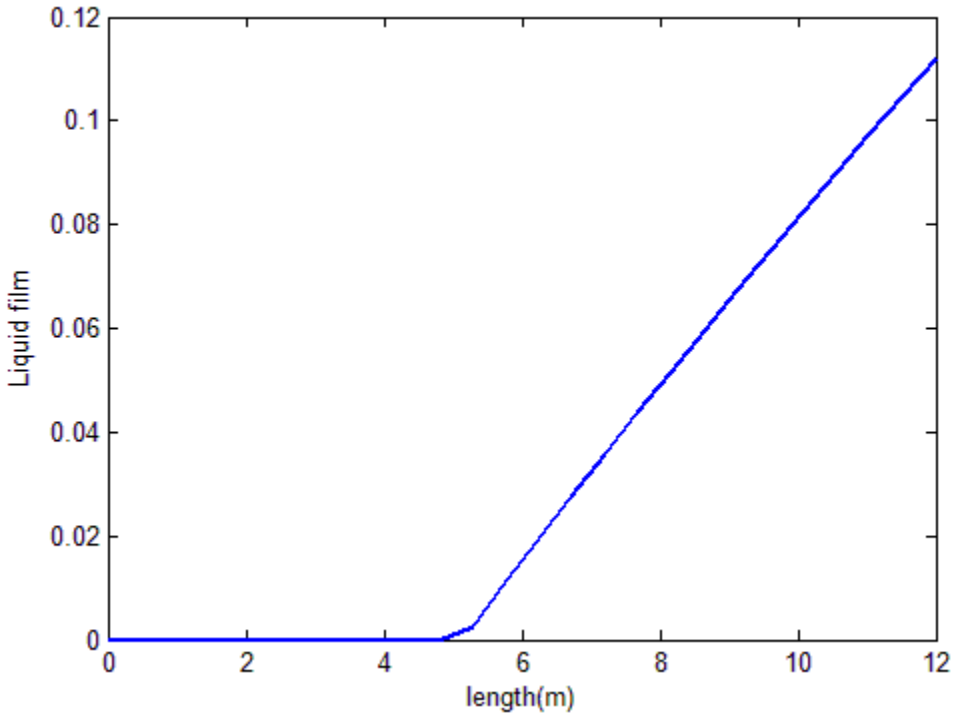

Fig42. Condensate water

One of notes on the superheat program is that, if we enter the two phase region suddenly or we remain near the border of superheat-saturate for a long time, because of their significant difference, the program will eventually end up in divergence (or getting stuck in infinite loops). In addition, choosing big steps results in wrong answer and sometimes, even increasing in the temperature of steam. Also, choosing very small steps results in qualities higher than one and consequently, divergence.

In this example, the length of heat exchanger is considered to be large enough that the entire superheat vapor, entered into it, condenses at the end of it.

Inner pipe inner D (m)	Inner pipe outer D (m)	Outer pipe inner D (m)	Outer pipe (m)
9e-3	11e-3	14e-3	16e-3

Water flux (kg/m2/s)	Steam flux (kg/m2/s)	Water T (c)	Water P (kpa)	Steam T (c)	Steam P (kpa)	Length (m)
400	40	22	500	300	500	30

Due to great heat transfer in the two phase region, passing this region and reaching the single phase region of condensate is a crucial task, because in common condition, the temperature of water will rise to a level that transferring heat to it will eventually stop and divergence or lack of convergence happens so there is no opportunity for steam to lose all its energy and condenses. For overcoming the handicap, the length of pipe is considered very large (30m) and, also, the flow rate of steam was decreased by decreasing its flux and the passing area of steam. Also, the flow rate of water was increased by its flux and its passing area, so we can assure that the temperature of water won't rise rapidly.

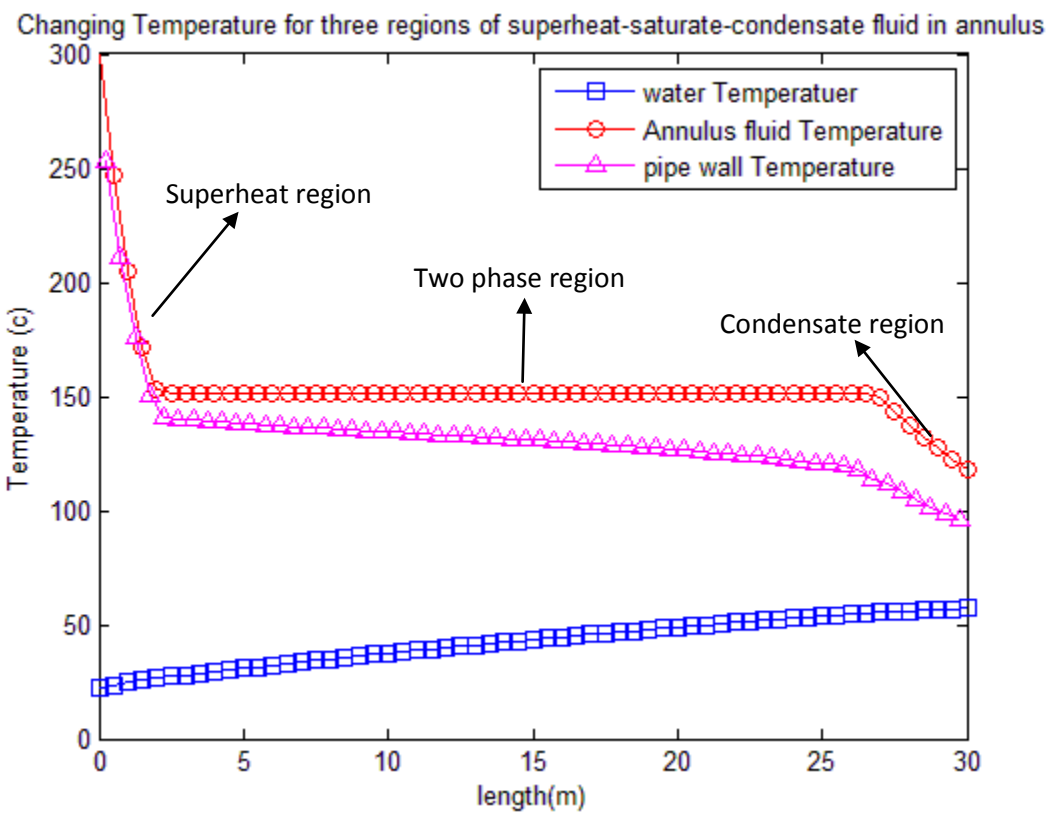

Fig 43. Changing temperature of steam for a long heat exchanger.

Like the previous example and as it was explained, in the single phase region of superheated steam, the reduction in temperature is high but in the two phase region the reduction in temperature is approximately constant. However, in the single phase region of condensate water, the reduction in temperature is, again, tangible. However, because the specific heat capacity of water is higher than steam and also, its convection heat transfer coefficient is less than steam, the rate of reduction in its temperature will be lower.

At the inlet section of pipe, due to high temperature of steam and high convection heat transfer coefficient of steam relative to that of inner pipe water, the temperature of pipe wall is near to steam temperature. However, as the condensate water increases, the convection heat transfer coefficient of outer pipe fluid decreases. This phenomena, continues to the point that the heat transfer coefficient of inner pipe water and outer pipe fluid get closer to each other, at this circumstances, the pipe wall temperature gets closer to the average of them.

As the condensate water increases, the heat transfer coefficient and consequently, the heat transferred to water decreases. Therefore, the rate of increasing the temperature of subcooled water decreases and consequently, creation of condensate decreases. The plots show these facts very well.

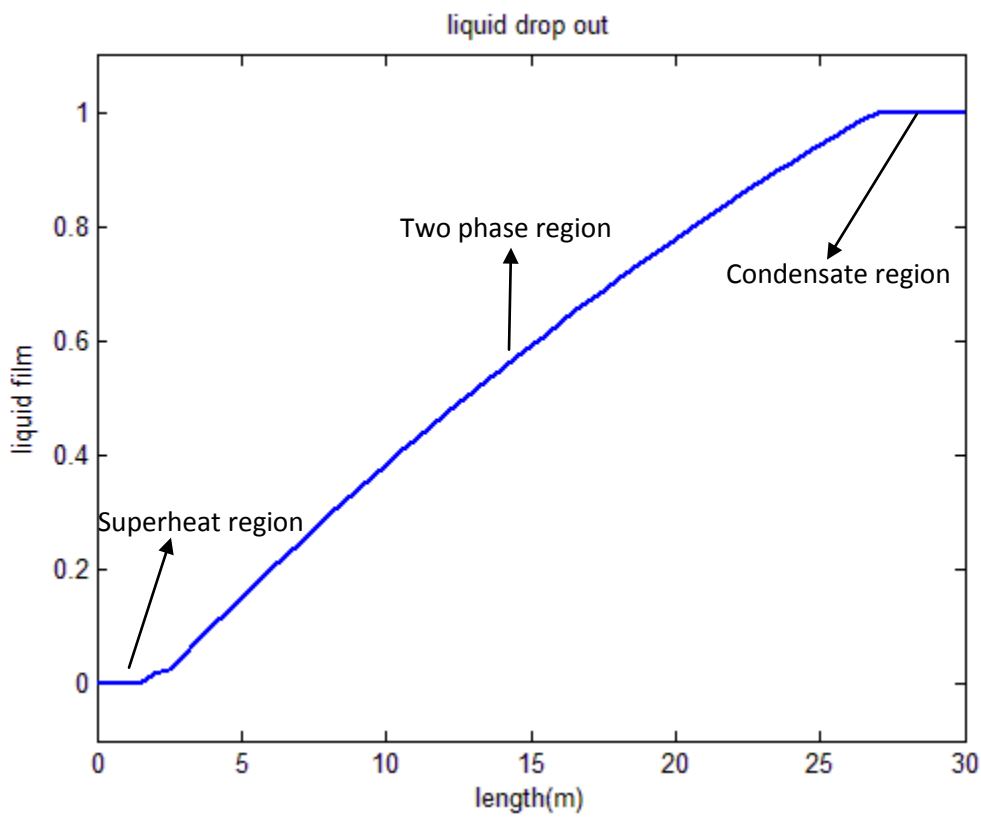

Fig 44. Liquid condensate for superheat entering.

An important point, concerning the programs of this example, is that in each region, in addition to use suitable steps, appropriate experimental correlations, also, is required. These correlations must give the same results in the borders of the regions or in another words, they must be

continuous. This criteria is rarely satisfied in the common correlations, for example if we implement “Monrad” equation for the steam region, “Chatto” equation for the two phase region and “Gielinislki” for the single phase condensate region, these equations give different results in the borders, this predicament will originate inappropriate results (increasing temperature or enthalpy) when we are going from one region to another. In order to overcome this problem, a suitable correlation which is in relation to quality of steam, is used.

1-8-6 Study of two dimensional wall and heat transfer with environment:

In almost all previous cases, we have premised one dimensional wall and no heat transfer with environment. Nevertheless, the real phenomenon is not protected from heat convection with its surrounding environment; hence, it is intended to eliminate this unrealistic assumption in this case study.

Isolation thickness(default)	Inner pipe inner D (m)	Inner pipe outer D (m)	Outer pipe inner D (m)	Outer pipe (m)
36e-3	8e-3	9.5e-3	14e-3	16e-3

Air T (c)	Water flux (kg/m2/s)	Steam flux (kg/m2/s)	Water T (c)	Water P (kpa)	Steam T (c)	SteamP (kpa)	Length (m)	isolation rows
20	300	100	15	1000	175	500	7	10

In the final part of case two, the effect of having two dimensional inner pipe walls was explained.

If just one point across the pipe is considered which steam and water, both, have contact with it; practically, wall has no effect on the final results, whether it concerns either its material or its thickness. This outcome makes sense. Nevertheless, if more than one layer of meshes is considered for the pipe, both indicated criteria become important.

In the outer pipe, however, three mechanism of heat transfer exist. Forced convection between outer pipe and steam, conduction between pipe and isolation and inside isolation and also, free convection between isolation and surrounding air.

For both, inner pipe wall and outer pipe wall, following method is used for indexing:

From the inlet section, the indexing of first layer wall starts and ends at the outlet section of that layer, similarly, for the next layer which is in a higher radius, this procedure is repeated.

In the outer pipe wall, block center grids are used while for the inner pipe layers (which are set to have two layer grids) the corner point gridding method is used.

In this case, the most conspicuous phenomena are the reduction of steam enthalpy and as a result, growth in condensed water. All other results are in direct influence of these phenomena and can be explained, through this point of view.

Table 9- effect of isolation thickness on quality and insulation-air contact temperature.

Without Insulator		Ins. Thickness=1mm		Ins. Thickness=5mm		Ins. Thickness=10mm	
Quality	Ins.-Air contact T	Quality	Ins.-Air contact T	Quality	Ins.-Air contact T	Quality	Ins.-Air contact T
1	169.s0307	1	151.8321	1	115.6384	1	87.3003
0.9943	169.1506	0.9958	151.8972	0.9962	115.6868	0.9964	87.3393
0.9888	169.1408	0.9918	151.8896	0.9925	115.6816	0.9931	87.3357
0.9833	169.1323	0.9879	151.8834	0.9888	115.6773	0.9897	87.3328
0.9778	169.1246	0.9839	151.878	0.9852	115.6737	0.9863	87.3303
0.9723	169.1175	0.98	151.8733	0.9816	115.6705	0.983	87.3282
0.9669	169.1107	0.976	151.869	0.978	115.6676	0.9797	87.3263
0.9614	169.1042	0.9721	151.8651	0.9744	115.665	0.9764	87.3245
0.956	169.0978	0.9682	151.8615	0.9708	115.6626	0.9731	87.3229
0.9506	169.0915	0.9644	151.8581	0.9673	115.6604	0.9698	87.3215
0.9453	169.0853	0.9605	151.8548	0.9637	115.6583	0.9666	87.3201
0.9399	169.0791	0.9567	151.8518	0.9602	115.6564	0.9634	87.3188
0.9346	169.0729	0.9529	151.8488	0.9567	115.6545	0.9602	87.3176
0.9292	169.0667	0.949	151.846	0.9533	115.6527	0.957	87.3165
0.9239	169.0605	0.9453	151.8432	0.9498	115.651	0.9538	87.3154
0.9186	169.0543	0.9415	151.8405	0.9464	115.6494	0.9506	87.3144
0.9134	169.048	0.9377	151.8379	0.9429	115.6478	0.9475	87.3134
0.9081	169.0416	0.934	151.8354	0.9395	115.6462	0.9444	87.3124
0.9029	169.0352	0.9303	151.8329	0.9361	115.6447	0.9413	87.3115
0.8977	169.0288	0.9266	151.8304	0.9327	115.6433	0.9382	87.3106
0.8925	169.0222	0.9229	151.828	0.9294	115.6418	0.9351	87.3097
0.8873	169.0156	0.9192	151.8256	0.926	115.6404	0.932	87.3089
0.8821	169.0089	0.9156	151.8232	0.9227	115.639	0.929	87.3081
0.8769	169.002	0.912	151.8208	0.9194	115.6377	0.926	87.3073
0.8718	168.8596	0.9083	151.7423	0.9161	115.5804	0.923	87.2625
0.8665		**0.9046**		**0.9127**		**0.9198**	

Ins. Thickness=20mm		Ins. Thickness=40mm	
Quality	Ins.-Air contact T	Quality	Ins.-Air contact T
1	84.5486	1	79.6902
0.9963	84.6111	0.9958	79.9348
0.9927	84.6077	0.9918	79.9323
0.9891	84.605	0.9878	79.9298
0.9856	84.6026	0.9838	79.9276
0.9821	84.6005	0.9798	79.9256
0.9786	84.5987	0.9759	79.9239
0.9751	84.597	0.972	79.9223
0.9717	84.5955	0.968	79.9208
0.9682	84.5941	0.9641	79.9194
0.9648	84.5928	0.9603	79.9181
0.9614	84.5915	0.9564	79.9168
0.958	84.5903	0.9526	79.9156
0.9546	84.5892	0.9487	79.9144
0.9513	84.5881	0.9449	79.9133
0.9479	84.5871	0.9411	79.9122
0.9446	84.5861	0.9374	79.9111
0.9413	84.5851	0.9336	79.91
0.938	84.5842	0.9299	79.909
0.9347	84.5833	0.9261	79.908
0.9315	84.5824	0.9224	79.907
0.9282	84.5816	0.9187	79.906
0.925	84.5807	0.9151	79.905
0.9218	84.5798	0.9114	79.9034
0.9186	84.5118	0.9078	79.6533
0.915		**0.904**	

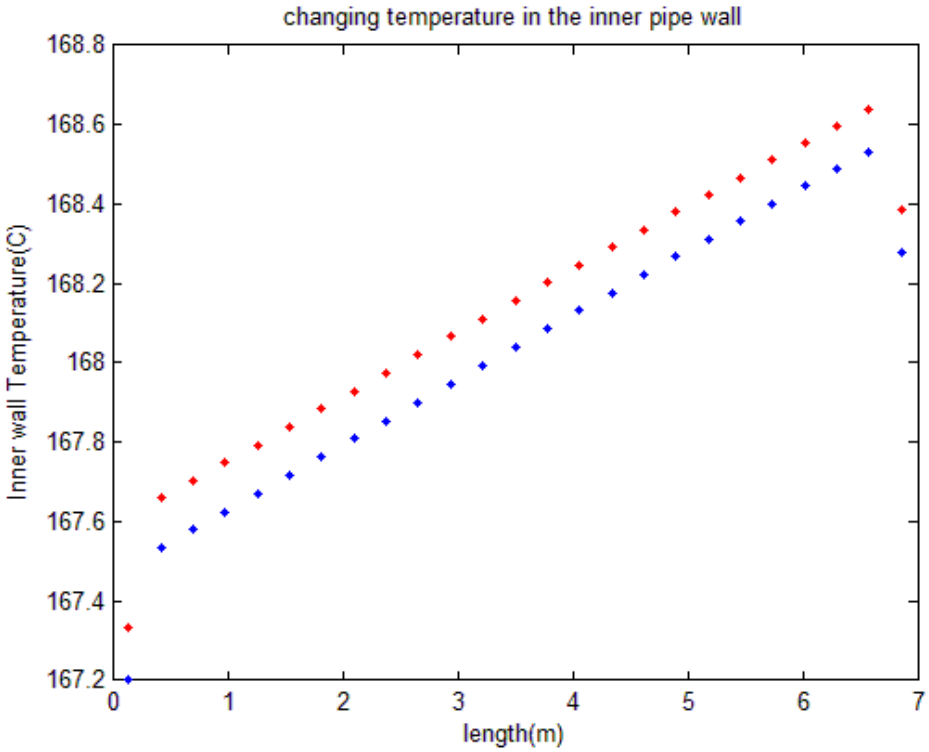

Fig 45. Profile of temperature for two dimensional inner pipe wall (two mesh across the pipe).

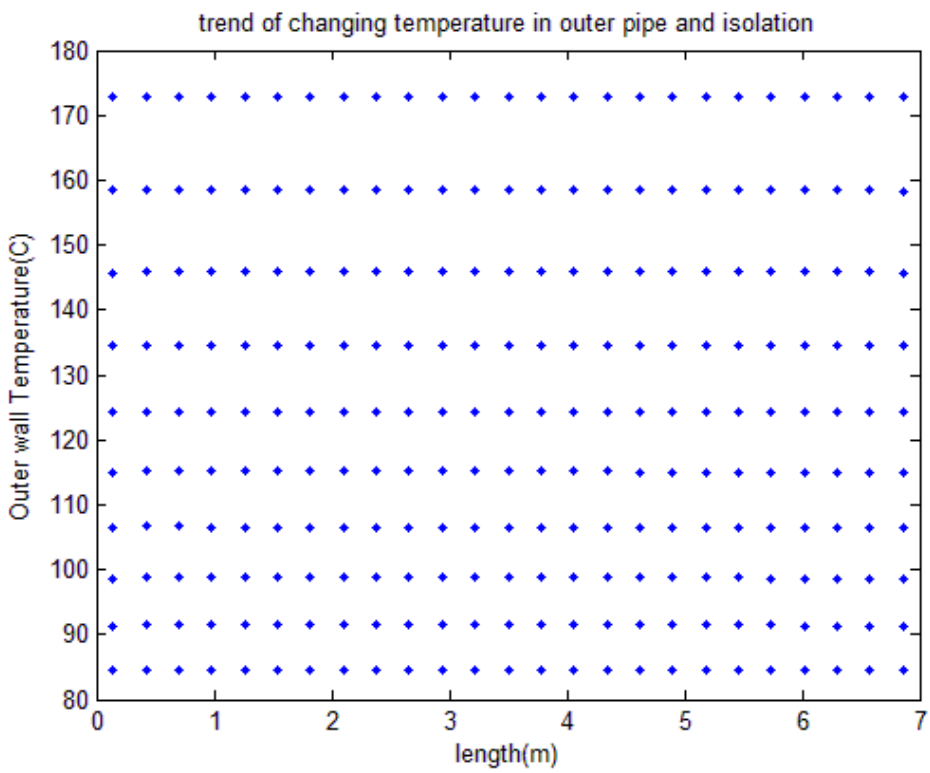

Fig 46. Profile of temperature for two dimensional isolation and outer wall.

Another point, concerning the results, is that considering the free convection heat transfer coefficient of air and also conduction heat transfer coefficient of isolation, the critical radius should be very thin, this means that by increasing the thickness of isolation more than this critical radius, the amount of heat transferred to environment increase due to surface extension and hence, condensed liquid boosts, which is out of interest. In other words, as the thickness of isolation increases, its temperature which is contact with air and, even, its gradient decreases, but, on the other hand, the heat transfer increases as its contact surface with air increases. Therefore, until the critical radius is reached, the heat transfer decreases as the thickness of isolations increases but further increasing above this critical radius increases the heat transfer. Data of the table advocates this claim.

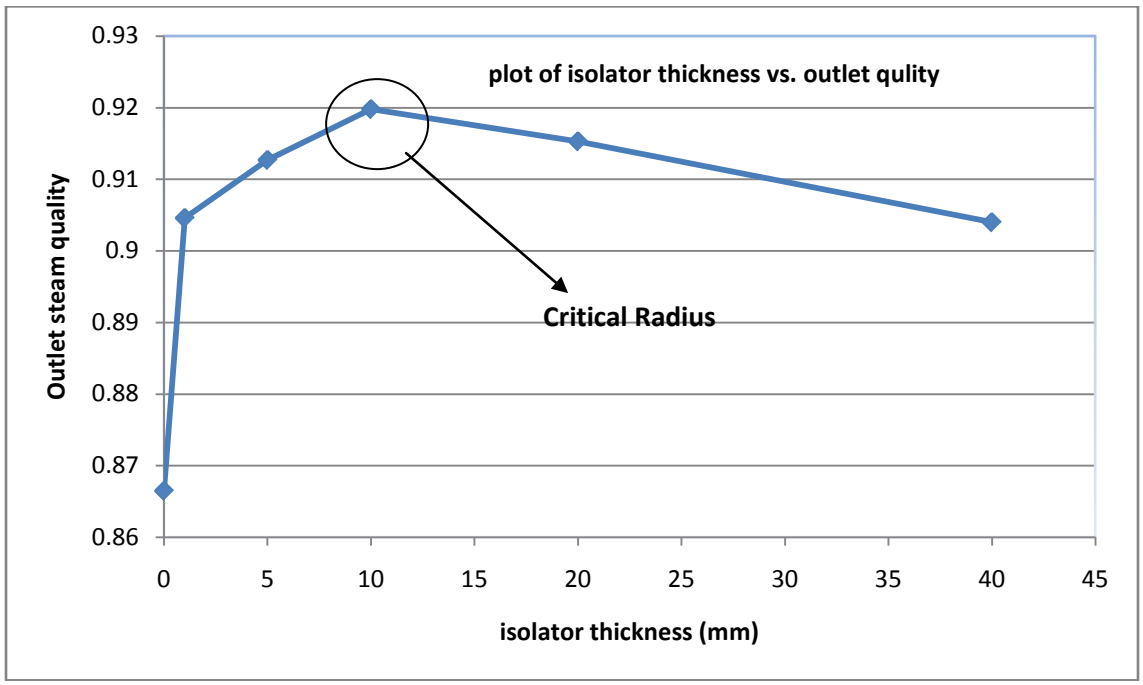

Fig 47. Finding Critical Radius

1-9 Challenges and rewards

1. During establishing the algorithm, we didn't remember some concepts; this gave us the opportunity of restudy Heat transfer and Thermodynamic books again.
2. The second drawback that was encountered during this project associates with correlation using. Some of the correlations appeared to give unrealistic results. It was because the condition of using that correlation had not been considered and yet the correlation was implemented, for example Dobson and Chatto correlation only gives reliable results when flux is more than 500 kg/s/m2. This ignorance was one of the causes of divergence. However, we could figure it out by checking the code and results of it line by line.
3. As we had accustomed to concurrent indexes, during Countercurrent flow coding, the indexing of the equations made our mind confused. This made us to work out the whole algorithm again on paper.
4. The most important problem we encountered during the project was the divergence of unsteady explicit codes. We had, meticulously, reviewed the algorithm and even the codes, line by line, over and over. All the variables had been scrutinized for times. We were looking for a small bug in the program which was causing divergence in a very special strange manner. This bug had caused the value of outer fluid enthalpy to oscillate impalpably and then cause the program to diverge. It deterred the project form progressing for three whole days. We were to give up hopelessly that suddenly we seized the culprit. A very subtle bug that we had been warned against in the course. We had chosen the time steps a little bit high and the steam flow rate was not reasonable enough to remain in the state of saturate vapor due to high pressure drop.
5. During implicit codes, the jacobian matrix demonstrated singularity, ill condition and as a result divergence. It was a little hard to understand what was really wrong. The bug was found to be inappropriate indexing of the equations. Some of

the equations were rewritten and some of them didn't even participate in the jacobian matrix.

6. In coding the implicit algorithm, we decided to write the Newton method, first, and then incorporate the House-Holder-Broyden method into it. The convergence time for steady sate implicit was about 17 seconds (for 20 meshes each layer) which was too high. However, after implementing House-Holder-Broyden method, the time was diminished to 4 seconds which was astonishing.
7. Maybe one of the greatest opportunities of this project was to work with graphic environment of Matlab, which is really fun.

Chapter 2

Hermite Polynomials

2-1 Outlines

1. Can we go further than **Hermite-19**?
2. Reducing encountered errors.(round off and global)

2-2 Objective

The objective of this chapter is to acquire Hermite equations roots using Bairsotow algorithm.

2-3 Introduction

Hermite polynomials are among the famous equations that have enormous application in science. They have been studied thoroughly and many of their properties are known. Hermite Polynomials can be derived using below recursive method.

$$H_0(x) = 1$$

$$H_1(x) = 2x$$

$$\text{———————————————————}$$

$$H_{n+1}(x) = 2xH_n(x) - 2nH_{n-1}(x)$$

The initial guess for Bairstow algorithm is very crucial. It is believed that initial guess will also affect the final error in the roots but we are going to explain why such an idea may not always be the case.

For the sake of simplicity and order of the report, we don't stray deep into details, copy-pasting the properties and application of these polynomials; but useful web pages and PDFs are attached to the delivered CD.

2-4 Assumptions

1. The convergence criteria in Bairstow algorithm is set to 10^{-17}.
2. If the initially guessed "r" and "s" fail to give appropriate quadratic factor after 10000 times modification, the program will be ceased for initial guess change.

2-5 Program Flowchart

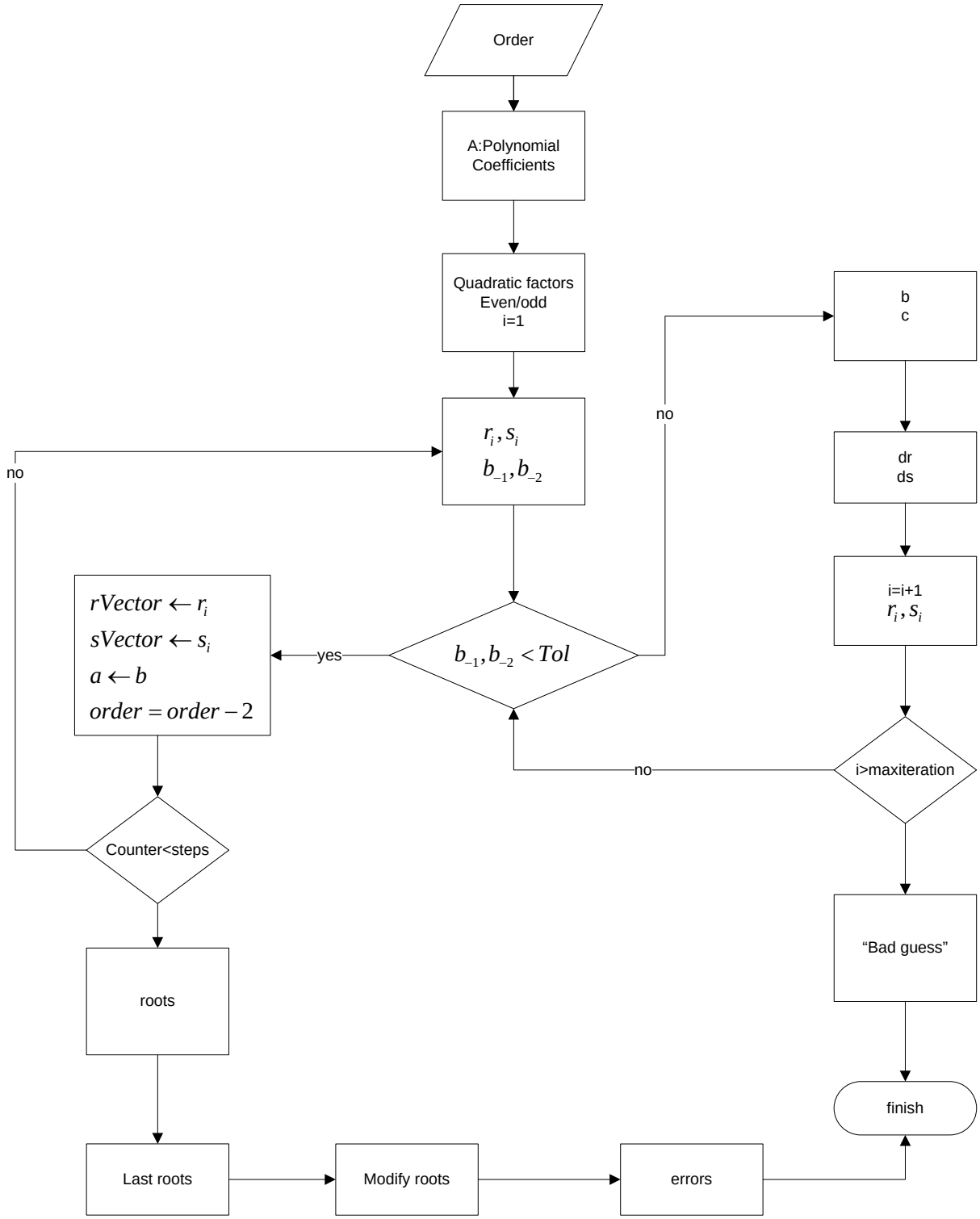

Flowchart 9- Bairstow algorithm

2-6 Program Results

Roots of H15(x)	Error of H15(x)
-4.499990707309390	0.018565177917
-3.669950373404430	-0.002391099930
-2.967166927905600	-0.000011920929
-2.325732486173850	-0.000000715256
-1.719992575186490	-0.000002503395
-1.136115585210920	0.000001192093
-0.565069583255578	0.000001430511
0.000000000000004	0.000002279802
0.565069583255576	-0.000000059605
1.136115585210920	-0.000001192093
1.719992575186490	-0.000008463860
2.325732486173860	0.000023841858
2.967166927905600	0.000057220459
3.669950373404420	-0.004496812820
4.499990707309390	-0.086036205292

Roots of H16(x)	Error of H16(x)
-4.688738939305820	0.088531494141
-3.869447904860120	-0.001205444336
-3.176999161979930	-0.000564575195
-2.546202157847460	0.000061035156
-1.951787990916250	-0.000003814697
-1.380258539198880	-0.000003814697
-0.822951449144656	-0.000001907349
-0.273481046138152	-0.000000417233
0.273481046138152	0.000000119209
0.822951449144622	0.000141143799
1.380258539198940	0.000473022461
1.951787990916250	0.000015258789
2.546202157847490	0.000083923340
3.176999161980010	-0.000335693359
3.869447904860130	0.000350952148
4.688738939305820	0.088531494141

Roots of H17(x)	Error of H17(x)
-4.871345193674400	-2.165496826172
-4.061946675875570	-0.017333984375
-3.378932091141460	0.001235961914
-2.757762915703850	0.000190734863
-2.173502826666630	0.000297546387
-1.612924314221230	-0.000015258789
-1.067648725743450	0.000000000000
-0.531633001342655	-0.000003814697
0.000000000000000	0.000008588932
0.531633001342655	0.000001907349
1.067648725743450	-0.000015258789
1.612924314221230	0.000015258789
2.173502826666620	0.000297546387
2.757762915703910	-0.000488281250
3.378932091141460	-0.001235961914
4.061946675875570	0.017333984375
4.871345193674400	2.165496826172

Roots of H18(x)	Error of H18(x)
-5.048364008874460	6.513671875000
-4.248117873568100	0.152343750000
-3.573769068486090	0.014648437500
-2.961377505531620	0.004394531250
-2.386299089166690	0.000000000000
-1.835531604261630	-0.000122070313
-1.300920858389610	-0.000061035156
-0.776682919267412	0.000122070313
-0.258267750519096	0.000045776367
0.258267750519097	-0.000038146973
0.776682919267412	0.000000000000
1.300920858389610	-0.000061035156
1.835531604261620	0.000000000000
2.386299089166650	-0.001953125000
2.961377505531580	0.000976562500
3.573769068486290	-0.010253906250
4.248117873568100	0.152343750000
5.048364008874460	6.513671875000

Roots of H19(x)	Error of H19(x)
-5.220271690537450	-272.686035156250
-4.428532806603830	-8.492675781250
-3.762187351963980	-0.729492187500
-3.157848818347550	-0.001953125000
-2.591133789794680	0.010742187500
-2.049231709850610	0.000976562500
-1.524170619393530	0.000488281250
-1.010368387134310	0.000488281250
-0.503520163423888	-0.000122070313
0.000000000000000	-0.000117545686
0.503520163423888	0.000000000000
1.010368387134310	-0.000244140625
1.524170619393520	0.002929687500
2.049231709850620	0.000244140625
2.591133789794560	-0.023681640625
3.157848818347350	-0.008789062500
3.762187351963800	0.604003906250
4.428532806603830	8.492675781250
5.220271690537450	272.686035156250

Roots of H20(x)	Error of H20(x)
-5.387480890011200	-3871.687500000000
-4.603682449550670	2.687500000000
-3.944764040115420	2.250000000000
-3.347854567383220	0.531250000000
-2.788806058428150	0.140625000000
-2.254974002089300	-0.085937500000
-1.738537712116600	0.000000000000
-1.234076215395320	0.007812500000
-0.737473728545394	-0.000976562500
-0.245340708300901	-0.000610351563
0.245340708300901	0.000732421875
0.737473728545394	0.001953125000
1.234076215395320	-0.003906250000
1.738537712116600	0.000000000000
2.254974002089300	-0.085937500000
2.788806058428160	-0.093750000000
3.347854567383240	-0.406250000000
3.944764040115420	2.250000000000
4.603682449550750	17.187500000000
5.387480890011200	-3871.687500000000

2-7 Challenges

Although we could reduce the errors associated with Hermite-17 and Hermite-18 by changing the initial guess of Bairstow algorithm but all the attempts for proceeding further were in vain. This handicap can be wisely attributed to the round off errors and will be discussed furthermore.

For controlling round off errors, we have some tips. First, in order to decrease the magnitude of round-off errors and to lower the possibility of overflow/underflow errors, we can make the intermediate result as close to 1 as possible in consecutive multiplication/division processes. According to this rule, when computing $x\,y/z$, we program the formula as

1. $(x\,y)/z$ when x and y in the multiplication are very different in magnitude,
2. $x(y/z)$ when y and z in the division are close in magnitude, and
3. $(x/z)\,y$ when x and z in the division are close in magnitude.
4. Also, we can use Horner method in constructing polynomials to mitigate the effect of round off errors.

The results of implementing above methods showed to be very effective, but the reduction in Hermite-19 errors was not satisfactory and still was high. Another conversation between the members of the group led to the conclusion that manipulating Matlab epsilon would be effective; a proposal which unfortunately was failed as we couldn't figure out the Matlab epsilon alteration. The reasons for settling such an agreement and summing up the argument are listed below:

1. First defendant for the rationality of this conclusion is what below figure illustrates.

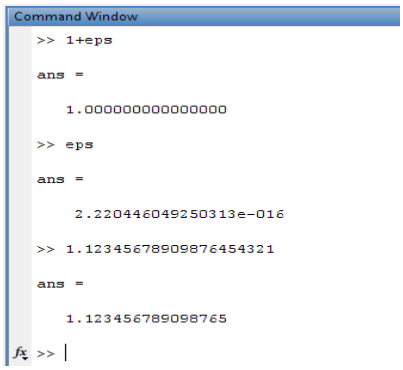

Fig48. Truncation of the numbers (round off errors) in Matlab.

2. Second reason is that we assumed if there's any root, it would be near detected root, closer than 10^{-3} (this assumption make sense as we know that the difference in the sign of Hermite polynomial changes around this root) so we prepared a program for exploring any possible root having little error in this domain, an approach which was unsuccessful. The initial guesses were generated through random numbers and the results were checked programmatically, this idea was also in vain.

Using above methods, it is possible to reduce the errors but, still, two main problems remain unresolved for high orders of hermite polynomials (more that 19). The first is propagation of large errors and the second is the convergence problem. The first associates with the precision of our computer and even used software (at least in our estimation) but the second originates in initial guess. For overcoming the first problem, which starts around hermite 15, the tolerance was reduced, so the attained roots were more precise and the errors diminished very easily up to hermite 19. The second problem during hermite work relates to initial guesses for high order polynomials. Inappropriate initial guess had made the program to get stuck in infinite loops or attained roots were zeros. This problem was so complicated that the initial guess of hermite 16 and 17 were, totally, unsuitable for hermite 18 and 19. So, we had to find, for every polynomial, a specific initial guess which was appropriate for it. Another idea was to implement different initial guesses for various polynomials. It was anticipated that because the distant roots to the zero had more errors, if they are calculated first, then the victory will emerge. This hope had contrary results; therefore the idea was, immediately, purged from minds because finding near zero roots was more promising. Therefore, the only left problem, still, was dealing with large errors. The errors are larger for distant roots from zero. It is obvious that for these roots, a little bit change in the root will result in a huge error. For example $\Delta x = 10^{-10}$ change in the root of hermite 18 causes a tremendous error of$\Delta y = 10^{6}$ which makes handling the errors hard. And as a result because matlab can't identify precisions more than 10^{-15}, hermite 19 roots can't be attained with desired precision.

Another idea which crossed our minds was to use Windows 64 bit with Matlab 64 bit. We were absolutely sure that this idea is going to work and we can, at last, meet hermite 19 precise roots

(of course up to 32 digits after point). Unfortunately, this idea, like some of others, was nothing more than self delusion.

These reasons were more than enough for bringing the Hermite homework to an end.

2-8 Program GUI

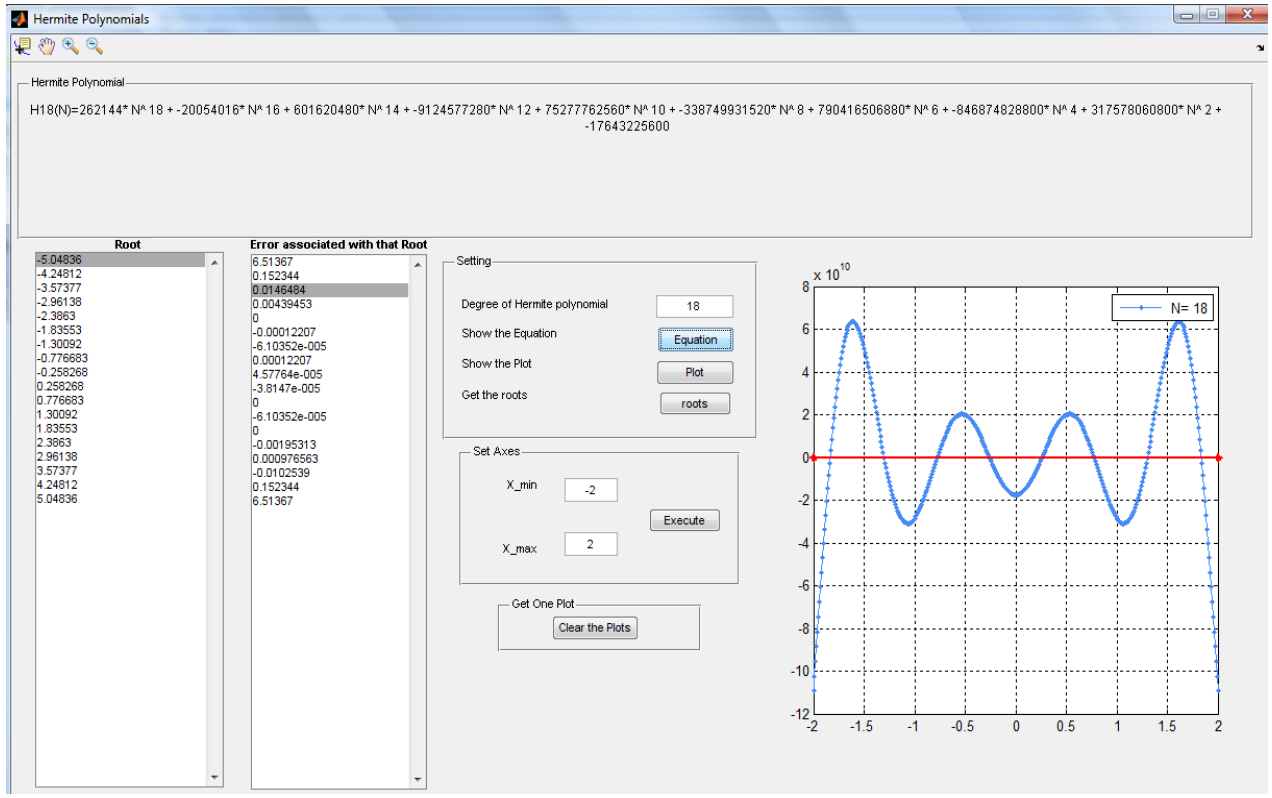

Fig49. Hermite polynomials GUI

Chapter 3

Cubic Spline Interpolation

3-1 Outlines

1. Performing the Spline homework for various boundary conditions.
2. Friendly user interface

3-2 Objective

The objective of this chapter is to interpolate all the properties of saturated vapor using Cubic Spline on about 75 known points.

3-3 Introduction

Splining the saturated vapor table is necessary, as we know these properties don't follow linear behavior and don't change gradually. This problem gets worse, when few data are available for estimation of unknown points.

3-4 Assumptions

1. For estimating the unknown point, all the known data (75 points) will participate.
2. ASME steam table (attached to the report) is used for the known data.

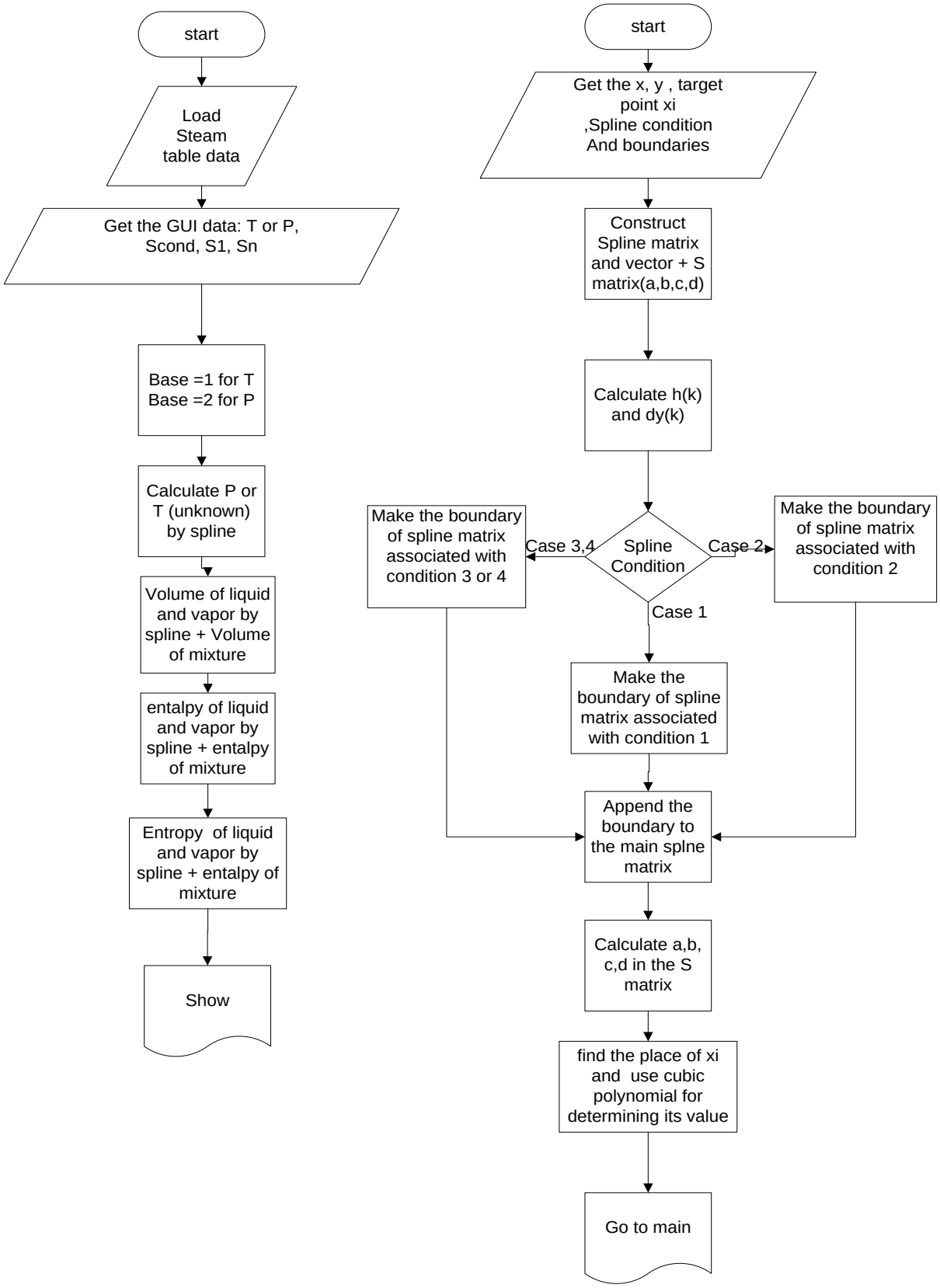

Flowchart 10– Spline homework

3-5 Program results

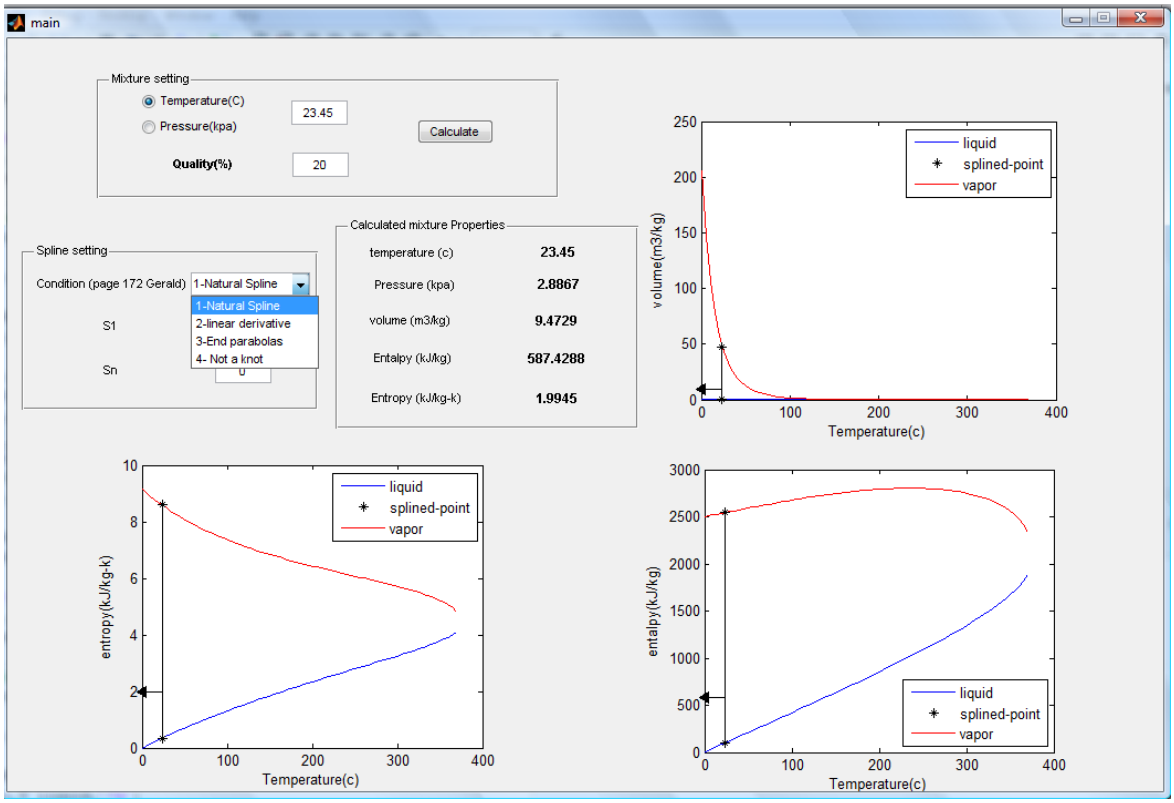

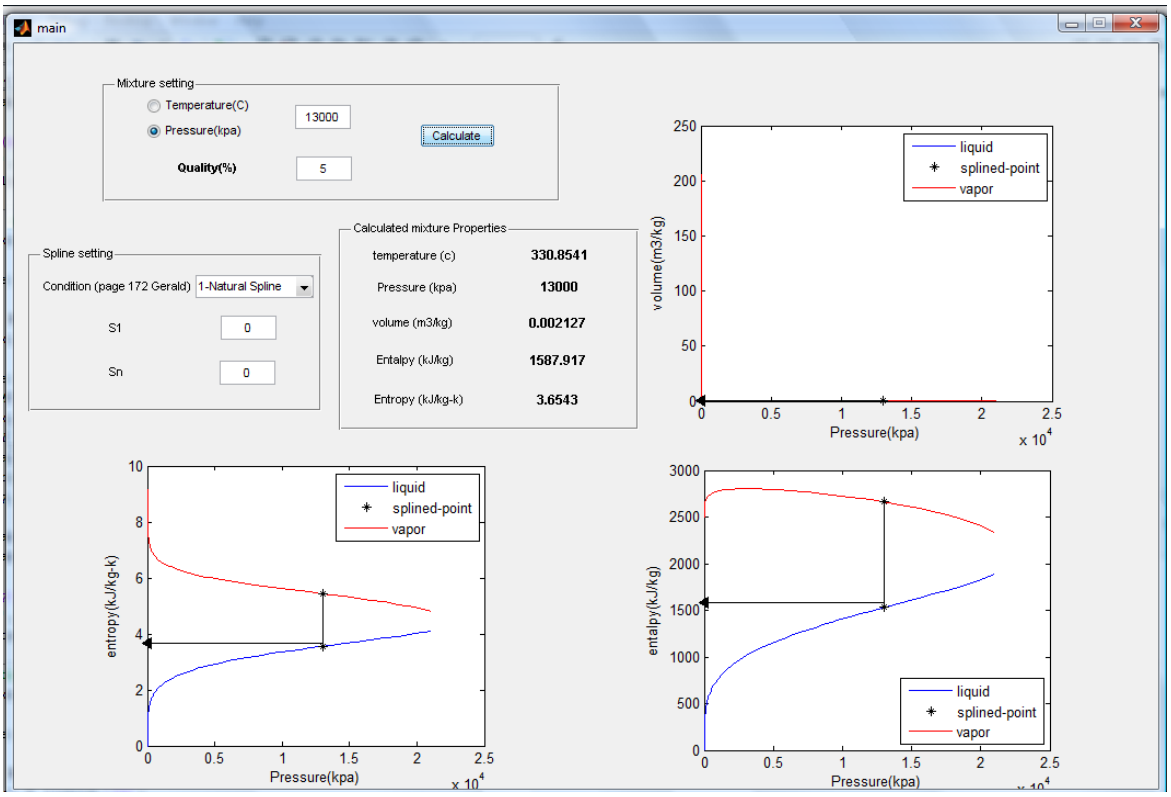

Suggestions and future works

1. The program of steady state and even unsteady state can be changed to intelligent based programs, it means that if the change in the phases inverses due to high pressure drop and less heat transfer from steam, the steam shows superheat behavior rather than saturated behavior, then the properties of superheated steam must be used, therefore, the seam quality won't proceed the value of one and the program won't diverge.
2. The programs associated with explicit unsteady state can be changed to an mesh wise program, it means that the program can have the capability of modifying the mesh size and time intervals, so, it ensures its convergence.
3. The case associated with inlet superheated vapor and outlet subcooled water in the outer pipe can be solved using implicit methods, therefore, not only we can validate the explicit results but also it is possible to simulate the problem for counter-current flows.
4. Beautiful design problems can be created and solved. This means that if the inlet flux and temperature of water and temperature of steam were known, then we find the inlet flux of steam. These sort of problems can be solved using explicit methods simply by trial and error, however solving them through implicit methods requires adaptations of codes.
5. The important point relates to the assumption of having one dimensional in Z direction, this assumption will be illegal if the diameter f pipe is large relative to its length, therefore, two dimensional grids are required, some of the efforts which is necessary for such modeling is listed below:
   A. Due to less pressure drop, it is possible to assume that pressure drop is constant in both inner and outer pipes. This eases the problem and reduces the unknowns.
   B. The Neumann condition appears as boundary condition in r=0 and Drichlet condition shows up at inlet section of the pipe, this complicates discretized equations associated with each grid.
   C. Indexing the grids and the procedure of dealing with them is very important.

However, we think solving this problem, although looking somehow tough, is feasible because "if you believe you can do a thing or not, either way, you are right - Henry Ford".

Thank you for reading this work